MONO-CYCLOPROPENONE CAGED DIBENZOCYCLOOCTYNE TRIAZOLE: A FAST-REACTING, WATER SOLUBLE SPAAC REAGENT

by

CHRISTOPHER JOSEPH MOLNAR

(Under the Direction of Vladimir V. Popik)

ABSTRACT

The use of strain-promoted azide-alkyne cycloadditions (SPAAC) has become increasingly popular due to its high efficiency and wide applicability. It has been used for probing cell metabolism, analyzing drug uptake, functionalizing material surfaces, among many other applications. SPAAC, as the name implies, requires an azide and a cyclic alkyne. Many of these cyclic alkyne reagents are hydrophobic due to the interplay between stability and reactivity. This also presents a challenge when attempting to utilize these reactions in aqueous conditions. Here, we report the synthesis, characterization, and kinetic analysis of dibenzocyclooctyne-triazole-EG_4-OH (DIBOT): a fast-reacting, water soluble cyclooctyne, as well as its precursors. The precursor, mono-cyclopropenone caged dibenzocyclooctyne-triazole-EG_4-OH (MC-DIBOT) is capable of photo-initiated decarbonylation. Both MC-DIBOT and DIBOT are water soluble, which allows us to analyze the reaction kinetics of the SPAAC reaction in aqueous solutions. We also plan to study the effects of water on the rate of the IEDDA reaction between DIBOT and 3,6-bipyridyl-1,2,4,5-tetrazine.

We also report the attempted synthesis of a water soluble bis-cyclopropenone caged dibenzocyclooctadiyne SPAAC reagent (WS-BC-DIBOD). It has been shown that each of the acetylene units of dibenzocyclooctadiyne (DIBOD) undergo the SPAAC reaction at significantly different rates. A compound such a WS-BC-DIBOD would allow for analysis of how the inclusion of water affects the rate of slower SPAAC reactions.

INDEX WORDS: Click chemistry, Bioorthogonal, SPAAC, Azide, IEDDA, Tetrazine ligation, pyTz, Photo-click, Cross-coupling, Rate-enhancement, Cyclopropenone, Dibenzocyclooctyne-triazole, Dibenzocyclooctadiyne

MONO-CYCLOPROPENONE CAGED DIBENZOCYCLOOCTYNE TRIAZOLE: A FAST-REACTING, WATER SOLUBLE SPAAC REAGENT

by

CHRISTOPHER JOSEPH MOLNAR

B.S., Westminster College, 2014

A Dissertation Submitted to the Graduate Faculty of The University of Georgia in Partial Fulfillment of the Requirements for the Degree

DOCTOR OF PHILOSOPHY

ATHENS, GEORGIA

2022

MONO-CYCLOPROPENONE CAGED DIBENZOCYCLOOCTYNE TRIAZOLE: A FAST-REACTING, WATER SOLUBLE SPAAC REAGENT

by

CHRISTOPHER JOSEPH MOLNAR

Major professor: Vladimir V. Popik

Committee: Richard W. Morrison

Robert S. Phillips

Electronic Version Approved:

Ron Walcott
Vice Provost for Graduate Education and Dean of the Graduate School
The University of Georgia
December 2022

DEDICATION

I would like to dedicate this work to my family, the Molnars and Lamaines; my parents, Dan and Christy Molnar, for continued love and support throughout my life; and my late grandparents, Helen and John Molnar, whom I wish I could have shared the completion of this journey with.

ACKNOWLEDGEMENTS

First and foremost, I would like to thank Dr. Popik for his patience, support, and understanding. I could not have done some of the intricate instrumental setup and modifications without his help. He has also helped tremendously in scrutinous data interpretation. I would also like to thank my committee, Dr. Phillips and Dr. Morrison, for their support throughout my graduate career. Additionally, I would like to thank Dr. Dennis Phillips and Dr. Chau-Wen Chou of the PAMS facility and Earle Adams of the NMR facility. I would be remiss not to also thank all the Popik lab members, past and present, that have been instrumental in my growth: Dr. Dewey Sutton, Dr. Masha Sutton, Dr. Chris McNitt, Dr. Nannan Lin, Dr. Kun Wang, Dr. Chen Zhao, Dr. Shubham Sharma, Dr. Zichun Ren, Ayesha Nisathar, Shrey Patel, Patrick Foster, Rohan Bhavsar, and Shivani Nagode. Next, I would like to thank Emily Chopra for her hard work and studiousness. Last, but certainly not least, I would like to thank my girlfriend Monica LaGatta for her unfailing love, support, and encouragement throughout my graduate endeavors.

Table of Contents

List of Figures

List of Tables

List of Schemes

List of Abbreviations

ADIBO.....Aza-dibenzocyclooctyne
BCN .....Bicyclo[6.1.0]non-4-yne
Bis-MC-DIBOT .....Bis-monocyclopropenone caged dibenzocyclooctyne-triazole
BSA..... Bovine Serum Albumin
CuAAC .....Copper-catalyzed azide-alkyne cycloaddition
DIBO.....Dibenzocyclooctyne
DIBOD.....Dibenzocyclooctadiyne
DIBOT ..... Dibenzocyclooctyne-triazole
DIFO ..... Difluorocyclooctyne
DiMOC .....Dimorpholino-dibenzocyclooctadiyne
HSA.....Human serum albumin
IEDDA ..... Inverse electron demand Diels-Alder
MC-DIBOD .....Mono-cyclopropenone caged dibenzocyclooctadiyne
MC-DIBOT..... Mono-cyclopropenone caged dibenzocyclooctyne-triazole
ODIBO.....Oxa-dibenzocyclooctyne
PBS .....Phosphate-buffered saline
pyTz 3,6-bipyridyl-1,2,4,5-tetrazine
SPAAC.....Strain-promoted azide-alkyne cycloaddition
TCO.....Trans-cyclooctene
TEG.....Tetraethylene glycol
TMDIBO..... Tetramethoxy dibenzocyclooctadiyne
Trx.....Thioredoxin
WS-BC-DIBOD..... Water-soluble bis-cyclopropenone caged dibenzocyclooctadiyne

CHAPTER 1

INTRODUCTION AND LITERATURE REVIEW

The term click chemistry was first described by Dr. Barry Sharpless as "[Reactions that are] modular, wide in scope, give very high yields, generate only inoffensive byproducts that can be removed by nonchromatographic methods, and [are] stereospecific."[1] Of these many click reactions, Sharpless notes that one example, 1,3-dipolar cycloaddition, "is about as good as a reaction can get." In his 1963 review, Dr. Rolf Huisgen describes a variety of 1,3-dipolar cycloaddition reactions; one of which is the reaction between organic azides and acetylenes to form 1,2,3-triazoles (Figure 1.1).[2] The utility of this particular Huisgen cycloaddition reaction has been investigated by numerous groups ever since.

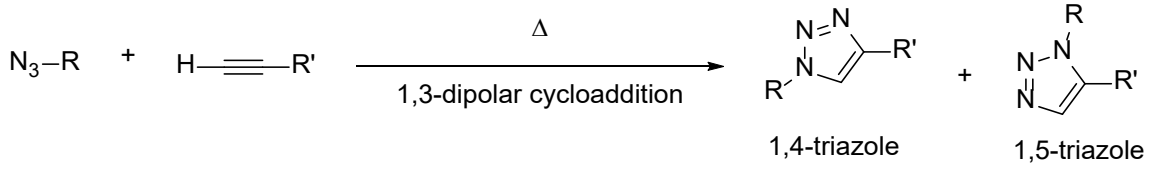

Figure 1.1 1,3-dipolar cycloaddition between an organic azide and terminal acetylene.

1.1 Bioorthogonal reactions

Building upon the idea of click chemistry introduced by Sharpless, Dr. Carolyn Bertozzi coined the term "bioorthogonal" in 2003[3] and defined it as a "chemical reaction that neither interact[s] with nor interfere[s] with a biological system." Bioorthogonal reactions are most useful for biomolecular imaging, and there are numerous examples in the literature of this.[4-8] One of the first examples of a bioorthogonal reaction is the Bertozzi model for Staudinger ligation (Figure 1.2).[3] In this reaction, a triphenyl phosphine methyl ester derivative is conjugated to *N*-

azidoacetylgalactosamine through a Staudinger ligation. The drawback to this method of click conjugation is that the Staudinger reaction is rather slow (k_2 = 2.5 ± 0.2 × 10^{-3} M^{-1} s^{-1}) and competing oxidation of the phosphine reagents leading to long incubation times and significant background labeling.[9]

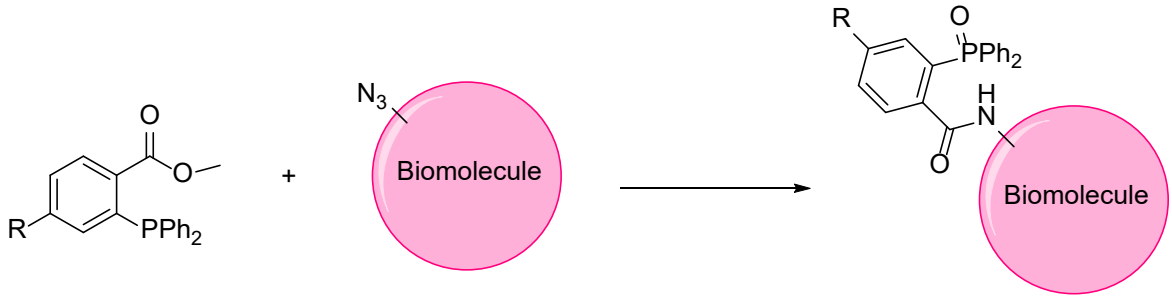

Figure 1.2 Bertozzi model for Staudinger ligation.

Certain functional groups can be deemed bioorthogonal if they meet these criteria: They are inert in biological systems, they react selectively, and they are nontoxic. It is also beneficial for these functional groups to be small, though it is not a requirement of biorthogonality. For these reasons, the azide functional group is commonly used as a bioorthogonal moiety. The azide group is small and highly stable under physiological conditions, making it the most continent handle for biomolecular modification.[10] Azide moieties can be introduced into biological substrate via chemical or metabolic methods. Chemical modification involves a direct chemical reaction on a natural biomolecule (Figure 1.3 A).[11-12] Metabolic insertion of an azide group requires incorporating the azide on an unnatural amino acid or unnatural monosaccharide and allowing the cell to metabolize these azide-modified substrates (Figure 1.3 B).[13-14] Both methods have been well studied and are sufficient for incorporating azide into a substrate of interest.

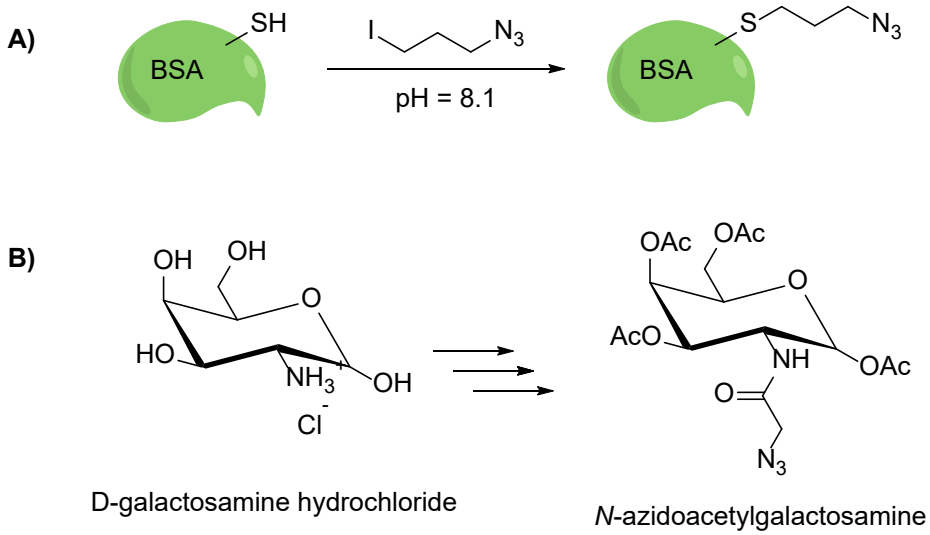

Figure 1.3 Chemical introduction of azide into (A) BSA and (B) monosaccharide.

1.1.1 Copper(I) Catalyzed Azide-Alkyne Cycloaddition (CuAAC)

In his original report, Sharpless describes azide-alkyne cycloadditions between azides and electron deficient internal alkynes. These reactions were performed in water or toluene as the solvent at moderately high temperatures.[1] Then, a little over a year after the initial report, Sharpless published a paper on the CuAAC reaction.[15] In this example, catalytic amounts of copper(II) sulfate and sodium ascorbate are added to the reaction mixture (Figure 1.4). The result of adding these additional reagents is an enhanced rate of reaction at lower temperatures and higher preference for the 1,4 regioisomer. Unfortunately, using copper to catalyze the reaction limits its applicability to *ex vivo* implementation.

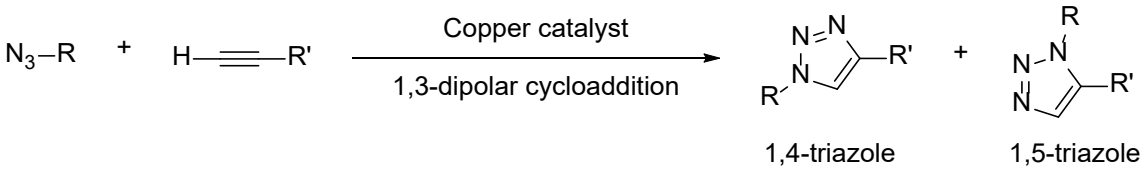

Figure 1.4 CuAAC between organic azide and terminal alkyne

1.1.2 Strain Promoted Azide-Alkyne Cycloaddition (SPAAC)

Wittig and Krebs first noted in 1961 that the reaction between a strained cycloalkyne and an azide results in an "explosive" reaction that yields a triazole via a 1,3-dipolar cycloaddition (Figure 1.5 A).[16] Then, in 2004, 43 years after Wittig and Krebs observed what is considered the first example of a SPAAC reaction, Bertozzi applied SPAAC to label protein within a living cell (Figure 1.5 B).[17] Inspired initially by Sharpless' work on CuAAC, Bertozzi's goal was to eliminate the need for toxic Cu(I) and make azide-alkyne cycloadditions viable bioorthogonal reactions. She was successful in her endeavors and this work initiated a boom in the field of bioorthogonal chemistry that is still ongoing.

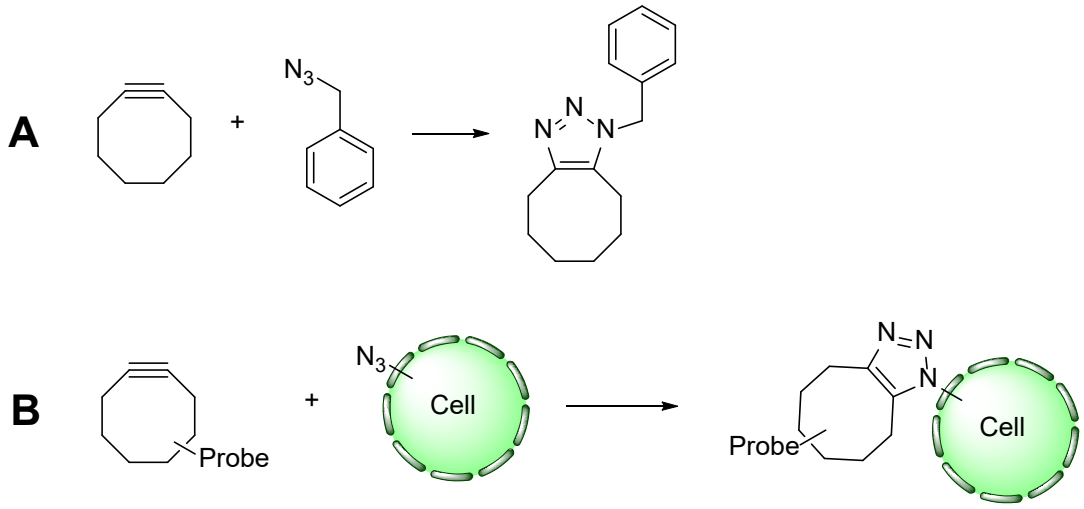

Figure 1.5 Wittig and Krebs 1,3-dipolar cycloaddition of cyclooctyne with phenylazide (A). Bertozzi model of cell labeling via 1,3-dipolar cycloaddition (B).

In 2008, Houk et. al. would look further into the major driving force for the SPAAC reaction.[18] Bertozzi had initially proposed that the major driving force was release in strain energy in going from cyclooctyne to triazole but did not perform computational analysis to support this claim. Houk analyzed three azide-alkye reactions using density functional theory and frontier molecular orbital theory calculations. In all cases, the azide was phenyl azide, while the alkynes

were acetylene, cyclooctyne, and difluorocyclooctyne (DIFO). Houk found that the activation energy for the transition states of acetylene-azide, cyclooctyne-azide and DIFO-azide are 16.2, 8.0, and 6.0 kcal/mol respectively. The unfavorable distortion of the azide N-N-N bond angle (173° → 138°) and the acetylene H-C-C bond angle (180° → 158°, 166°) account for the higher activation energy of the acetylene-azide transition state and aligns with the observed sluggish reaction. In both cyclooctyne-azide and DIFO-azide transition states, the distortion angles are not as pronounced, with the azide N-N-N bond angle only distorting to 142° and 143° respectively and the C-C-C bond angles at 153° and 155° in the ground state of cyclooctyne. In summation of Houk's results, the pre-distortion of the cyclooctyne bonds and reduced distortion of the azide N-N-N bond angle lead to a lower activation energy and an earlier transition state in both cyclooctyne and DIFO (Figure 1.6). In addition, the difluoro substituent on DIFO increases the electronic interactions, leading to a further reduction in activation energy and increased rate of azide-alkyne cycloaddtion reaction.

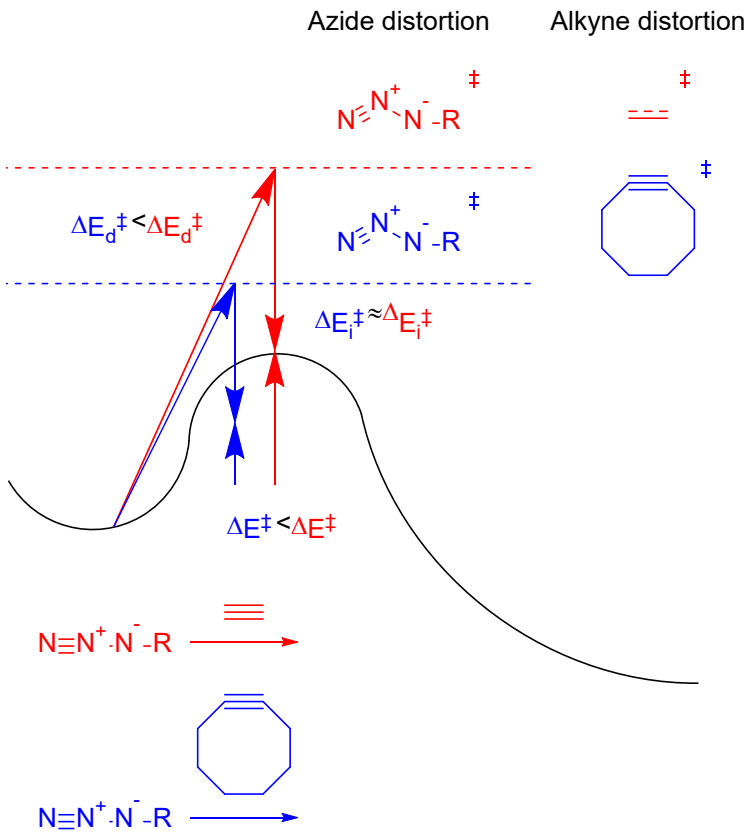

Figure 1.6 Reaction coordinate diagram illustrating difference between azide-acetylene reaction and azide-cyclooctyne reaction.

1.2 Reactivity, Selectivity, and Stability of SPAAC Reagents

The following sections comprise a non-exhaustive list of SPAAC reagents in chronological order of published synthesis, which will serve to outline the progress that has been made in the design of faster, more stable, and more selective cyclooctynes.

1.2.1 DIFO

Bertozzi first reported the synthesis of difluorinated cyclooctyne (DIFO) in 2007.[19] Their main goal in developing this compound was to increase the SPAAC reaction rate relative to the Staudinger ligation ($k_2 = 2.5 \pm 0.2 \times 10^{-3}$ M^{-1} s^{-1}). This was going to be achieved by installation of the difluoromethylene moiety adjacent to the acetylene. The electron-withdrawing nature of this moiety should enhance the ring strain which would lead to enhanced reaction rates. An added

benefit of using the difluoromethylene unit is that it is biologically inert and not a Michael acceptor.

The kinetic analysis of DIFO revealed that the second-order rate constant is 7.6 x 10^{-2} $M^{-1}s^{-1}$, which is 17-63 times higher than for Staudinger ligation. Additionally, DIFO was found to be stable in aqueous conditions and did not react with thiols (2-mercaptoethanol), making it amenable to biological applications. This result prompted *in vitro* and *in vivo* labeling studies, which were also successful (Figure 1.7).

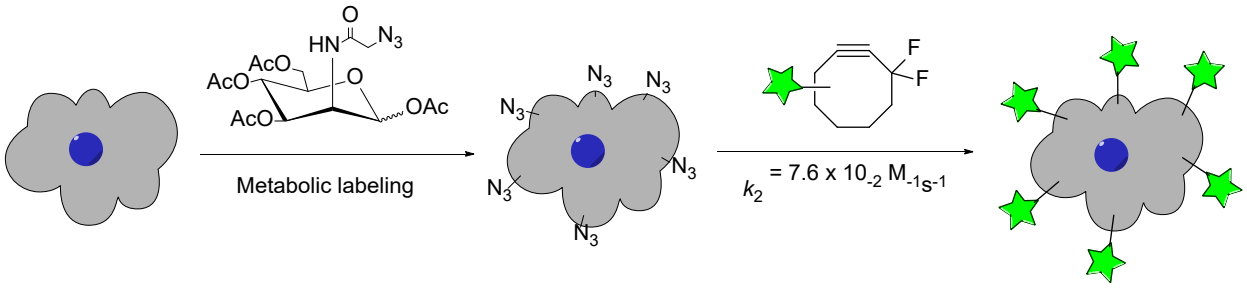

Figure 1.7 Jurkat cell labeling experiment with DIFO probe. Azide was incorporated metabolically using $Ac_4ManNAz$.

However, a subsequent analysis of DIFO in 2010 revealed that it is not as stable as was originally reported.[31] It was discovered that DIFO reacts with cysteine at a rate comparable to that of its reaction with azide. Tandem mass spectrometry analysis revealed that the products are likely formed from the addition of cysteine to the acetylene of DIFO. Thus, while DIFO showed promise initially, it is still subject to undesired side-reactions *in vivo*.

1.2.2 DIBO

In 2008, the Boons group developed dibenzocyclooctyne (DIBO) as the next generation of strained cyclooctyne reagents.[20] The idea behind the design of DIBO was to further increase the ring strain on the acetylene while also providing conjugation to the alkyne. An additional benefit of installing flanking benzene groups is the *ortho* hydrogens which would shield the alkyne from nucleophilic attack (Figure 1.8).

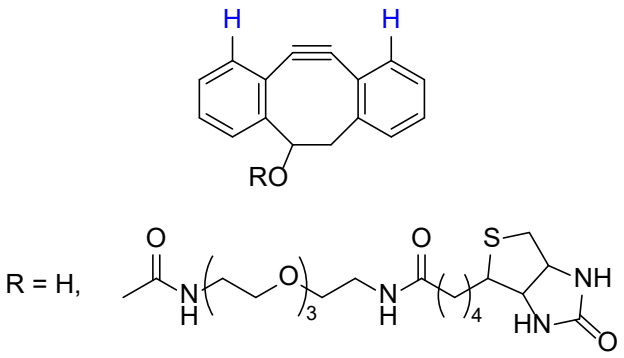

Figure 1.8 Structures of DIBO reported by Boons et. al. *Ortho* hydrogens are shown in blue.

After synthesizing DIBO, they tested the stability and found that it has an excellent shelf life and does not readily react with thiols or amines. It does, however, react with azides to yield the triazole products as desired. When testing the reactivity, they performed the experiment in both methanol and a 1:4 water/acetonitrile solution. The second-order rate constant for the SPAAC reaction in methanol was found to be 0.17 $M^{-1}s^{-1}$ and in 1:4 water/acetonitrile was found to be 2.3 $M^{-1}s^{-1}$. The authors did not provide any theories as to why the rate was enhanced in partially aqueous conditions. However, the reported rates are between 2-30 times greater than those of DIFO.

1.2.3 ADIBO

In 2010, the Delft group published the first report of the synthesis of an aza-dibenzocyclooctyne (ADIBO) that they called DIBAC (Scheme 1.1).[21] They analyzed the kinetics of the reaction of two of their DIBAC compounds with benzyl azide in deuterated methanol and found the second-order rate constant to be between 0.29 – 0.31 $M^{-1}s^{-1}$. They also looked at the reaction between DIBAC and 2-azidopropanoic acid in deuterated water and found the second-order rate constant to be 0.36 $M^{-1}s^{-1}$: slightly higher than the rate constant in methanol, however, not as marked of a rate increase as was observed with DIBO in aqueous conditions.

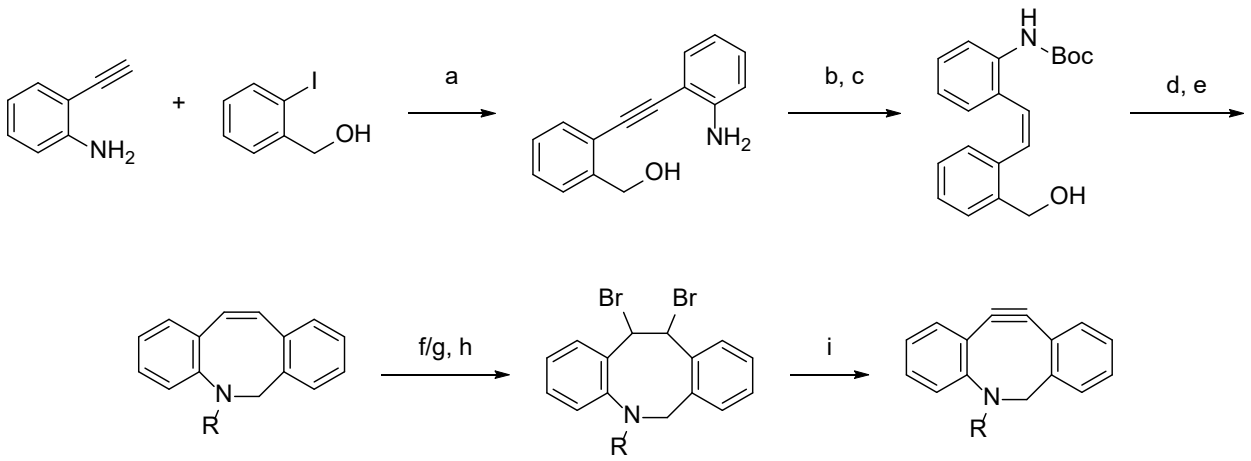

Scheme 1.1 Synthesis of DIBAC as reported by Delft et. al. Reagents and conditions: (a) $PdCl_2(PPh_3)_2$, CuI, Et_3N, THF, N_2/H_2-atmosphere, r.t., 4 h (99%); (b) Boc_2O, THF, 70 °C, 2 d (83%); (c) 10% Pd/$BaSO_4$, quinoline, H_2, MeOH, r.t., 1.5 h (95%); (d) Dess–Martin periodinane, $NaHCO_3$, CH_2Cl_2, r.t., 40 min (90%); (e) (1) 2 M HCl in EtOAc, r.t., 1 h; (2) $NaBH_4$, H_2O, r.t., o.n. (100%); (f) CbzCl, Na_2CO_3, H_2O, CH_2Cl_2, r.t., 3 h (86%); (g) $ClCOC_3H_6CO_2Me$, Et_3N, CH_2Cl_2, r.t., 1.5 h (94%); (h) Br_2, CH_2Cl_2, 0 °C, 2 h (**f**: 67%, **g**: 81%); (i) KO^{t}Bu, THF, 0 °C → r.t., o.n. (**f**), −40 °C, 2 h (**g**) (**f**: 87%, **g**: 84%). Overall yield = 41% over 9 steps.

Then, a year later, our group would publish a paper on the same type of compound synthesized via a different route (Scheme 1.2).[22] The original paper was centered around the synthesis and application of ADIBO as a handle for surface functionalization. Due to the nature of the application, a second-order rate constant was not determined in this particular experiment. However, it would later be determined by our group in collaboration with Dr. Locklin's group for both the rate of surface modification and reaction in solution.[23] The second-order rate constant for the reaction of ADIBO with benzyl azide in methanol was reported to be 0.428 ± 0.054 $M^{-1}s^{-1}$, which is slightly higher than the value reported by Delft.

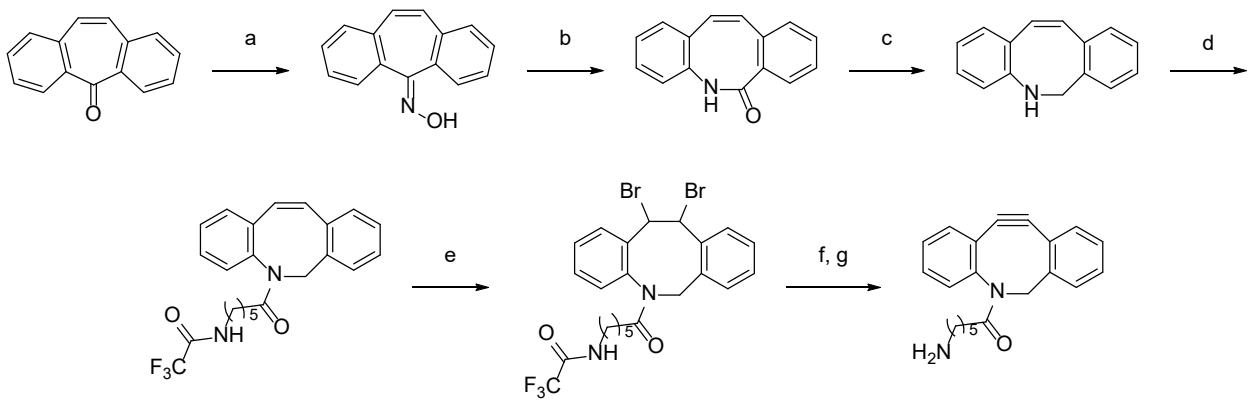

Scheme 1.2 Synthesis of ADIBO as reported by Popik et. al. Reagents and conditions: (a) $NH_2OH.HCl$, pyridine, 60%; (b) PPA, 125 °C, 73%; (c) $LiAlH_4$, ether, 58%; (d) pyridine, CH_2Cl_2, 71%; (e) pyridinium tribromide, 78%; (f) *t*-BuOK, THF, 88%; (g) K_2CO_3, aq MeOH, 58%. Overall yield = 7% in 7 steps.

1.2.4 BCN

Around the same time the experiments with ADIBO were conducted, Delft's group would also report on the strained cyclooctyne compound bicyclo[6.1.0]non-4-yne (BCN).[24] This compound incorporates a cyclopropane ring between carbons 5 and 6 of the cyclooctyne ring that has a functionalizable hydroxyl handle at the apex. BCN does not contain any aromatic units, which reduces its lipophilicity relative to dibenzocyclooctynes. It also comes in two forms, *exo* and *endo*, each of which have slightly different second order rate constants for reaction with benzyl azide. In a 3:1 CD_3CN:D_2O solution, the second-order rate constants were found to be 0.14 and 0.11 $M^{-1}s^{-1}$ for the *endo* and *exo* respectively. In a more polar 1:2 CD_3CN:D_2O solution, the second-order rate constants increased slightly to 0.29 and 0.19 $M^{-1}s^{-1}$ for the *endo* and *exo* respectively.

It was also reported that this compound does undergo undesired reactions with thiols (Figure 1.9).[25] To reduce undesired thiol reactions, Delft et. al. propose alkylating cell lysates with iodoacetamide. This method can only be effectively used *in vitro* as preincubation with live specimens will have deleterious effects on biological processes. The abundance of thiols in living

organisms, namely serum albumin and glutathione, is a major cause of high background labeling and reduced labeling sensitivity.

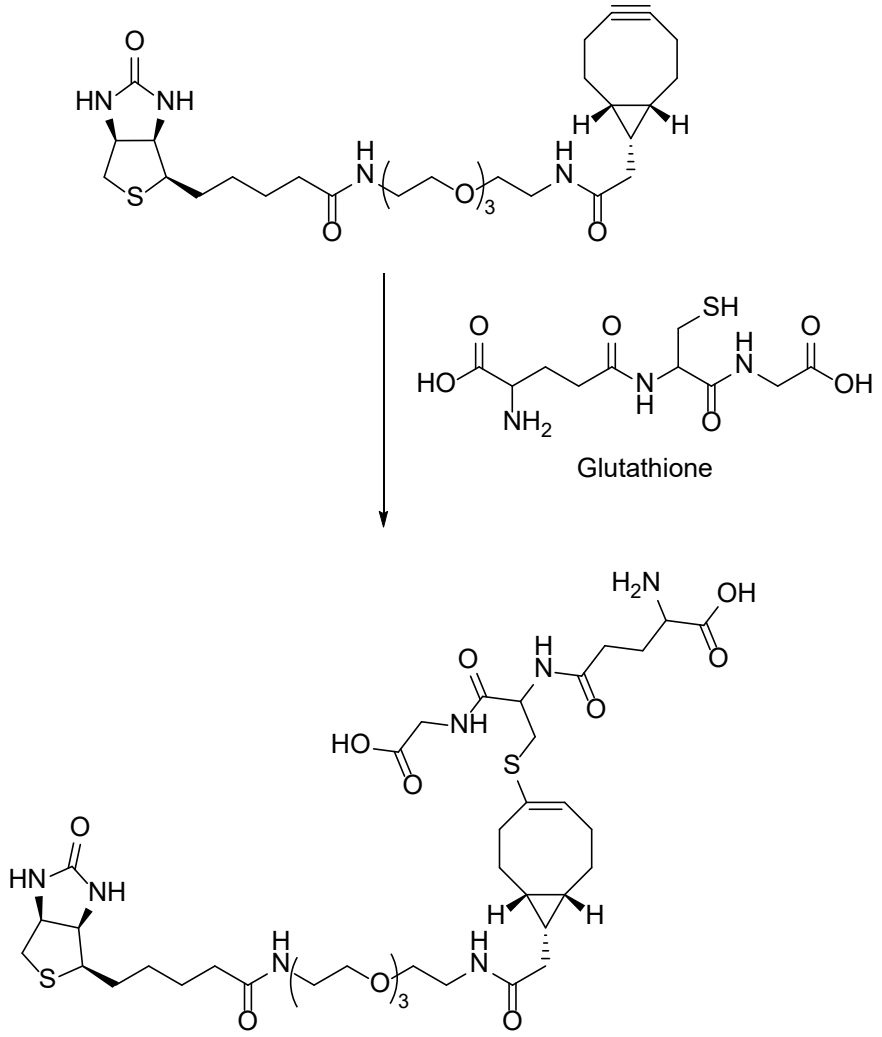

Figure 1.9 Thiol-yne reaction between BCN and glutathione. Addition product confirmed by mass spectrometry and NMR analyses.

1.2.5 BARAC

In early 2010, Bertozzi developed biarylazacyclooctynone (BARAC) to add to the library of strained dibenzocyclooctyne reagents.[26] This compound incorporates an amide opposite of the alkyne to increase the double-bond character of the bond opposite the alkyne. The desired goal was to increase the ring strain which would, in turn, increase the reactivity. However, they also

anticipated that this would significantly impact the stability of the alkyne. The kinetics experiments reveal that the SPAAC rate in organic solvent is enhanced compared to all previously mentioned cyclooctynes, giving a second-order rate constant of 0.96 $M^{-1}s^{-1}$ in acetonitrile. Unfortunately, the short lifetime and high instability of BARAC derivatives necessitates that they be stored neat and at 0 °C.

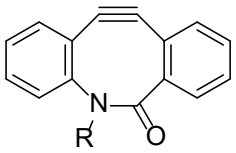

Figure 1.10 Structure of BARAC.

1.2.6 Summary and Limitations of SPAAC Reagents

The reactivity, selectivity, and stability of SPAAC reagents give insight into the features that allow the desired results to be achieved (Table 1.1). The reactivity of cyclooctynes that do not contain sufficient electron withdrawing substituents adjacent to the alkyne is lower than those with this feature. Additionally, the reactivity of cyclooctynes increases when the substituent opposite

Cyclooctyne	k_2 (x10^{-2} $M^{-1}s^{-1}$)	Solvent
DIFO	7.6	CD_3CN
DIBO	17 230	MeOD 1:4 D_2O/CD_3CN
DIBAC/ADIBO	29 – 31 36 42.8 ±5.4	MeOD D_2O MeOH
endo-BCN	14 29	3:1 CD_3CN/D_2O 1:2 CD_3CN/D_2O
exo-BCN	11 19	3:1 CD_3CN/D_2O 1:2 CD_3CN/D_2O
BARAC	96	CD_3CN

Table 1.1 Summary of cyclooctyne SPAAC reagents including experimentally determined second-order rate constants and solvent used for rate constant determination.

of the alkyne induces ring strain. However, increasing the reactivity comes at the cost of selectivity due to the increased electrophilicity of the alkyne moiety. The stability of the cyclooctyne also suffers when the reactivity increases, especially so with increased ring strain. This unfortunate relationship makes designing cyclooctyne SPAAC reagents challenging and limits their utility. Thus, other bioorthogonal click reactions have been explored as alternatives to SPAAC.

1.3 Inverse Electron Demand Diels-Alder (IEDDA) Reactions

The inverse electron demand Diels-Alder reaction is the complement to the standard Diels-Alder reaction. In a typical Diels-Alder reaction, the gap between the $HOMO_{diene}$-$LUMO_{dienophile}$ is small. On the other hand, in the inverse electron demand Diels-Alder reaction, the gap between the $HOMO_{dienophile}$-$LUMO_{diene}$ is small (Figure 1.7).[27] This relationship for IEDDA reactions implies that the $HOMO_{dienophile}$ energy should be increased and the $LUMO_{diene}$ energy should be decreased to reduce the band gap and increase the reaction rate. This band gap adjustment can be accomplished by incorporating electron-withdrawing groups on the diene and electron-donating groups on the dienophile.

The most popular IEDDA reaction for bioorthogonal applications is the tetrazine ligation. The tetrazine ligation reaction is composed of two parts: first, a [4 + 2] cycloaddition (rate limiting step) occurs between the diene and the tetrazine to give a bicyclic adduct. Then, the highly strained intermediate rapidly undergoes a retro-Diels Alder reaction to release N_2, giving either a dihydropyridazine (alkene dienophile) or pyridazine (alkyne dienophile) product.

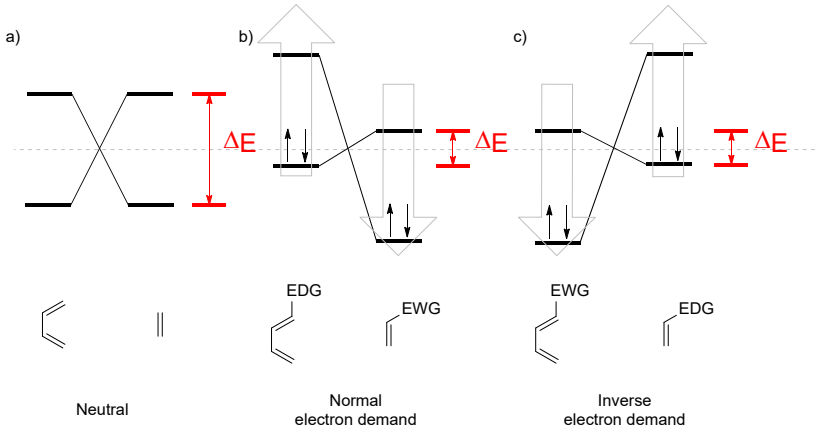

Figure 1.11 FMO models for (a) neutral, (b) normal, and (c) inverse electron demand Diels-Alder reactions.

1.3.1 Reactivity and Stability of Tetrazines in IEDDA Reactions

Tetrazines have been shown, by numerous groups, to have a wide range of stabilities and IEDDA reactivities. The observed general trend for stabilities is that tetrazines with better electron withdrawing groups and asymmetric substitution at the 2 and 6 position are less stable than those that are symmetric and have hydrogen or electron donating groups at the 2 and 6 positions (Figure 1.11).[26] These trends are in good alignment with what is observed for IEDDA reactivity of the dienophile, which may imply that tetrazine reactivity and stability are directly correlated. It is also known that tetrazines undergo hydrolysis and are susceptible to nucleophilic attack,[28] which makes their incorporation in biological settings challenging. Decomposition of tetrazines leads to either much less reactive dihydrotetrazines or benzonitriles.

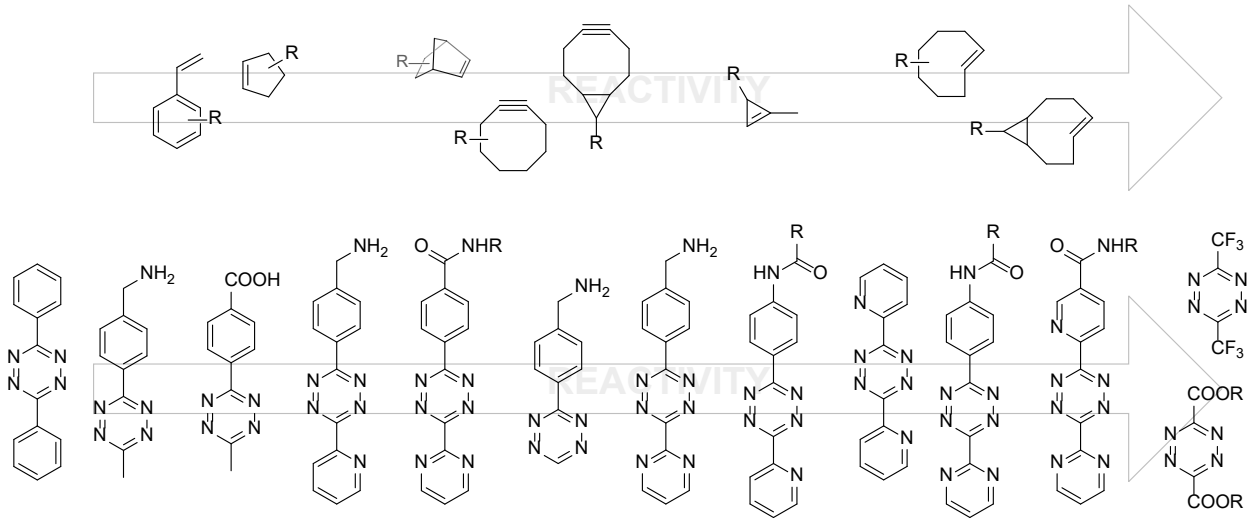

Figure 1.12 Reactivity scale of some dienophiles and tetrazines.

1.3.2 Reactivity of Dienophiles in IEDDA Reactions

In 1997, Sauer et. al. screened a wide array of dienophiles for IEDDA reactivity with 1,2,4,5-tetrazine.[29] They derived some "principle rules" for dienophile reactivities that will be summarized below:

1) Olefins react faster than acetylenes.

2) Cyclic olefins react faster the more ring strain is reduced in going to the product.

3) Enamines and ynamines have increased reactivity, presumably due to electron-donating ability.

4) Methoxy, ethoxy, trimethylsiloxy, and thioether substituents impart decreased reactivity due to dominating steric effects.

5) 1,2-disubstituted olefins are less reactive than 1,1-disubstituted olefins.

6) The substituent effect for substituted styrenes and phenylacetylenes is minimal.

These "rules" illustrate the interplay between electronic effects, steric effects, and ring strain in determining the reactivity of dienophiles with tetrazine.

1.3.3 Examples of Tetrazine Ligation in Biological Settings

In 2008, Fox et. al. reported that the IEDDA reaction between trans-cyclooctene (TCO) and 3,6-di(pyridin-2-yl)-1,2,4,5-tetrazine proceeds at a very high rate (k_2 = 2000 $M^{-1}s^{-1}$) and is amenable to bioorthogonal applications (Figure 1.8).[30] The main drawback to this method is that the range of tetrazines is limited due to the instability of various 3,6-disubstituted tetrazines. Additionally, it is not always feasible to incorporate bulky, hydrophobic compounds like trans-cyclooctene in biological systems. It has also been reported that the reaction between 3,6-disubstituted tetrazines and cyclooctynes proceeds at a significantly slower rate (or no reaction occurs) than with trans-cyclooctene under physiological conditions.[31-33] This significant difference in the reactivity of tetrazines with different dienophiles allows for enhanced mutual orthogonality between SPAAC and IEDDA reactions.[31-32]

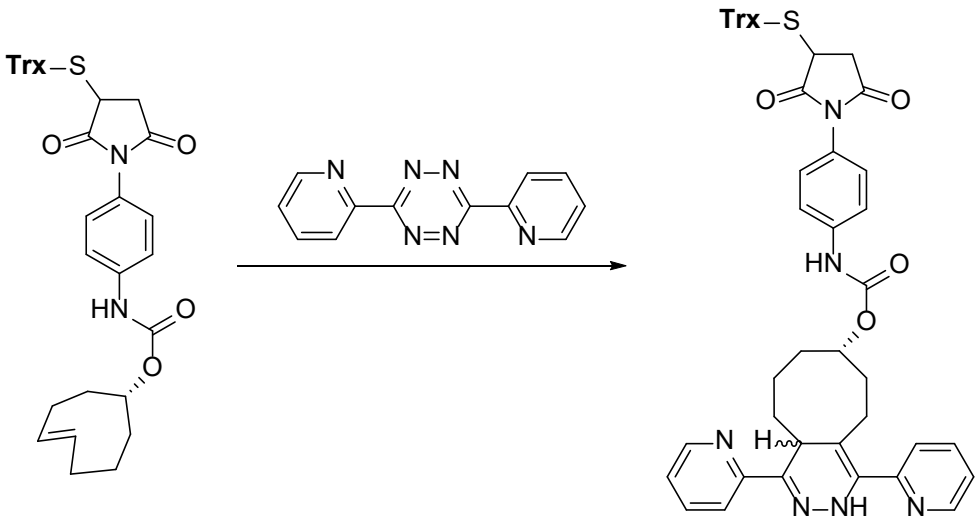

Figure 1.13 IEDDA reaction between pyTz and trans-cyclooctene used by Fox et. al.

In 2016, Augustyns et. al. synthesized and screened a number of tetrazines for use in bioorthogonal pretargeting.[34] They synthesized a total of ten different tetrazines and analyzed their stabilities in PBS and pure fetal bovine serum (FBS). They found that tetrazines with electron-

donating groups were the most stable, as was expected. They also observed that the stability and reactivity were inverses of each other, i.e. the more stable the tetrazine, the less reactive it was and vice versa. They selected the tetrazine with the best combination of stability and reactivity and used it to create an antibody-tetrazine conjugate. They then used a pretargeting approach to label human ovarian adenocarcinoma cells with TCO-fluorescent probes (Figure 1.13). Conjugation of the tetrazine did not significantly affect the reactivity of the tetrazine and the TCO-fluorescent probes could effectively label the cancer cells at concentrations as low as 50 nM.

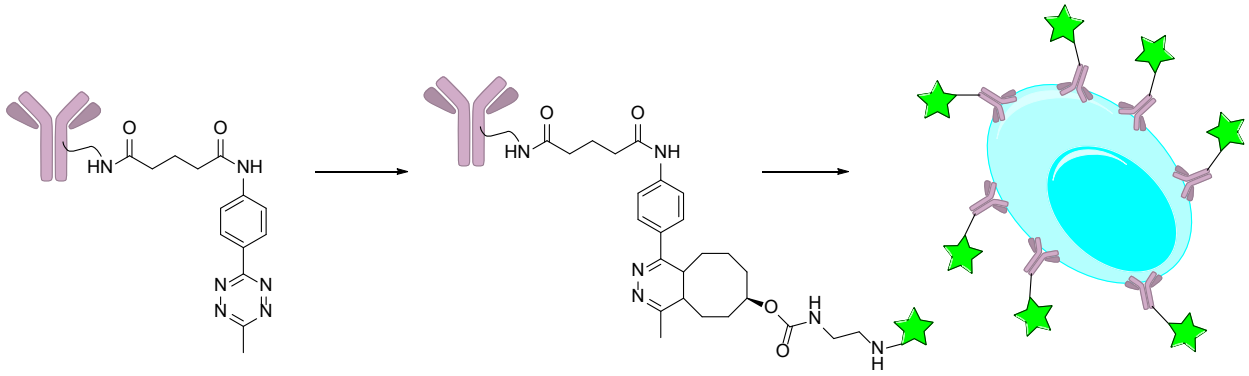

Figure 1.14 Pretargeting approach using tetrazine ligation. Tetrazine is covalently bound to antibodies which then undergo IEDDA reaction with TCO-probe. Antibody-probes are then introduced to cancer cells and labeling is observed.

1.3.4 Summary and Limitations of Tetrazine Ligation

Tetrazine ligation has emerged as one of the fastest bioorthogonal click reactions. The mechanism of the reaction and the properties of the reagents have been studied and are reasonably well-understood. Examples in the literature have shown how useful this reaction can be for rapid labeling of desired biomolecules. However, the high reactivity of tetrazines comes at a cost. Many of the tetrazines that undergo IEDDA reactions with suitable dienophiles are highly unstable in biological conditions. Tetrazines are highly susceptible to hydrolysis and nucleophilic attack. Another challenge that must be overcome in tetrazine ligations is that many dienophiles that are commonly used are hydrophobic, which makes it difficult to use them as the functional handle

within the biological system of interest. TCO is particularly problematic as it is known to bury itself within proteins, rendering up to 90% of TCO handles unreactive.[35]

1.4 Limitations of Bioorthogonal Click Reactions

While click reactions have a wide range of applications and, in particular, the SPAAC reaction has been deemed the "cream of the crop",[1] there are a number of improvements that could be made. First, most example bioorthogonal click reactions require a large excess of one of the reagents to achieve rates on the scale of biological processes. In biological imaging studies, this problem significantly increases background noise and off-labeling. Thus, the need for improved spatiotemporal control of click ligation is needed. Additionally, the aqueous solubility of most click reagents is rather low. This issue brings into question the efficiency of click reactions under biological conditions. Furthermore, it has been shown that cyclooctynes and tetrazines are susceptible to nucleophilic attack and decomposition in buffers and biologically mimetic conditions. Therefore, the introduction of water-soluble side chains or functional groups and the introduction of a protecting group for the acetylene moiety of cyclooctynes should circumvent these problems.

1.5 Summary and Goals of the Project

Click reactions are extremely robust, atom economic, and widely used in a variety of fields including organic synthesis, chemical biology, and material science. For organic synthesis and material science applications, CuAAC, SPAAC, and IEDDA reactions are applicable. However, chemical biology applications are only viable with SPAAC and IEDDA as the use of highly cytotoxic copper(I) catalysts limits the use of CuAAC in biological systems. For SPAAC reactions, the most used 1,3-dipole is azide due to its small size and ease of installation. On the other hand, the most used dipolarophiles are cyclooctyne derivatives which are bulkier and more hydrophobic

than azide. For tetrazine ligations, 3,6-disubstituted-1,2,4,5-tetrazines are clicked together with TCO or another electron-rich dienophile. However, this reaction is limited due to the instability of the tetrazines in aqueous conditions and the need to use trans-cyclooctene as the dienophile. To address these issues, there is a need for a cyclooctyne reagent that fits the following criteria: (1) is significantly more water soluble than currently known cyclooctynes, (2) is protected from undesired side-reactions at the acetylene, and (3) is capable of reacting with azides at a rate comparable to tetrazine ligation in aqueous conditions.

1.6 References

1. Kolb, H. C.; Finn, M. G.; Sharpless, K. B. Click Chemistry: Diverse Chemical Function from a Few Good Reactions. *Angewandte Chemie International Edition* **2001**, *40* (11), 2004-2021.

2. Huisgen, R. 1,3-Dipolar Cycloadditions. Past and Future. *Angewandte Chemie International Edition in English* **1963**, *2* (10), 565-598.

3. Hang, H. C.; Yu, C.; Kato, D. L.; Bertozzi, C. R. A metabolic labeling approach toward proteomic analysis of mucin-type O-linked glycosylation. *Proceedings of the National Academy of Sciences* **2003**, *100* (25), 14846-14851.

4. Carroll, L.; Evans, H. L.; Aboagye, E. O.; Spivey, A. C. Bioorthogonal chemistry for pre-targeted molecular imaging - progress and prospects. *Organic & Biomolecular Chemistry* **2013**, *11* (35), 5772-5781.

5. Debets, M. F.; van Hest, J. C. M.; Rutjes, F. P. J. T. Bioorthogonal labelling of biomolecules: new functional handles and ligation methods. *Organic & Biomolecular Chemistry* **2013**, *11* (38), 6439-6455.

6. Borrmann, A.; van Hest, J. C. M. Bioorthogonal chemistry in living organisms. *Chemical Science* **2014**, *5* (6), 2123-2134.

7. Shih, H.-W.; Kamber, D. N.; Prescher, J. A. Building better bioorthogonal reactions. *In vivo chemistry • Mechanisms* **2014**, *21*, 103-111.

8. Gong, Y.; Pan, L. Recent advances in bioorthogonal reactions for site-specific protein labeling and engineering. *Tetrahedron Letters* **2015**, *56* (17), 2123-2132.

9. Lin, F. L.; Hoyt, H. M.; van Halbeek, H.; Bergman, R. G.; Bertozzi, C. R. Mechanistic Investigation of the Staudinger Ligation. *Journal of the American Chemical Society* **2005**, *127* (8), 2686-2695.

10. Carrico, I. S. Chemoselective modification of proteins: hitting the target. *Chemical Society Reviews* **2008**, *37* (7), 1423-1431.

11. Arumugam, S.; Popik, V. V. Sequential "Click" – "Photo-Click" Cross-Linker for Catalyst-Free Ligation of Azide-Tagged Substrates. *The Journal of Organic Chemistry* **2014**, *79* (6), 2702-2708.

12. van Dongen, S. F. M.; Teeuwen, R. L. M.; Nallani, M.; van Berkel, S. S.; Cornelissen, J. J. L. M.; Nolte, R. J. M.; van Hest, J. C. M. Single-Step Azide Introduction in Proteins via an Aqueous Diazo Transfer. *Bioconjugate Chemistry* **2009**, *20* (1), 20-23.

13. Kiick, K. L.; Saxon, E.; Tirrell, D. A.; Bertozzi, C. R. Incorporation of azides into recombinant proteins for chemoselective modification by the Staudinger ligation. *Proceedings of the National Academy of Sciences* **2002**, *99* (1), 19.

14. Prescher, J. A.; Dube, D. H.; Bertozzi, C. R. Chemical remodelling of cell surfaces in living animals. *Nature* **2004**, *430* (7002), 873-877.

15. Rostovtsev, V. V.; Green, L. G.; Fokin, V. V.; Sharpless, K. B. A stepwise huisgen cycloaddition process: copper (I)-catalyzed regioselective "ligation" of azides and terminal alkynes. *Angewandte Chemie* **2002**, *41* (14), 2596-2599.

16. Wittig, G.; Krebs, A. On the existence of low-membered cycloalkynes. I. *Chemische Berichte* **1961**, *94*, 3260-3275.

17. Agard, N. J.; Prescher, J. A.; Bertozzi, C. R. A Strain-Promoted [3 + 2] Azide−Alkyne Cycloaddition for Covalent Modification of Biomolecules in Living Systems. *Journal of the American Chemical Society* **2004**, *126* (46), 15046-15047.

18. Ess, D. H.; Jones, G. O.; Houk, K. N. Transition States of Strain-Promoted Metal-Free Click Chemistry: 1,3-Dipolar Cycloadditions of Phenyl Azide and Cyclooctynes. *Organic Letters* **2008**, *10* (8), 1633-1636.

19. Baskin, J. M.; Prescher, J. A.; Laughlin, S. T.; Agard, N. J.; Chang, P. V.; Miller, I. A.; Lo, A.; Codelli, J. A.; Bertozzi, C. R. Copper-free click chemistry for dynamic *in vivo* imaging. *Proceedings of the National Academy of Sciences* **2007**, *104* (43), 16793.

20. Ning, X.; Guo, J.; Wolfert, M. A.; Boons, G.-J. Visualizing Metabolically Labeled Glycoconjugates of Living Cells by Copper-Free and Fast Huisgen Cycloadditions. *Angewandte Chemie International Edition* **2008**, *47* (12), 2253-2255.

21. Debets, M. F.; van Berkel, S. S.; Schoffelen, S.; Rutjes, F. P. J. T.; van Hest, J. C. M.; van Delft, F. L. Aza-dibenzocyclooctynes for fast and efficient enzyme PEGylation via copper-free (3+2) cycloaddition. *Chemical Communications* **2010**, *46* (1), 97-99.

22. Kuzmin, A.; Poloukhtine, A.; Wolfert, M. A.; Popik, V. V. Surface Functionalization Using Catalyst-Free Azide−Alkyne Cycloaddition. *Bioconjugate Chemistry* **2010**, *21* (11), 2076-2085.

23. Orski, S. V.; Sheppard, G. R.; Arumugam, S.; Arnold, R. M.; Popik, V. V.; Locklin, J. Rate Determination of Azide Click Reactions onto Alkyne Polymer Brush Scaffolds: A Comparison of Conventional and Catalyst-Free Cycloadditions for Tunable Surface Modification. *Langmuir* **2012**, *28* (41), 14693-14702.

24. Dommerholt, J.; Schmidt, S.; Temming, R.; Hendriks, L. J. A.; Rutjes, F. P. J. T.; van Hest, J. C. M.; Lefeber, D. J.; Friedl, P.; van Delft, F. L. Readily Accessible Bicyclononynes for

Bioorthogonal Labeling and Three-Dimensional Imaging of Living Cells. *Angewandte Chemie International Edition* **2010**, *49* (49), 9422-9425.

25. van Geel, R.; Pruijn, G. J. M.; van Delft, F. L.; Boelens, W. C. Preventing Thiol-Yne Addition Improves the Specificity of Strain-Promoted Azide–Alkyne Cycloaddition. *Bioconjugate Chemistry* **2012**, *23* (3), 392-398.

26. Jewett, J. C.; Sletten, E. M.; Bertozzi, C. R. Rapid Cu-Free Click Chemistry with Readily Synthesized Biarylazacyclooctynones. *Journal of the American Chemical Society* **2010**, *132* (11), 3688-3690.

27. Knall, A.-C.; Slugovc, C. Inverse electron demand Diels-Alder (iEDDA)-initiated conjugation: a (high) potential click chemistry scheme. *Chemical Society reviews* **2013**, *42 12*, 5131-5142.

28. Karver, M. R.; Weissleder, R.; Hilderbrand, S. A. Synthesis and Evaluation of a Series of 1,2,4,5-Tetrazines for Bioorthogonal Conjugation. *Bioconjugate Chemistry* **2011**, *22* (11), 2263-2270.

29. Sauer, J.; Heldmann, D. K.; Hetzenegger, J.; Krauthan, J.; Sichert, H.; Schuster, J. 1,2,4,5-Tetrazine: Synthesis and Reactivity in [4+2] Cycloadditions. *European Journal of Organic Chemistry* **1998**, *1998* (12), 2885-2896.

30. Blackman, M. L.; Royzen, M.; Fox, J. M. Tetrazine Ligation: Fast Bioconjugation Based on Inverse-Electron-Demand Diels−Alder Reactivity. *Journal of the American Chemical Society* **2008**, *130* (41), 13518-13519.

31. Chen, W.; Wang, D.; Dai, C.; Hamelberg, D.; Wang, B. Clicking 1,2,4,5-tetrazine and cyclooctynes with tunable reaction rates. *Chemical Communications* **2012**, *48* (12), 1736-1738.

32. Karver, M. R.; Weissleder, R.; Hilderbrand, S. A. Bioorthogonal Reaction Pairs Enable Simultaneous, Selective, Multi-Target Imaging. *Angewandte Chemie International Edition* **2012**, *51* (4), 920-922.

33. Schoch, J.; Staudt, M.; Samanta, A.; Wiessler, M.; Jäschke, A. Site-Specific One-Pot Dual Labeling of DNA by Orthogonal Cycloaddition Chemistry. *Bioconjugate Chemistry* **2012**, *23* (7), 1382-1386.

34. Maggi, A.; Ruivo, E.; Fissers, J.; Vangestel, C.; Chatterjee, S.; Joossens, J.; Sobott, F.; Staelens, S.; Stroobants, S.; Van Der Veken, P.; wyffels, L.; Augustyns, K. Development of a novel antibody–tetrazine conjugate for bioorthogonal pretargeting. *Organic & Biomolecular Chemistry* **2016**, *14* (31), 7544-7551.

35. Rahim, M. K.; Kota, R.; Haun, J. B. Enhancing Reactivity for Bioorthogonal Pretargeting by Unmasking Antibody-Conjugated trans-Cyclooctenes. *Bioconjugate Chemistry* **2015**, *26* (2), 352-360.

CHAPTER 2

MONO-CYCLOPROPENONE CAGED DIBENZOCYCLOOCTYNE-TRIAZOLE (MC-DIBOT): A WATER SOLUBLE, PHOTOACTIVATABLE SPAAC REAGENT

2.1 Introduction

Our group has studied and developed a diverse array of strained cyclooctyne compounds that are amenable to SPAAC reactions. Some examples of these compounds that we have studied or are currently studying include BCN,[1] DIBO,[2] ADIBO,[3] and ODIBO.[4] In addition, we have also reported the synthesis of cyclopropenone-caged derivatives of DIBO, ADIBO, and ODIBO (Figure 2.1).[5] The cyclopropenone protecting group is photolabile, yielding carbon monoxide and acetylene.

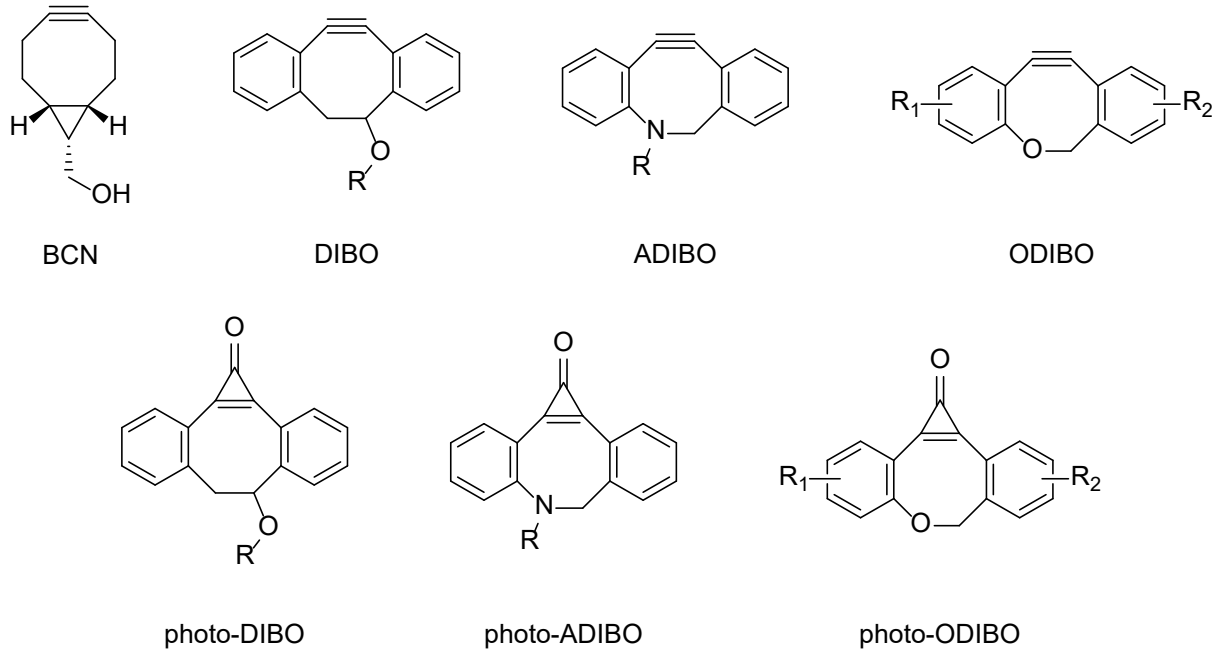

Figure 2.1 Cyclooctyne SPAAC reagents and cyclopropenone-caged SPAAC reagents

Most strained cycloalkynes contain only one alkyne functionality. This limits their potential use relative to a compound with multiple strained alkynes. A diyne species could be used as a crosslinking reagent that reacts readily with two different azide species, or two different azide functionalities on the same molecule. One such compound is dibenzocyclooctadiyne or DIBOD. This compound was first synthesized by Sondheimer in 1974 and is sometimes referred to as the Sondheimer diyne.[6] Since this initial discovery, the synthetic scheme has been improved (Scheme 2.1).[7]

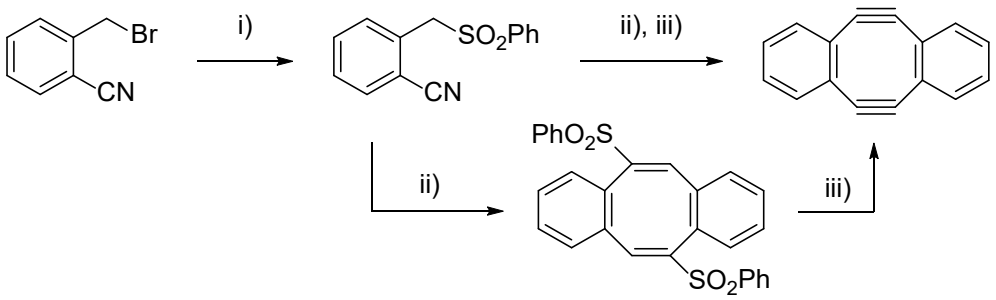

Scheme 2.1 Otera method for synthesis of DIBOD (2.5). Reagents and conditions: i) $NaSO_2Ph$, DMF, 80 °C, 2 h. ii) LiHMDS, $ClOP(OEt)_2$, THF, -78 °C, 30 min, rt, 1.5 h. iii) LDA, THF, -78 °C, 2 h.

Several publications have reported on this compound and its properties. Each of the strained alkynes of DIBOD are capable of performing a SPAAC reaction. All attempts to isolate a mono-triazole intermediate have been unsuccessful; the bis-triazole products and unreacted starting material were isolated due to the significant rate difference between the first and second SPAAC reaction.[8] The rate of the second SPAAC reaction has been reported to be 185 times faster than the first.[9] The reported value, however, may not be entirely accurate as the authors were not able to isolate the intermediate strained alkyne. Seeing that this was an indirect estimate of the rate, we wanted to isolate the second stained alkyne and observe its behavior and properties directly.

2.2 Synthesis

To achieve the goal of asymmetric alkyne protection, two methods were developed based on the Hu-Prakash procedure of protecting alkynes as gem-difluorinated cyclopropenes.[10] The first method involves complete protection of both alkyne moieties as difluorocyclopropenes (Scheme 2.2 A). This is followed by hydrolysis on wet silica gel to afford the cyclopropenones. After generating the cyclopropenones, selective deprotection by UV irradiation affords MC-DIBOD (Figure 2.2). The selective deprotection is possible due to the large difference in quantum yield for each decarbonylation. The quantum yield of photo-DIBOD is 0.05 when using 350 nm irradiation, while the quantum yield of MC-DIBOD is 0.006 when using 350 nm irradiation.

The second method involves synthetically generating the mono-cyclopropenone product directly by modifying the reaction conditions (Scheme 2.2 B). By using a reduced amount of sodium iodide and trifluoromethyl trimethyl silane, only one difluorocyclopropene is generated. Then, hydrolysis, as mentioned above, affords MC-DIBOD directly without a photochemical step. Each method has advantages and disadvantages. The selective photochemical deprotection method requires more time and materials, but often affords high yields of very pure product. The direct synthetic method requires less time and materials, but often affords lower yields of product and a multitude of byproducts.

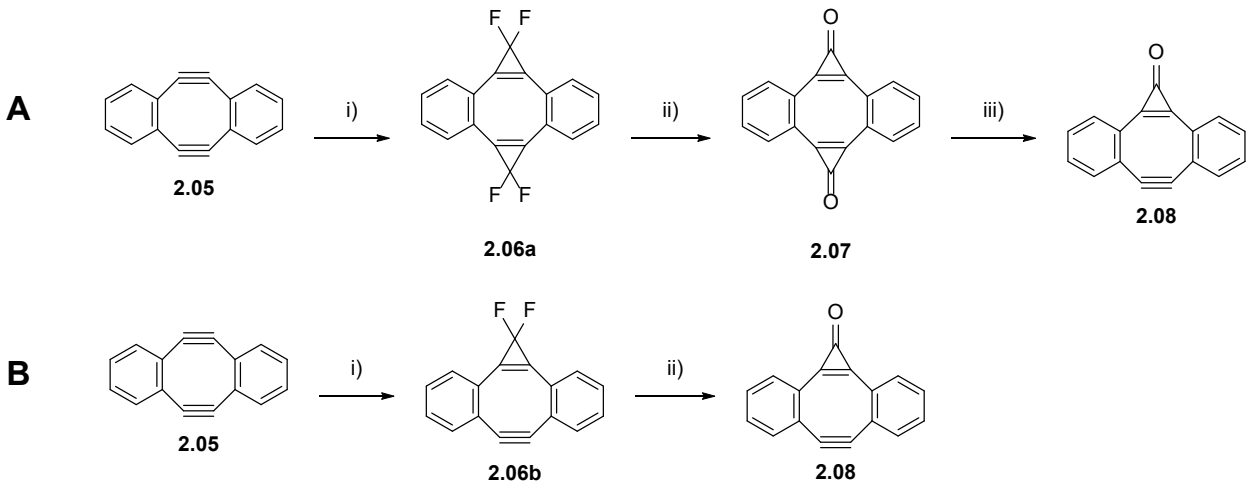

Scheme 2.2 Hu-Prakash method for cyclopropenone protection of DIBOD. Reagents and conditions: Pathway A: i) 4x NaI, 4.2x $TMSCF_3$, THF, 110 °C, 2 h. ii) wet silica gel, 1 d. iii) 350 nm, DCM (Φ_{350nm} = 0.05). Pathway B: i) 0.5x NaI, 0.5x $TMSCF_3$, THF, 110 °C, 2 h. ii) wet silica gel, 1 d.

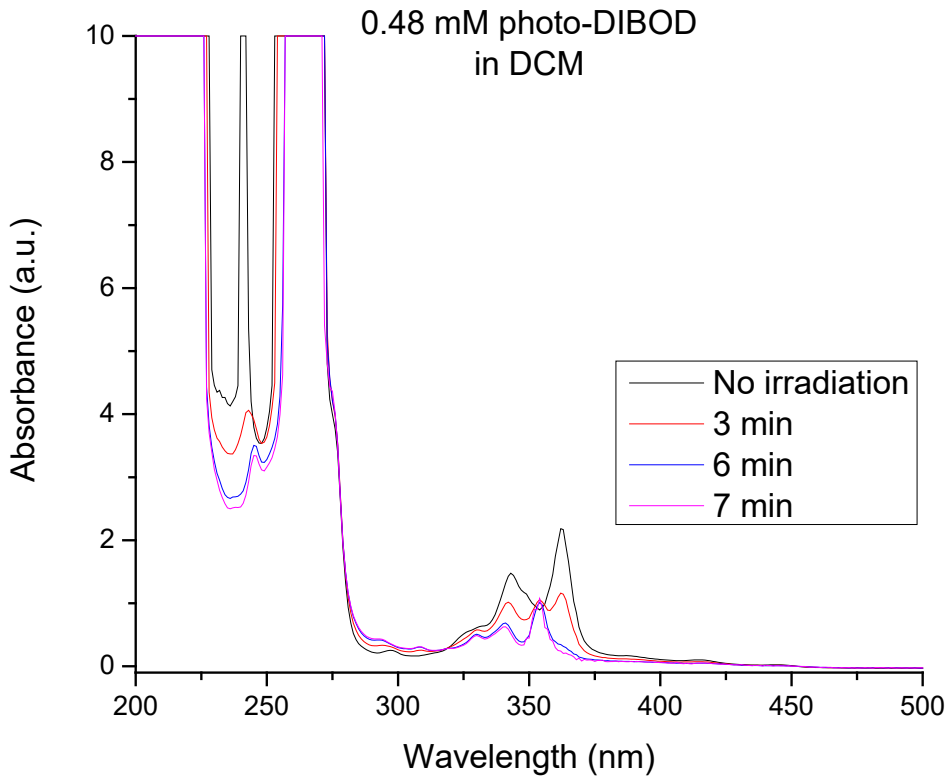

Figure 2.2 UV-Vis traces of the photochemical conversion of photo-DIBOD to MC-DIBOD. The hypsochromic shift in the absorbance maximum at 363 nm to 354 nm indicates the conversion.

With MC-DIBOD on hand, we could now do two things: Improve the aqueous solubility of the parent MC-DIBOD by clicking on a water-soluble azide linker and isolate the second strained alkyne and observe its reaction and decomposition rate. To do so, we incorporated an oligoethylene glycol side chain in the first SPAAC reaction on the exposed strained alkyne of MC-DIBOD. Fortunately, this modification worked as expected affording mono-cyclopropenone caged dibenzocyclooctyne triazole (MC-DIBOT) for further study. The cyclopropenone protecting group can be removed by irradiation with 300 nm light (Φ_{300nm} = 0.09). The product of this photo-irradiation step has been named dibenzocyclooctyne triazole (DIBOT).

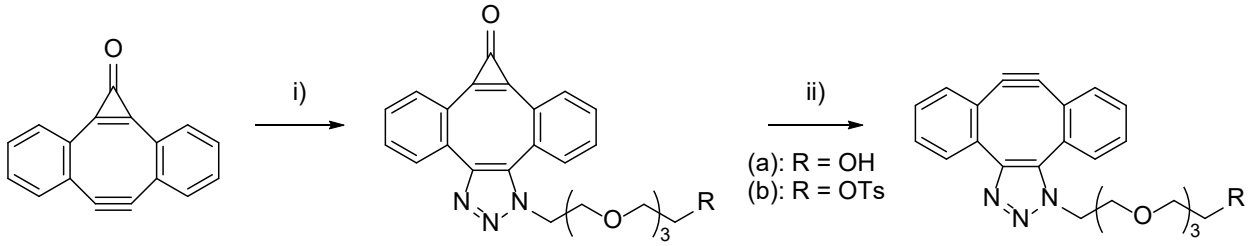

2.08 **2.09a** **2.09b** **2.10a** **2.10b**

Scheme 2.3 Synthesis of MC-DIBOT and DIBOT. Reagents and conditions: i) N_3-EG_4-R, DCM, rt, 6 h. ii) 300 nm, DCM (Φ_{300nm} = 0.09).

2.3 Chemical and Photochemical Properties of MC-DIBOT

Cyclopropenones have been shown to possess high thermal stability, requiring temperatures in excess of 130°C for decarbonylation to occur.[11] However, cyclopropenones are susceptible to addition reactions. Thus, proper care must be taken when storing these compounds, as storage in hydroxylic solvents, especially methanol, can lead to decomposition of the cyclopropenone moiety of MC-DIBOT. Additionally, even small amounts of base can cause hydrolysis of cyclopropenones to yield acrylic acid derivatives (Scheme 2.4). This is more likely to occur with diarylcyclopropenones than with dialkylcyclopropenones due to the stabilizing effect of aromatic groups on the carbanion transition state.

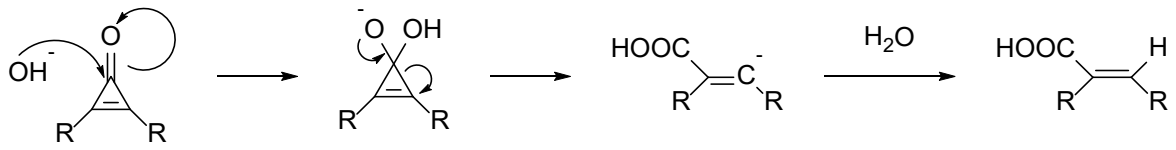

Scheme 2.4 Hydrolysis of cyclopropenones in basic conditions.

We investigated the stability of MC-DIBOT stored in methanol under ambient conditions in the dark using UV-Vis analysis (Table 2.1). The half-life of MC-DIBOT in methanol under these conditions was found to be approximately 15 days. We decided to also test the stability in two additional solvents: THF and 5% DMSO/phosphate buffer. In THF, the half-life was found to be longer than 15 days and in 5% DMSO/phosphate buffer, the half-life was found to be approximately 5 days. Analysis by mass spectrometry reveals that the most prominent decomposition products are those of methanolysis or hydrolysis, which correlates well with previously reported results.[11-12]

Solvent	Half-life (s)
THF	> 15 days
Methanol	14.6 ± 2.4 days
5% DMSO/Phosphate buffer (pH = 7.4)	5.3 ± 0.3 days

Table 2.1 Half-lives of MC-DIBOT in three solvents. Data were acquired by UV-Vis.

Additionally, we probed the electrophilicity of the cyclopropenone of MC-DIBOT by incubation with cysteamine. Originally, we hoped to investigate the competition between thiol addition and SPAAC on the acetylene of DIBOT. However, due to the relatively short half-life of DIBOT, we attempted to add the cysteamine and azide mixture to MC-DIBOT and then irradiate the samples. Unfortunately, this revealed the highly electrophilic nature of the cyclopropenone of MC-DIBOT as a new byproduct was formed within minutes of adding the cysteamine and azide

mixture. Mass spectrometry analysis reveals that the byproduct is the addition product of cysteamine on MC-DIBOT.

MC-DIBOT possesses two absorbance bands: a medium intensity broad band at 310 nm (ε = 6400 ± 100 $M^{-1}cm^{-1}$), and a high intensity sharp band at 239 nm (ε = 32300 ± 800 $M^{-1}cm^{-1}$). Upon irradiation with 300 nm light, the band at 310 nm is bleached and a new high intensity sharp band arises at 263 nm (Figure 2.3). These results agree with prior work on other compounds similar to MC-DIBOT. Irradiation with 350 nm and 420 nm light also bleaches the band at 310 nm, however the irradiation time required for conversion to the product is significantly increased.

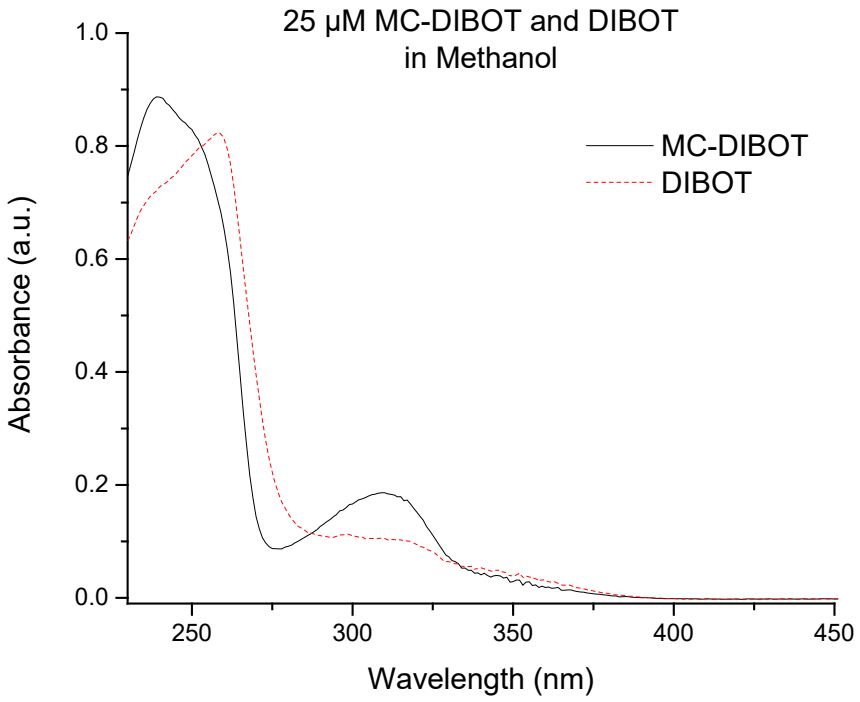

Figure 2.3 UV-Vis traces of a 25 μM sample of MC-DIBOT in methanol before (solid, black) and after (dashed, red) irradiation (300 nm, 30 seconds). ε_{310nm} = 6400 ± 100 $M^{-1}cm^{-1}$ and ε_{239nm} = 32300 ± 800 $M^{-1}cm^{-1}$.

What distinguishes MC-DIBOT from previously synthesized MC-DIBOT-like compounds is the incorporation of the tetraethylene glycol (TEG) tail. Incorporation of TEG significantly

increases the overall water solubility of MC-DIBOT, making it soluble in aqueous solutions up to millimolar concentrations. This increase in aqueous solubility allowed us to examine the SPAAC reaction rate in aqueous-organic solutions.

2.4 SPAAC Reactions with DIBOT

DIBOT is capable of undergoing SPAAC reactions with organic azides. To analyze the SPAAC reaction kinetics of this compound, we chose to use the same azide that was clicked onto the first acetylene moiety due to its water solubility. Additionally, we monitored the kinetics of the reaction in a variety of organic solvents and in two aqueous-organic solvent mixtures.

2.4.1 SPAAC Reaction with DIBOT in Organic Solvents

The SPAAC reaction between DIBOT and TEG-azide was performed in three different organic solvents: methanol, tetrahydrofuran, and acetonitrile. This reaction was found to be second-order and the kinetic evaluation was performed under pseudo first-order conditions using a minimum 10-fold excess of azide. The rate equation for a second order process is given by equation 2.1:

$$\text{Rate} = k_2[\text{A}][\text{B}] \qquad \text{(Eq 2.1)}$$

If we have a large excess of one reagent over the other, in this case reagent B, the change in concentration of the excess reagent is insignificant relative to the limiting reagent. Thus, we can define the observed rate constant (k_{obs}) as follows:

$$k_{\text{obs}} = k_2[\text{B}] \qquad \text{(Eq 2.2)}$$

Applying the observed rate constant into equation 2.1, we obtain a rate equation that is first-order:

$$\text{Rate} = k_{\text{obs}}[\text{A}] \qquad \text{(Eq 2.3)}$$

The integrated rate law for a first-order reaction gives an exponential function:

$$[\text{A}] = [\text{A}]_0 e^{(-k_{\text{obs}} * \text{t})} \qquad \text{(Eq 2.4)}$$

Solving the integrated rate law for k_{obs} and plotting k_{obs} vs [B] gives k_2 for the SPAAC reaction (Appendix C).

Spectroscopic measurement of the change in DIBOT concentration was performed by observing the disappearance of the band at 263 nm in all cases. The observed rate constants were then plotted against the concentration of excess TEG-azide and were fit to a linear regression. The slope of the line generated by this fitting is the second-order rate constant for the SPAAC reaction of DIBOT with TEG-azide. The data are summarized below (Table 2.2). These second-order rate constants for SPAAC reaction represent the fastest SPAAC reactions between dibenzocycloocytne and azide in organic solvents reported to date.

Solvent	k_2 (M^{-1} s^{-1})
THF	17 ± 1
Acetonitrile	30 ± 1
Methanol	55 ± 2

Table 2.2 Second-order rate constant of SPAAC reaction between DIBOT and TEG-azide in three organic solvents.

2.4.2 SPAAC Reaction with DIBOT in Aqueous-Organic Solvent Mixtures

After analyzing the kinetics of the SPAAC reaction in organic solvents, we turned our attention to the SPAAC reaction in aqueous-organic solvent mixtures. Numerous experimenters have observed a 1,3-dipolar cycloaddition rate enhancement when the reaction is performed in water.[4, 13-15] However, the cause of this observed rate enhancement has not been thoroughly established or exhaustively evaluated. Burke and Breslow attribute the rate enhancement to a combination of three components: 1) the hydrophobic effect, 2) increased polarity of the transition state in aqueous solutions and 3) hydrogen-bonding effects in the transition state. Our goal, in performing these experiments, was to corroborate previous observations and provide a scaffold for further evaluation of the rate enhancement effect.

The kinetic analysis was performed in the same way as described in section 2.4.1. However, instead of changing the excess concentration of azide, the amount of water in the solvent mixture was adjusted with each sample. To accurately observe the reaction as it progressed, a modification of our existing instrumentation had to be done. In short, we attached an LED (300 nm) perpendicular to the observation beam of our Cary 60 UV-Vis spectrophotometer so that we could simultaneously irradiate and observe the UV spectrum of the sample. Using this setup, we were able to observe the reaction in methanol-water and THF-water mixtures with water contents ranging from 0-70% or 0-90% for methanol and THF respectively. The second-order rate constants were determined by dividing the observed rate constants by the concentration of TEG-azide. Then, the second-order rate constants were plotted against the concentration of water in each sample. In doing so, we observed an exponential growth in the second-order rate constant as the concentration of water increased. Upon observing this trend, we looked to compare the Gibbs energy of activation to the dielectric constant of the solvent mixture. The trend that we observed when looking at these values fit well to a linear model. Using this linear model, we could extrapolate the Gibbs energy of activation at the dielectric constant of water (Table 2.3, Appendix C). In doing so, we found that the second-order rate constant for the SPAAC reaction in neat water is nearly 10-fold higher than in the organic solvents tested. The terminal functionality on the TEG linker did not seem to have any impact on the extrapolated rate constant.

Compound	Organic solvent	Maximum water content (%)	Extrapolated k_2 in neat H_2O (M^{-1} s^{-1})
DIBOT-OH	THF	90	375 ± 29
DIBOT-OH	Methanol	70	561 ± 180
DIBOT-OTs	THF	90	434 ± 43
DIBOT-OTs	Methanol	80	487 ± 74

Table 2.3 DIBOT aqueous-organic SPAAC kinetics data

2.4.3 Protein Labeling Experiment

To illustrate the applicability of DIBOT as an extraordinarily fast-reacting cyclooctyne for bioorthogonal labeling, we chose to perform a model protein-labeling assay using BSA and fluorescein-azide. In this experiment, BSA-azide was prepared and incubated with MC-DIBOD to install the MC-DIBOT functional handle (Scheme 2.5). Next, the MC-DIBOT-BSA conjugate was incubated with an equimolar amount of fluorescein-azide. Control samples were prepared either without fluorescein-azide, or with fluorescein-azide incubated in the dark. The remaining samples were irradiated with 300 nm light for 2-10 minutes.

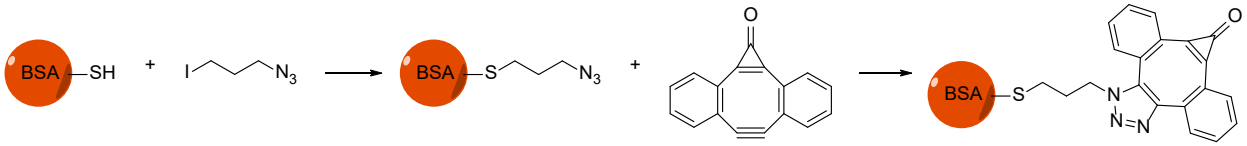

Scheme 2.5 Preparation of MC-DIBOT-BSA.

All samples were immediately denatured and transferred to SDS-PAGE gel. After running the gel, it was observed that all samples containing fluorescein-azide were labeled by the fluorescein. There was also another relatively large component of the samples (~17 kDa) that was also strongly fluorescent. The gel was then stained with Coomassie blue. Oddly, the anomalous compound was not stained by the Coomassie blue, only the BSA conjugates were stained. This experiment could be repeated with purification steps along the way to prevent unusual observations.

2.5 Modular Construction of PET Agents Using MC-DIBOD

In collaboration with the lab of Dr. Zibo Li at UNC Chapel Hill, we have demonstrated the utility of MC-DIBOD for a modular click chemistry approach to constructing PET (positron emission tomography) agents containing ^{18}F.[16] ^{18}F is one of the most used isotopes from radiolabeling due to its relatively long half-life (110 minutes) and low positron energy.

Currently, there are challenges facing the introduction of ^{18}F into bioorthogonal probes, limiting their *in vivo* efficiency. The synthetic methods for rapid introduction ^{18}F into organic compounds can require harsh conditions. Also, while SPAAC reagents with one cycloalkyne functionality have been used for PET imaging, one of the prosthetic groups must be covalently bound to the SPAAC reagent by other methods. This presents a challenge in the clinical setting where technicians may not be skilled in organic synthesis methods. Lastly, the PET agents can have variable biodistribution profiles and low stability in *in vivo* conditions.

Using a modular approach with MC-DIBOD overcomes most of the aforementioned challenges (Figure 2.4). First, SPAAC reactions require no catalysts and proceed under mild conditions. Also, the unique design of MC-DIBOD (one exposed acetylene moiety and one photo-caged acetylene) allows for more varied ^{18}F and targeting ligand synthon design as neither the ^{18}F nor targeting ligand synthon must be covalently bound to the core MC-DIBOD by other methods. Therefore, synthons can be designed to be lipophilic or hydrophilic prior to cross-coupling. The cyclopropenone protecting group also allows for sequential addition of synthons. In addition, the significant rate enhancement of the second acetylene moiety relative to the first leads to very rapid formation of the cross-coupled final product. Lastly, the bis-triazole products are very stable in biological conditions.

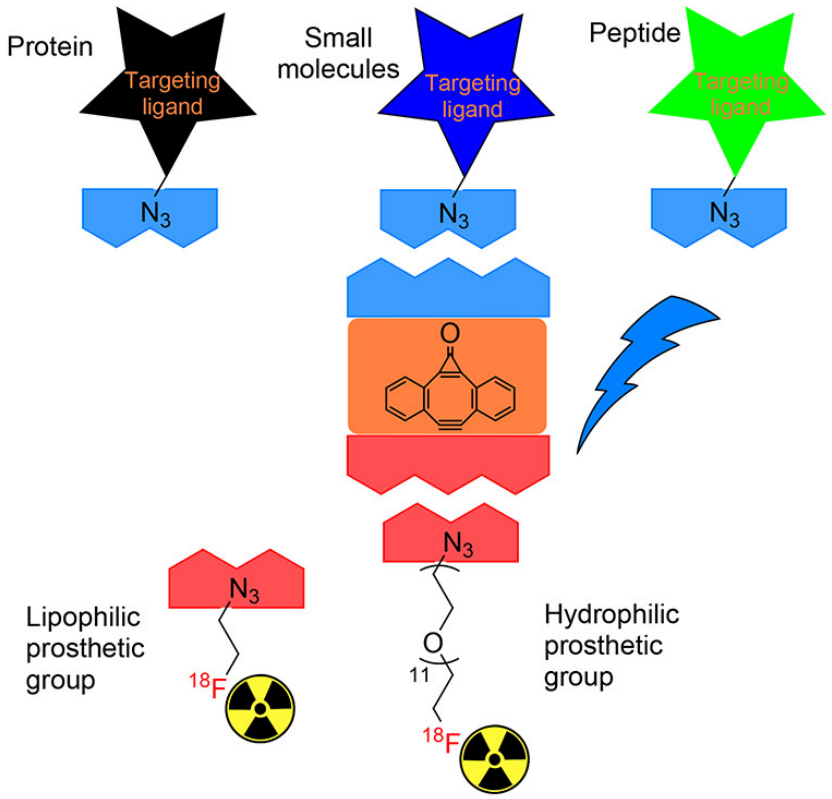

Figure 2.4 Modular approach to PET labeling using MC-DIBOD. First, the prosthetic group is covalently bound to MC-DIBOD by SPAAC. Then, irradiation of the MC-DIBOT-^{18}F unveils the second cycloalkyne moiety which reacts with azide-functionalized targeting ligands.

Two synthetic routes were evaluated: (A) SPAAC with ligand synthon first and (B) SPAAC with ^{18}F synthon first (Figure 2.5). It was found that route B is more efficient than route A. From here, a small library of azide-containing targeting ligands were coupled to either a lipophilic or hydrophilic ^{18}F-azido synthons. These cross-coupled PET tracers were then tested in animal models (mice). The i*n vivo* study demonstrated the advantage of the ability to modify the lipophilicity and hydrophilicity of the prosthetic groups as the absolute tumor uptake was greater in the lipophilic tracer than the hydrophilic tracer. MC-DIBOT-^{18}F was also tested for its ability to rapidly label protein (HSA). The DIBOT-^{18}F was capable of labeling even low concentrations of HSA, demonstrating the feasibility of this approach for low concentration cross-couplings.

a) Route A inefficient for the second click-coupling

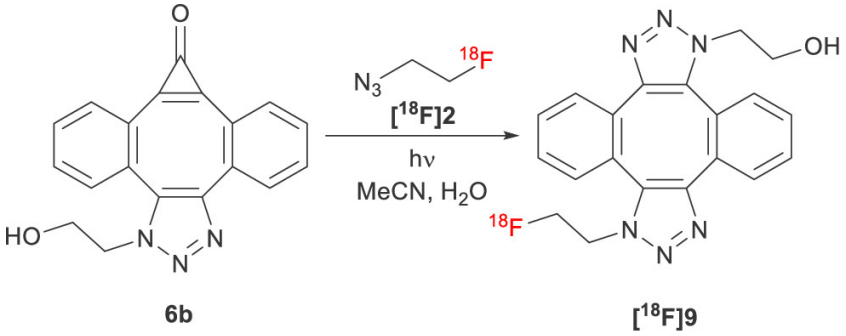

6b Concentration (mM)	Conversion[a,b]
0.32	26%
0.63	46%
1.27	58%
3.17	92%

b) Route B offers higher efficiency for the second click-coupling

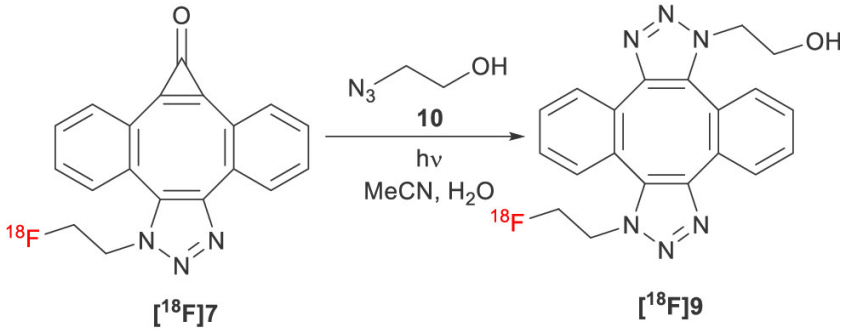

Azide **10** Concentration (μM)	RCY[a,c]
6	21%
60	60%
600	84%

Figure 2.5 Comparison of synthetic routes A and B for MC-DIBOT PET tracers. Route A requires a high concentration of MC-DIBOT to afford reasonable yields of bis-triazole products. Route B achieves moderate yields with much lower concentrations than route A.

In summary, MC-DIBOD is an effective linchpin for the modular construction of PET agents. The sequential SPAAC steps allow more variability in synthon design. In addition, decarbonylation of the MC-DIBOT intermediates can be achieved with 350-420 nm irradiation in as little as 10 minutes. Both *ex vivo* and *in vivo* experiments also provide evidence for the applicability of this method.

2.6 IEDDA Reactions with DIBOT

We have also found that DIBOT can undergo the IEDDA reaction with 3,6-bipyridyl-1,2,4,5-tetrazine under ambient conditions. Kinetic measurements of the reaction have been performed in dichloromethane and methanol. These measurements were performed under pseudo first-order conditions using the tetrazine as the excess reagent. The tetrazine possess a very intense absorbance band at 295 nm and a weaker band at 540 nm (Figure 2.6). Due to the overwhelming intensity of the 295 nm band, and the significant overlap with the cyclopropenone band (310 nm), we decided to monitor the change of the weaker 540 nm band. The rate constant of the IEDDA reaction for this system was found to be 11 ± 1 M^{-1} s^{-1} and 56 ± 3 M^{-1} s^{-1} in DCM and methanol respectively (Appendix C). Attempts to monitor the reaction in aqueous-organic solvent mixtures are currently underway.

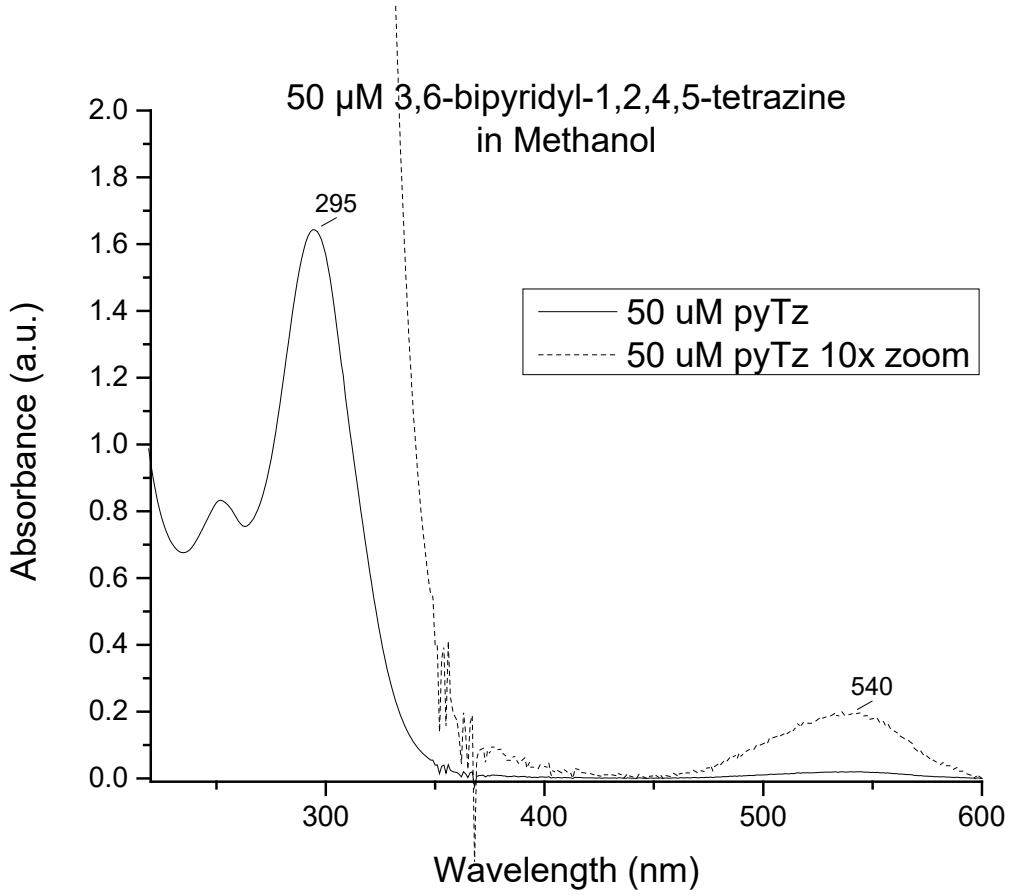

Figure 2.6 UV-Vis spectrum of a 50 µM sample of 3,6-bipyridyl-1,2,4,5-tetrazine in methanol showing the absorbance bands at 295 nm (solid trace) and 540 nm (dashed trace).

2.7 Bis-DIBOT for Ultrafast Cross-Couplings

Several publications have reported the use of two dibenzocyclooctynes linked by a polymer or oligomer chain that can act as a crosslinker between two azides.[17-18] However, these examples use unprotected strained alkyne reagents that react at a slower rate than DIBOT and the crosslinking density cannot be controlled very easily. Thus, we developed a crosslinker based on MC-DIBOT. By clicking two molecules of MC-DIBOD onto bis-azido-TEG, we have synthesized bis-MC-DIBOT (Scheme 2.6). Upon irradiation with 300 nm light, this molecule undergoes decarbonylation in the same way as MC-DIBOT, to give bis-DIBOT. So far, we have only

analyzed its reaction with bis-azido-TEG (Mass spectra, Appendix B; kinetics data, Appendix C). However, this preliminary experiment shows that the bis-DIBOT prefers to form a cyclic product in the presence of bis-azido-TEG regardless of reagent ratio (Scheme 2.7). If used in a polymer that is decorated with multiple azide substituents, we anticipate rapid and controllable cross-linking can be achieved.

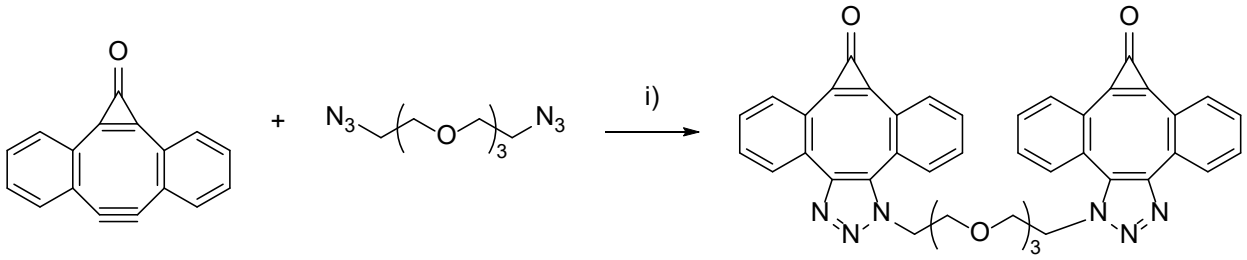

Scheme 2.6 Synthesis of bis-MC-DIBOT. Reagents and conditions: i) DCM, rt, 16 h.

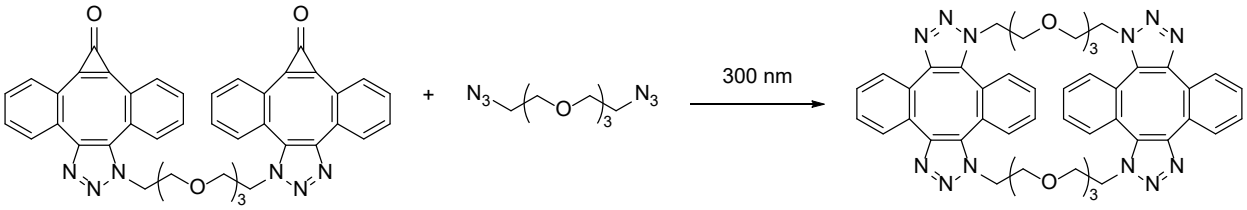

Scheme 2.7 Photochemical generation of bis-DIBOT leading to macrocyclic product. Irradiation of bis-MC-DIBOT with 300 nm light leads to bis-DIBOT which reacts with bis-azido-TEG.

2.8 Summary

We have synthesized a water soluble cyclopropenone-caged dibenzocyclooctyne derivative (MC-DIBOT) that can be photochemically decarbonylated to reveal the acetylene moiety (DIBOT). The SPAAC reaction of TEG-azide with DIBOT represents the fastest reported SPAAC reaction of its type reported to date. Additionally, owing to the enhanced water solubility of DIBOT, we have analyzed the SPAAC reaction in various aqueous-organic solvent systems. Extrapolation of the data indicates that the SPAAC reaction is enhanced 10-fold in neat water relative to the rate in organic solvents. Also, we have investigated the IEDDA reaction of DIBOT

with 3,6-bipyridyl-1,2,4,5-tetrazine and found that it proceeds with a rate comparable to the SPAAC reaction. Finally, we synthesized a bis-MC-DIBOT derivative that could be used as a photo-activatable crosslinker for azide decorated polymers.

2.9 Future Directions

Current interests with MC-DIBOT involve modification of the terminal hydroxy group of the TEG tail. For example, substitution with a tertiary or quaternary amine could further enhance the water solubility of the compound allowing for more accurate rate measurements in neat water. Other possible end groups include biotin (Western Blot), fluorescent probes, or polarizable functionalities. As mentioned previously, bis-DIBOT could be used as a crosslinker for the rapid formation of hydrogels or other highly crosslinked materials. Additionally, we could investigate the potential use of MC-DIBOT as an electrophilic warhead for drug delivery. Further, DIBOT could be used to decorate material surfaces that are coated with azide moieties. We hope to continue exploring the vast array of possible uses for the MC-DIBOT and DIBOT family of compounds, as this list merely scratches the surface.

2.10 Experimental Procedures

All solvents used for reactions were purified and dried using an MBRAUN SPS-5 solvent purification system. All reagents were purchased from Sigma Aldrich, VWR, or Fischer Scientific and used as received unless otherwise noted. Flash chromatography was performed using 40-63 μm silica gel. Electronic spectra and kinetics data for samples in organic solvents were collected using a Cary 300 Bio UV-Vis spectrophotometer. Kinetics data for samples in aqueous-organic solvent mixtures were recorded using a Cary 60 UV-Vis spectrophotometer equipped with a 300 nm LED diode array. Photolyses of samples were conducted using a Rayonet photoreactor

equipped with sixteen 4W 300, 350, or 420 nm fluorescent lamps. All NMR spectra were recorded on a 400 MHz Bruker Ascend^{TM} 400 spectrometer using deuterochloroform or DMSO-d_6.

Synthetic Procedures

DIBOD (**2.05**) was prepared according to the Otera protocol.[7] Photo-DIBOD (**2.07**) was prepared according to the Popik protocol.[19] TEG-azide[20], TEG-azide-tosylate[21], and bis-azido-TEG[22] were prepared according to previously reported procedures. BSA-azide[12] was prepared according to previously reported procedures.

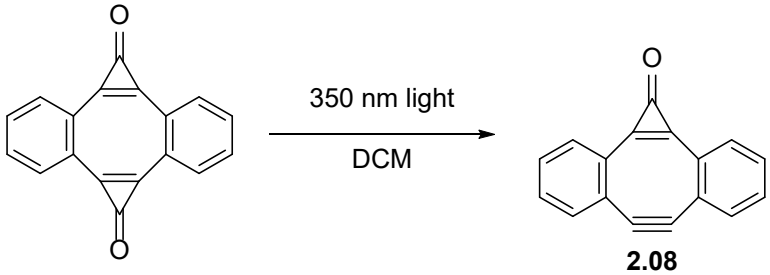

2.07 **2.08**

6,7-Dehydrodibenzo[*a*,*e*]cyclopropa[*c*][8]annulen-1-one (2.08). Photochemical method: 2.07 (54 mg, 0.210 mmol) was dissolved in DCM (1 L). The mixture was irradiated with 16x12" 350 nm wavelength lamps in a Rayonet reactor. The disappearance of the absorption band at 361 nm was followed by taking samples after 2, 3, and 4 minutes. The crude product mixture was then concentrated by solvent removal under vacuum and purified by flash chromatography (20% acetone/hexanes) to give 48 mg (quant.) of the product as a yellow solid. ^{1}H NMR: 7.59 – 7.51 (m, 2H), 7.20 (m, 4H), 6.94 – 6.86 (m, 2H). ^{13}C NMR: 150.83, 135.34, 133.83, 132.29, 130.23, 127.35, 125.33, 106.94.

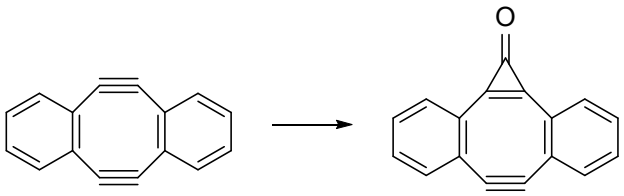

2.05 **2.08**

Direct synthesis of 2.08: 2.05 (400 mg, 0.80 mmol) was dissolved in THF (20 mL) in a pressure vessel. Next, NaI (144 mg, 0.96 mmol) was added and the mixture was degassed. Then, $TMSCF_3$ (0.118 mL, 0.80 mmol) was added and the mixture was heated to 110 °C for 2 hours. After this time, the reaction was quenched with saturate sodium bicarbonate. The crude product was extracted with DCM and washed with water and brine. The organic extracts were dried over anhydrous K_2CO_3 and the solvent was removed under vacuum. The crude difluorocyclopropene intermediate was then hydrolyzed on a wet silica gel column (1% H_2O, 50% DMC/hexanes) for 24 hours. The product was eluted with 20% acetone/hexanes to give 40 mg (22%) of the product as a bright yellow solid. ^{1}H NMR: 7.59 – 7.51 (m, 2H), 7.20 (m, 4H), 6.94 – 6.86 (m, 2H). ^{13}C NMR: 150.83, 135.34, 133.83, 132.29, 130.23, 127.35, 125.33, 106.94.

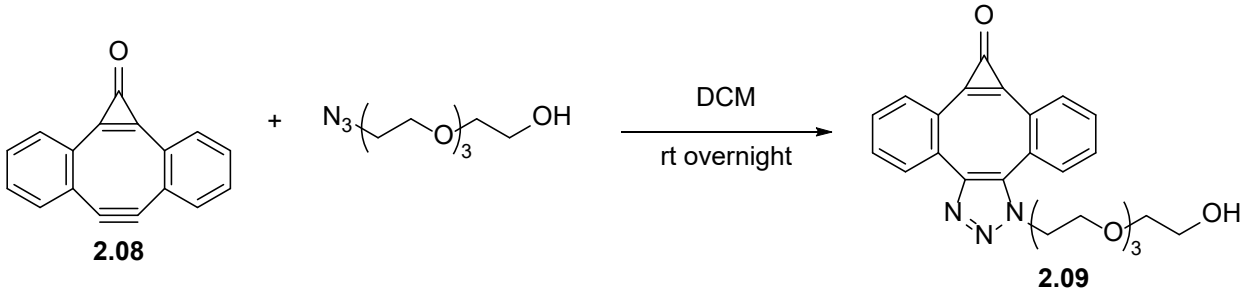

2.08 **2.09**

1-(2-(2-(2-(2-hydroxyethoxy)ethoxy)ethoxy)ethyl)dibenzo[3,4:7,8]cyclopropa[5,6]cycloocta [1,2-*d*][1,2,3]triazol-8(1*H*)-one (2.9). 2.8 (84 mg, 0.37 mmol) was dissolved in DCM (20 mL). Then, 11-azido-3,6,9-trioxaundecan-1-ol (161 mg, 0.74 mmol) was added. The mixture was stirred at room temperature overnight. The crude product mixture was concentrated and purified via chromatography (1% MeOH/DCM – 5% MeOH/DCM) to give 163 mg (98%) of the product as

an amorphous amber solid. ^{1}H NMR: 7.89 (dd, J = 7.8, 1.2 Hz, 1H), 7.72 (dd, J = 7.9, 1.3 Hz, 1H), 7.68 – 7.52 (m, 5H), 7.47 (td, J = 7.6, 1.3 Hz, 1H), 4.47 (ddd, J = 14.1, 6.6, 4.4 Hz, 1H), 4.31 (ddd, J = 14.1, 6.2, 4.3 Hz, 1H), 3.96 (ddd, J = 10.7, 6.6, 4.3 Hz, 1H), 3.87 (ddd, J = 10.4, 6.2, 4.4 Hz, 1H), 3.74 – 3.44 (m, 15H). ^{13}C NMR: 157.21, 154.45, 152.07, 142.69, 133.88, 133.75, 133.09, 132.36 (2C), 132.15, 131.53, 131.32, 130.48, 129.36, 128.64, 126.93, 124.43, 72.56, 70.62, 70.60, 70.38, 70.24, 69.47, 61.64, 48.90. ESI HRMS cald. $[M+H]^+$: $C_{25}H_{26}N_3O_5^+$ 448.1867, found: 448.1871.

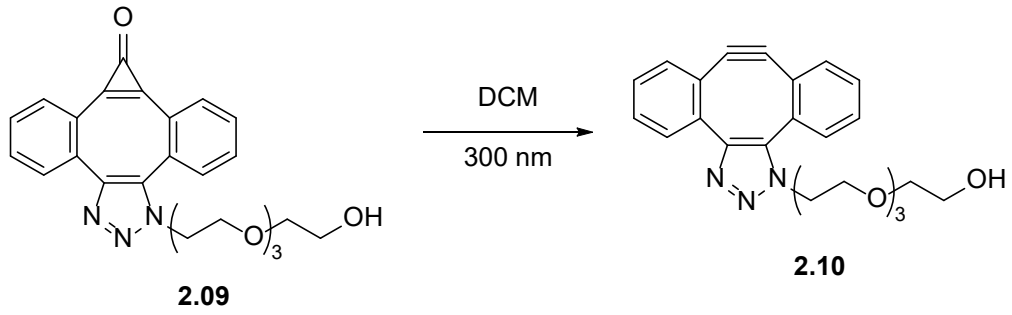

2.09 **2.10**

2-(2-(2-(2-(8,9-dehydro-1*H*-dibenzo[3,4:7,8]cycloocta[1,2-d][1,2,3]triazol-1-yl)ethoxy) ethoxy)ethoxy)ethan-1-ol (2.10). An amount of **2.09** dissolved in a suitable solvent is irradiated with 300 nm light. The amount of irradiation time is dependent on the starting amount of **2.09**. In dilute solutions, **2.10** is observed as the photolysis product (3 min $\leq t_{1/2} \leq$ 1.5 hours). UV-Vis: λ_{max} = 264 nm (ε = 32900 ± 500 $M^{-1}cm^{-1}$). ESI HRMS cald. $[M+H]^+$: $C_{24}H_{26}N_3O_4^+$ 420.1918, found: 420.1920.

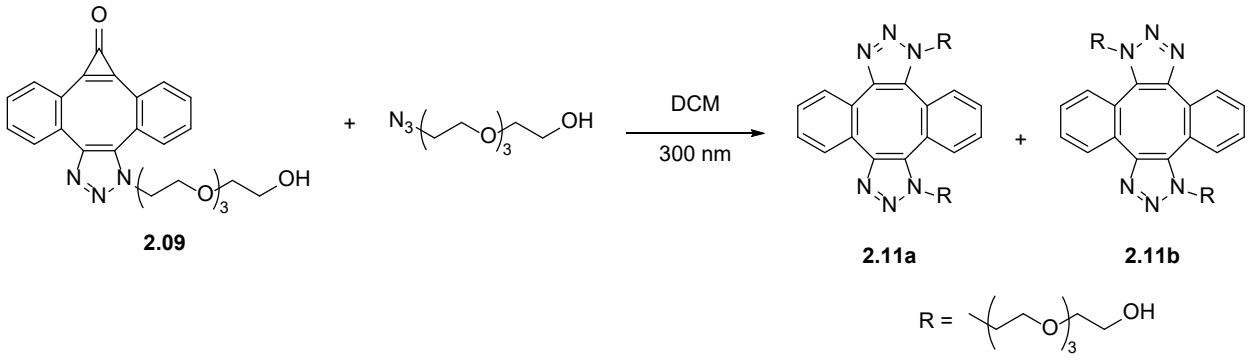

2,2'-((((((dibenzo[3,4:7,8]cycloocta[1,2-d:5,6-d']bis([1,2,3]triazole)-1,10-diylbis(ethane-2,1-diyl))bis(oxy))bis(ethane-2,1-diyl))bis(oxy))bis(ethane-2,1-diyl))bis(oxy))bis(ethan-1-ol) and **2,2'-((((((dibenzo[3,4:7,8]cycloocta[1,2-d:5,6-d']bis([1,2,3]triazole)-1,8-diylbis(ethane-2,1-diyl))bis(oxy))bis(ethane-2,1-diyl))bis(oxy))bis(ethane-2,1-diyl))bis(oxy))bis(ethan-1-ol) (2.11a and 2.11b).** *From MC-DIBOT*: **2.09** (158.4 mg, 0.354 mmol) and TEG-azide (155.2 mg, 0.708 mmol) were dissolved together in DCM (1 L). The flask was placed in the large Rayonet photoreactor (15 lamps, 300 nm) with a stir plate inside. The reaction mixture was irradiated for 25 minutes with 300 nm light and the product formation was checked by TLC. After sufficient decarbonylation/product formation, the solvent was removed under vacuum and the crude product was purified by chromatography (DCM – 10% MeOH/DCM) to give 188.8 mg (84%) of the final product as a yellow viscous, waxy semi-solid. The isomeric mixture could not be separated by standard chromatographic methods. ^{1}H NMR: 7.69 (dd, J = 7.3, 1.6 Hz, 1H), 7.64 (dd, J = 5.7, 3.4 Hz, 1H), 7.56 (s, 1H), 7.55 – 7.42 (m, 4H), 4.46 (dddd, J = 13.8, 9.0, 7.6, 4.8 Hz, 2H), 4.32 (dq, J = 14.4, 5.0 Hz,2H), 4.10 – 4.01 (m, 1H), 3.99 – 3.89 (m, 2H), 3.82 (dt, J = 10.2, 5.0 Hz, 2H), 3.75 – 3.70 (m, 6H), 3.69 – 3.47 (m, 40H). ^{13}C NMR: 145.72, 144.93, 135.47, 134.70, 132.74, 131.63, 131.44, 131.04, 130.50, 130.40, 130.16, 129.19, 129.09, 128.26, 126.52, 72.69, 72.63, 72.61, 70.71, 70.69, 70.63, 70.62,70.45, 70.42, 70.38, 70.28, 69.37, 69.33, 61.72, 61.70, 61.64, 50.74, 48.36, 48.21. ESI HRMS cald. $[M+H]^+$: $C_{32}H_{43}N_6O_8^+$ 639.3137, found 639.3141.

From DIBOT:

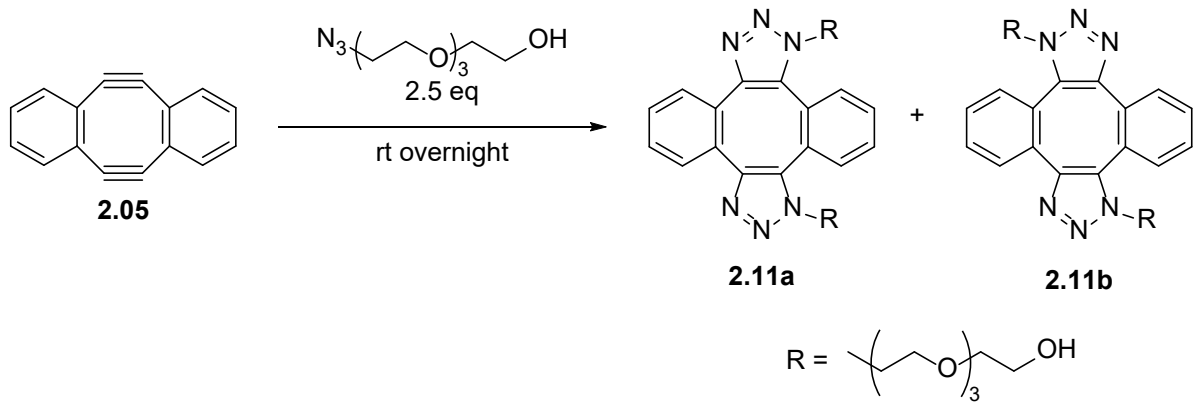

2.05 (200 mg, 0.41 mmol) was dissolved in DCM (10 mL). TEG-azide (219 mg, 1.03 mmol) was then added to the solution. The mixture was stirred at room temperature overnight. The solvent was then removed under vacuum and the product was purified by column chromatography (10% MeOH/DCM) to give 227 mg (89%) of the product as a yellow viscous, waxy semi-solid. The mixture of isomers could not be separated by standard chromatographic methods.

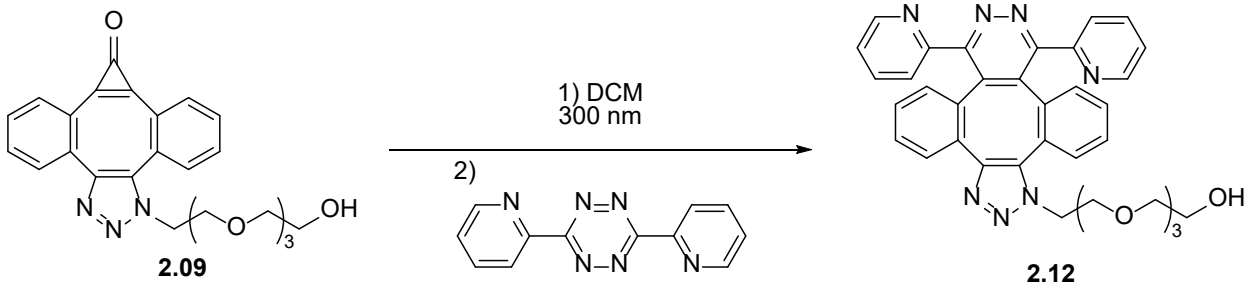

2-(2-(2-(2-(8,11-di(pyridin-2-yl)-1H-dibenzo[3,4:7,8][1,2,3]triazolo[4',5':5,6]cycloocta[1,2-d]pyridazin-1-yl)ethoxy)ethoxy)ethoxy)ethan-1-ol (2.12). 2.09 (10 mg, 0.02 mmol) was dissolved in DCM (1 mL). The solution was irradiated with 300 nm light (16x12" Rayonet photoreactor) for 5x4 minute intervals (20 minutes total). After each 4 minute interval, 1,3-bipyridyl-1,2,4,5-tetrazine (10 mM, 1.3 µL, 3.2 mg) was added and the solution was incubated for 10 minutes. After this time, it was noted that there was still a large amount of **2.09** remaining. Thus, an excess of pyTz (10 mM, 10 µL, 23.6 mg) was added and the mixture was irradiated for 20 additional minutes. After this time, the solution was incubated for an additional 2 hours. Next,

the solvent was removed under vacuum and the crude product was subjected to chromatography (50% acetone/hexanes) to give 6.8 mg (49%) of the product as a light orange, waxy semi-solid. ^{1}H NMR: 8.68 (d, J = 4.9 Hz, 1H), 8.21 (d, J = 4.8 Hz, 1H), 8.08 (d, J = 7.8 Hz, 1H), 7.83 – 7.72 (m, 1H), 7.56 (t, J = 8.5 Hz, 2H), 7.44 (d, J = 7.7 Hz, 1H), 7.35 – 7.27 (m, 2H), 7.23 (t, J = 6.4 Hz, 1H), 7.14 (dd, J = 7.7, 5.0 Hz, 1H), 7.05 (dt, J = 7.6, 3.8 Hz, 1H), 6.98 (t, J = 7.7 Hz, 1H), 6.86 (d, J = 7.8 Hz, 1H), 6.75 (d, J = 7.9 Hz, 1H), 4.79 – 4.68 (m, 1H), 4.66 – 4.54 (m, 1H), 4.31 – 4.20 (m, 1H), 4.12 – 4.03 (m, 1H), 3.71 – 3.53 (m, 12H). ESI HRMS cald. $[M+Na]^{+}$: $C_{36}H_{33}O_4N_7Na^{+}$ 650.2486, found 650.2505.

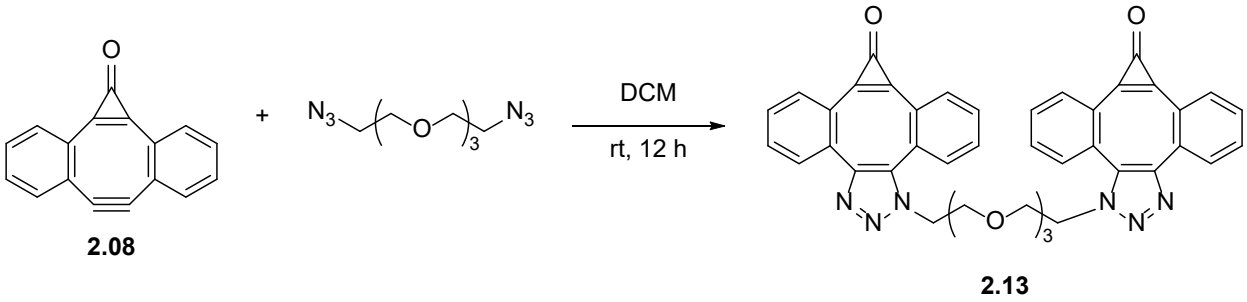

2.08 **2.13**

1,1'-(((oxybis(ethane-2,1-diyl))bis(oxy))bis(ethane-2,1-diyl))bis(dibenzo[3,4:7,8]cyclopropa [5,6]cycloocta[1,2-d][1,2,3]triazol-8(1H)-one) (2.13). Bis-azido-TEG (15.3 mg, 0.06 mmol) was dissolved in DCM. 2.08 (30 mg, 0.13 mmol) was added and the mixture was stirred at room temperature for 12 hours. The solvent was removed under vacuum and the product was purified by chromatography (50% acetone/hexanes) to give 8 mg (18%) of the product as a light yellow, waxy solid. ^{1}H NMR: 7.90 – 7.83 (m, 2H), 7.69 – 7.65 (m, 2H), 7.63 – 7.49 (m, 10H), 7.45 (tt, *J* = 7.6, 1.5 Hz, 2H), 4.45 – 4.37 (m, 2H), 4.31 – 4.22 (m, 2H), 3.99 – 3.92 (m, 2H), 3.86 – 3.79 (m, 2H), 3.52 – 3.43 (m, 8H). ^{13}C NMR:157.49, 154.67, 152.04, 142.83, 133.93, 133.87, 133.18, 132.53, 132.38, 132.28, 131.58, 131.41, 130.58, 129.47, 128.71, 127.11, 124.59, 70.74, 70.58, 69.60, 48.96.

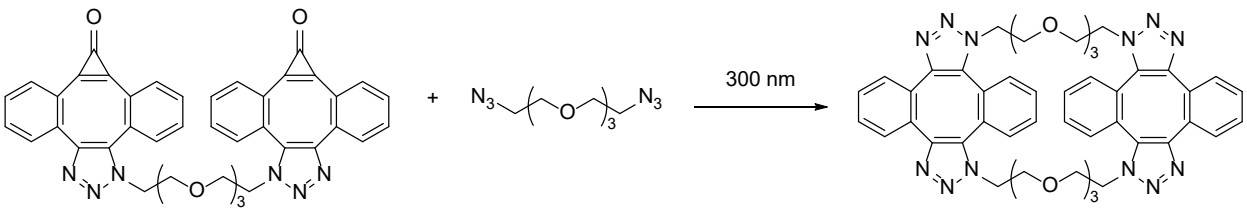

2.13 2.14

(4bZ,17Z,21bZ,34Z)-9,10,12,13,26,27,29,30-octahydro-5,34:17,22-bis([1,2]benzeno)dibenzo [f,q]tetrakis([1,2,3]triazolo)[1,5-d:5',1'-h:1'',5''-o:5''',1'''-s][1,12]dioxa[4,9,15,20]tetraaza cyclodocosine (2.14). A sample of **2.13** (30 μM in DCM) was prepared in a quartz cuvette and irradiated for 50 seconds with 300 nm light. Then, bis-azido-TEG (30 μM in DCM) was added. Upon azide addition, scanning kinetics analysis was performed (24 hours). After scanning kinetics analysis was complete, a sample was taken for MS analysis. Then, an excess of azide was added to the sample in the cuvette and this new sample was incubated an additional 24 hours before submitting a sample for MS analysis. Finally, another sample of **2.13** (30 μM in DCM) and bis-azido-TEG (300 μM in DCM) was prepared in a quartz cuvette and irradiated for 50 seconds with 300 nm light. After 24 hours incubation, a sample was submitted for MS analysis. ESI HRMS cald. $[M+H]^+$: $C_{48}H_{49}N_{12}O_6^+$ 889.3893, found 889.3890.

Protein Labeling Experiment:

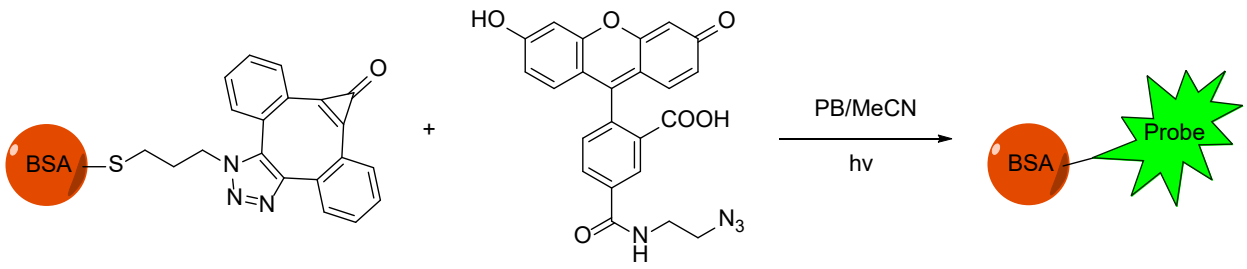

A 2 mg/mL stock solution of the BSA-DIBOT-MC and a 0.25 µg/mL stock solution of the FAM-N_3 were used to prepare 7 samples. A control sample of only the BSA-DIBOT-MC was prepared by adding 5 µL of the stock solution to 5 µL of phosphate buffer. The remaining 6 samples were prepared by mixing 5 µL of the BSA stock solution with 5 µL of the FAM-N_3 stock solution. Samples 3-7 were then irradiated with 300 nm light (Rayonet, 16 lamps) for 2, 4, 6, 8, and 10 minutes respectively. Then, 10 µL of sample prep solution containing beta-mercaptoethanol and bromophenol blue was added to each sample and they were boiled for 5 minutes. After this time, they were allowed to cool and immediately dispensed into the wells of the SDS-PAGE gel along with a ladder sample in well 15. The gel was allowed to run for approximately 30 minutes, observing the bands of the ladder move down to determine the stopping point. The gel was then imaged using a UV mode and then with Coomassie blue stain.

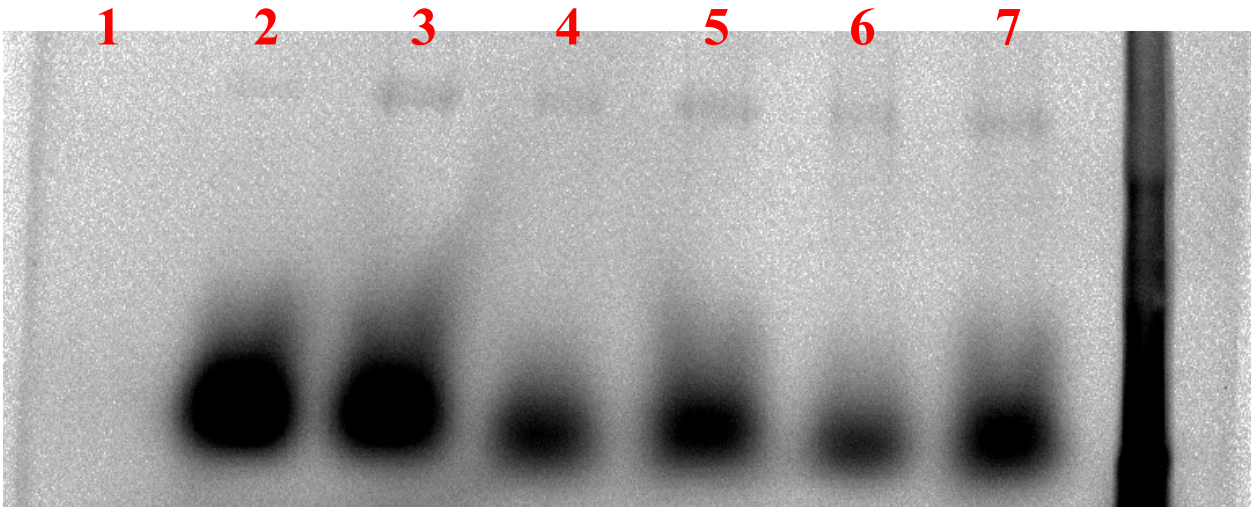

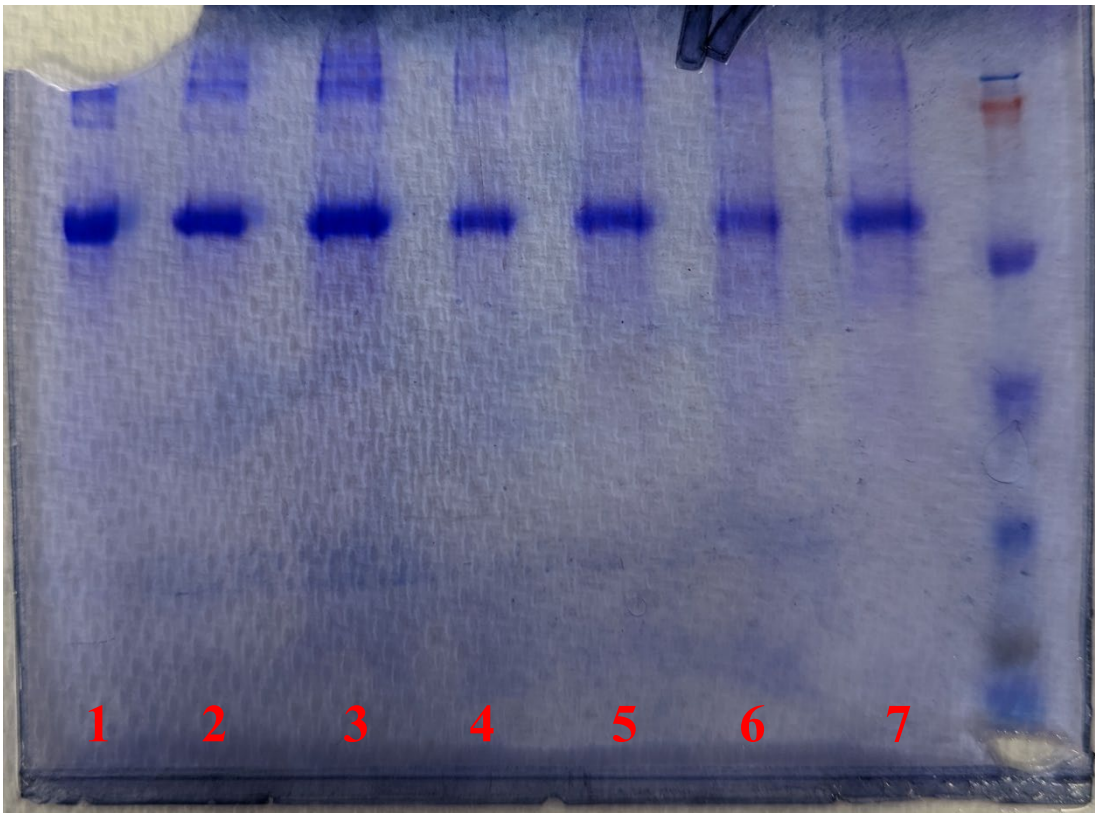

Lane	1	2	3	4	5	6	7
BSA-DIBOT-MC	+	+	+	+	+	+	+
FAM-N_3	-	+	+	+	+	+	+
Irradiation time (minutes)	0	0	2	4	6	8	10

2.11 References

1. Dommerholt, J.; Schmidt, S.; Temming, R.; Hendriks, L. J. A.; Rutjes, F. P. J. T.; van Hest, J. C. M.; Lefeber, D. J.; Friedl, P.; van Delft, F. L. Readily Accessible Bicyclononynes for Bioorthogonal Labeling and Three-Dimensional Imaging of Living Cells. *Angewandte Chemie International Edition* **2010**, *49* (49), 9422-9425.

2. Ning, X.; Guo, J.; Wolfert, M. A.; Boons, G.-J. Visualizing Metabolically Labeled Glycoconjugates of Living Cells by Copper-Free and Fast Huisgen Cycloadditions. *Angewandte Chemie International Edition* **2008**, *47* (12), 2253-2255.

3. Kuzmin, A.; Poloukhtine, A.; Wolfert, M. A.; Popik, V. V. Surface Functionalization Using Catalyst-Free Azide−Alkyne Cycloaddition. *Bioconjugate Chemistry* **2010**, *21* (11), 2076-2085.

4. McNitt, C. D.; Popik, V. V. Photochemical generation of oxa-dibenzocyclooctyne (ODIBO) for metal-free click ligations. *Organic & Biomolecular Chemistry* **2012**, *10* (41), 8200-8202.

5. McNitt, C. D. Development and application of photo-click reagents for spatial and temporal control of strain-promoted alkyne-azide cycloadditions (SPAAC). University of Georgia, **2016**.

6. Wong, H. N. C.; Garratt, P. J.; Sondheimer, F. Unsaturated eight-membered ring compounds. XI. Synthesis of sym-dibenzo-1,5-cyclooctadiene-3,7-diyne and sym-dibenzo-1,3,5-cyclooctatrien-7-yne, presumably planar conjugated eight-membered ring compounds. *Journal of the American Chemical Society* **1974**, *96* (17), 5604-5605.

7. Orita, A.; Hasegawa, D.; Nakano, T.; Otera, J. Double Elimination Protocol for Synthesis of 5,6,11,12-Tetradehydrodibenzo[a,e]cyclooctene. *Chemistry – A European Journal* **2002**, *8* (9), 2000-2004.

8. Kii, I.; Shiraishi, A.; Hiramatsu, T.; Matsushita, T.; Uekusa, H.; Yoshida, S.; Yamamoto, M.; Kudo, A.; Hagiwara, M.; Hosoya, T. Strain-promoted double-click reaction for chemical modification of azido-biomolecules. *Organic & Biomolecular Chemistry* **2010**, *8* (18), 4051-4055.

9. Chen, J.-Q.; Xiang, L.; Liu, X.; Liu, X.; Zhang, K. Self-Accelerating Click Reaction in Step Polymerization. *Macromolecules* **2017**, *50* (15), 5790-5797.

10. Wang, F.; Luo, T.; Hu, J.; Wang, Y.; Krishnan, H. S.; Jog, P. V.; Ganesh, S. K.; Prakash, G. K. S.; Olah, G. A. Synthesis of gem-Difluorinated Cyclopropanes and Cyclopropenes: Trifluoromethyltrimethylsilane as a Difluorocarbene Source. *Angewandte Chemie International Edition* **2011**, *50* (31), 7153-7157.

11. Potts, K.; Baum, J. Chemistry of cyclopropenones. *Chemical Reviews* **1974**, *74* (2), 189-213.

12. Sutton, D. A. Bis-and mono-cyclopropenone fused dibenzocyclooctadiynes: photoactivatable linchpins for sequential click ligations. University of Georgia, **2016**.

13. Warther, D.; Dursun, E.; Recher, M.; Ursuegui, S.; Mosser, M.; Sobska, J.; Krezel, W.; Chaubet, G.; Wagner, A. Plasma induced acceleration and selectivity in strain-promoted azide–alkyne cycloadditions. *Organic & Biomolecular Chemistry* **2021**, *19* (23), 5063-5067.

14. Rideout, D. C.; Breslow, R. Hydrophobic acceleration of Diels-Alder reactions. *Journal of the American Chemical Society* **1980**, *102* (26), 7816-7817.

15. Butler, R. N.; Cunningham, W. J.; Coyne, A. G.; Burke, L. A. The Influence of Water on the Rates of 1,3-Dipolar Cycloaddition Reactions: Trigger Points for Exponential Rate Increases in Water−Organic Solvent Mixtures. Water-Super versus Water-Normal Dipolarophiles. *Journal of the American Chemical Society* **2004**, *126* (38), 11923-11929.

16. Li, M.; Ma, X.; Molnar, C. J.; Wang, S.; Wu, Z.; Popik, V. V.; Li, Z. Modular PET Agent Construction Strategy through Strain-Promoted Double-Click Reagent with Efficient Photoclick Step. *Bioconjugate Chemistry* **2022**.

17. Zheng, J.; Smith Callahan, L. A.; Hao, J.; Guo, K.; Wesdemiotis, C.; Weiss, R. A.; Becker, M. L. Strain-Promoted Cross-Linking of PEG-Based Hydrogels via Copper-Free Cycloaddition. *ACS Macro Letters* **2012**, *1* (8), 1071-1073.

18. Hodgson, S. M.; Bakaic, E.; Stewart, S. A.; Hoare, T.; Adronov, A. Properties of Poly(ethylene glycol) Hydrogels Cross-Linked via Strain-Promoted Alkyne–Azide Cycloaddition (SPAAC). *Biomacromolecules* **2016**, *17* (3), 1093-1100.

19. Sutton, D. A.; Yu, S.-H.; Steet, R.; Popik, V. V. Cyclopropenone-caged Sondheimer diyne (dibenzo[a,e]cyclooctadiyne): a photoactivatable linchpin for efficient SPAAC crosslinking. *Chemical Communications* **2016**, *52* (3), 553-556.

20. Park, K. D.; Liu, R.; Kohn, H. Useful Tools for Biomolecule Isolation, Detection, and Identification: Acylhydrazone-Based Cleavable Linkers. *Chemistry & Biology* **2009**, *16* (7), 763-772.

21. Harrison, V. S. R.; Carney, C. E.; MacRenaris, K. W.; Waters, E. A.; Meade, T. J. Multimeric Near IR–MR Contrast Agent for Multimodal In Vivo Imaging. *Journal of the American Chemical Society* **2015**, *137* (28), 9108-9116.

22. Leaver, D. J.; Dawson, R. M.; White, J. M.; Polyzos, A.; Hughes, A. B. Synthesis of 1,2,3-triazole linked galactopyranosides and evaluation of cholera toxin inhibition. *Organic & Biomolecular Chemistry* **2011**, *9* (24), 8465-8474.

CHAPTER 3

WATER SOLUBLE BIS-CYCLOPROPENONE CAGED DIBENZOCYCLOOCTADIYNE

3.1 Introduction

The rate enhancement effect of performing SPAAC reactions and IEDDA reactions in aqueous conditions has been previously discussed. However, the rate enhancement effect has only been tested on the second acetylene moiety of DIBOT. Looking back at the DIBOD scaffold, adding water soluble functionalities branching from the aromatic rings could enhance the water solubility of the compound without needing to convert the first acetylene to triazole. Indeed, Otera et. al. have already reviewed the synthesis of various cyclooctadiyne compounds with flanking substituted benzyl or naphthyl groups.[1] Other groups have also successfully synthesized cyclooctadiynes with substituents on the aromatic rings.[2-3] Our goal was to generate a bis-cyclopropenone caged DIBOD derivative with hydrophilic substituents on the aromatic rings. This would allow us to investigate the rate enhancement effect of water on the first SPAAC reaction. In addition, it would offer enhanced spatiotemporal control over the cross-conjugation of two azides in aqueous media.

We envisioned two main pathways that could yield the desired water-soluble derivative of DIBOD: (a) Substitution of the aromatic ring prior to Wittig-Horner cyclization and subsequent double elimination or (b) Wittig-Horner cyclization of the methoxy-protected phenol followed by deprotection, substitution, and double elimination. Our group has already reported the successful implementation of pathway (a) in the synthesis of some DIBOD derivatives. Unfortunately, it was found that these compounds are insoluble in aqueous and organic solvents. It has been reported by

Luedtke et. al. that pathway (a) is effective for synthesizing DiMOC (**3.20**).[2] They report that DiMOC is soluble in aqueous conditions and is stable for up to several months when stored at low temperatures. Therefore, we have investigated both methods for the synthesis of a water soluble bis-cyclopropenone caged dibenzocyclooctadiyne (WS-BC-DIBOD) and its subsequent photo-deprotection and SPAAC reaction.

3.2 Synthesis and Characterization of Water Soluble DIBOD Derivative WS-BC-DIBOD-1

We start with 3-methyl anisole as the starting material. Aromatic bromination followed by a Rosenmund-von Braun reaction affords the aromatic nitrile. Next, bromination of the benzylic position and subsequent substitution with sodium benzene sulfinate affords the α-sulfone nitrile anisole. Deprotection of the methoxy group and subsequent Mitsunobu reaction installs the TBDPS-protected pentane glycol moiety. Reduction of the nitrile to the aldehyde using DIBAL affords the precursor that can undergo intermolecular Wittig-Horner cyclization to give an 8-membered ring intermediate which, upon double elimination of the sulfone substituents, yields the pentane glycol substituted DIBOD (Scheme 3.1).

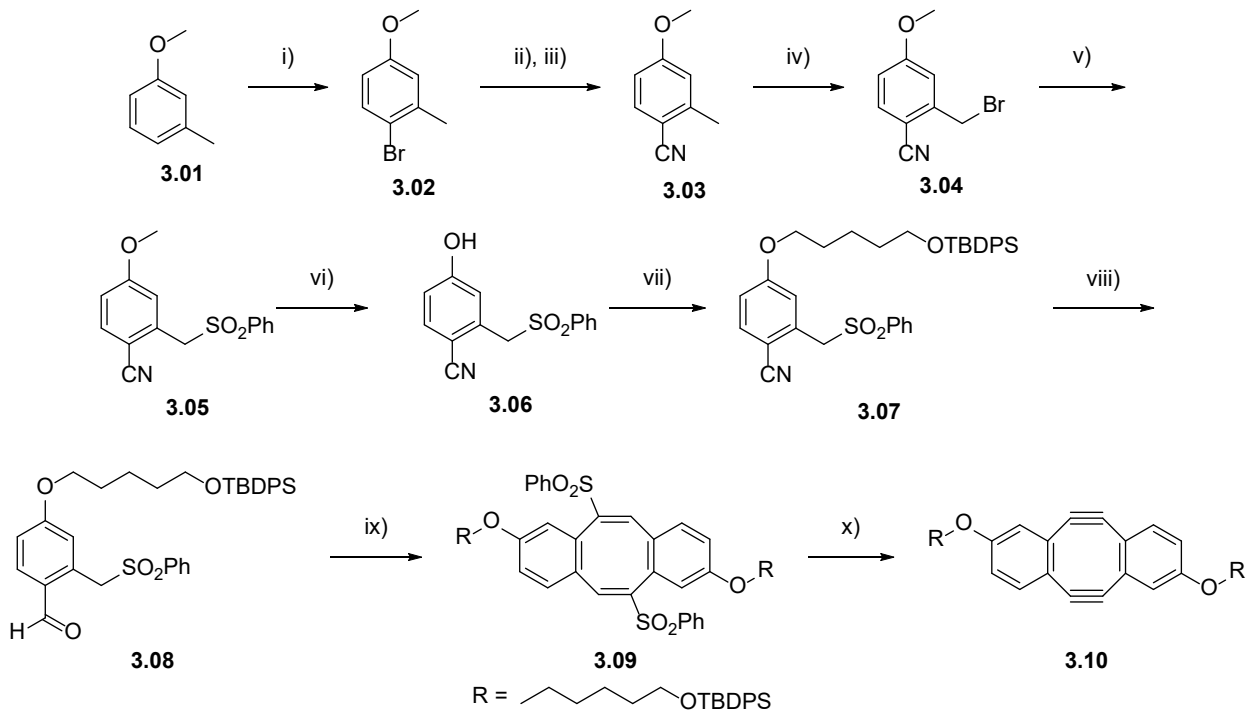

Scheme 3.1 Synthesis of WS-DIBOD-1. Reagents and conditions: i) NBS, MeCN, -10 °C – rt, 24 h. ii) CuCN, DMF, reflux, 12 h. iii) 1:1 diethylamine/H_2O, NaCN, 1 h. iv) NBS, AIBN, CCl_4, reflux, 2 h. v) $NaSO_2Ph$, DMF, 80 °C, 2 h. vi) BBr_3, DCM, *4* days. vii) 5-((tert-butyldiphenylsilyl)oxy)pentan-1-ol, triphenylphosphine, THF, -10 °C, DIAD, 16 h. *viii) DIBAL, DCM, -78 °C, 2 h. ix*) LiHMDS, $ClOP(OEt)_2$, -78 °C – rt, 2 h. x) LDA, -78 °C, 2 h.

At this stage, the next step would normally be to install the difluorocarbenes and hydrolyze them to yield the desired cyclopropenones. However, the TBDPS protecting group is labile to fluoride. Thus, we decided to exchange the TBDPS group for acetate protecting groups anticipating enhanced stability in the conditions for difluorocarbene addition (Scheme 3.2). The protecting group exchange worked without issue. However, after completing the difluorocarbene addition, we observed (by TLC) that a mixture of products was formed. The product mixture was subjected to chromatographic separation and the isolated products were analyzed by mass spectrometry. The product mixture appeared to contain compounds with varying amounts of cyclopropenone, trimethyl silyl ethers, and trifluoromethyl groups (appendix).

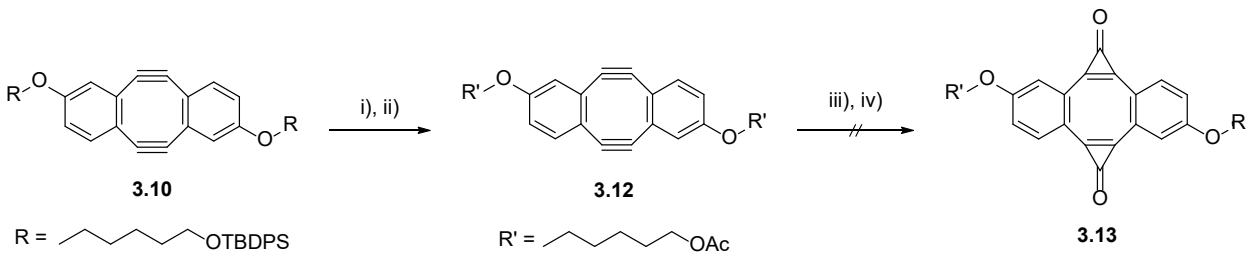

Scheme 3.2 Synthesis of WS-BC-DIBOD-1 from 3.*10*. Reagents and conditions: i) TBAF, THF, 2 h, DOWEX + $CaCO_2$. ii) DMAP, triethylamine, Ac_2O, 3 h. iii) NaI, $TMSCF_3$, THF, 110 °C, 2 h. iv) wet silica gel, 24 h.

Nonetheless, we decided to analyze the electronic spectra of the product mixture we obtained. Surprisingly, the electronic spectra appear to closely resemble those of photo-DIBOD and MC-DIBOD. There are two sharp bands at 375 nm and 354 nm, similar in shape and separation to photo-DIBOD (362 nm and 343 nm respectively). Irradiation of the compound with 350 nm light bleaches the bands at 375 nm and 354 nm and gives rise to a new sharp band at 365 nm. In addition, an intense band begins to increase in intensity at 292 nm. This is complementary to the changes observed in photo-DIBOD. When photo-DIBOD is irradiated with 350 nm light, the bands at 362 nm and 343 nm are bleached and a new sharp band appears at 354 nm.

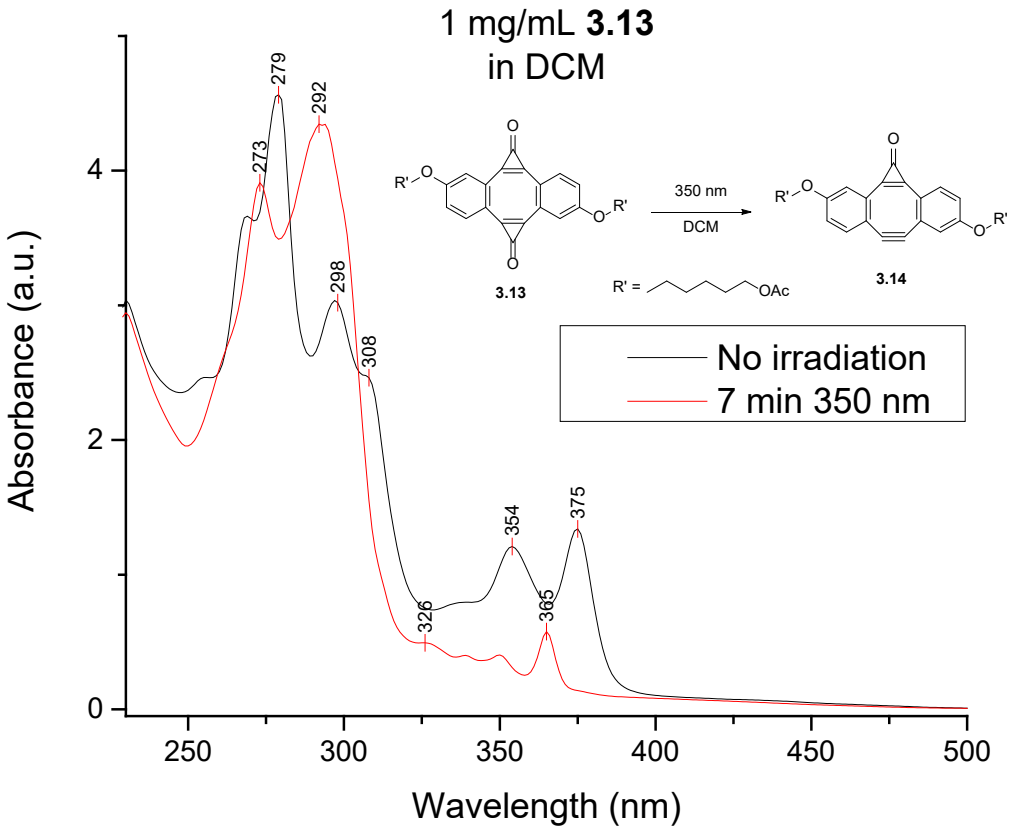

Figure 3.1 UV-Vis spectrum of a 1 mg/mL sample of **3.13** in DCM before (black trace) and after (red trace) irradiation with 350 nm light.

We were curious to see if the photolysis product would react with azide. Adding an excess of TEG-azide causes numerous changes to occur in the UV-Vis spectrum. Bands at 275 nm, 294 nm and 365 nm are bleached, while a broad band at 330 nm grows in intensity. Unfortunately, none of these absorbance changes fit to a simple first-order or second-order kinetics model.

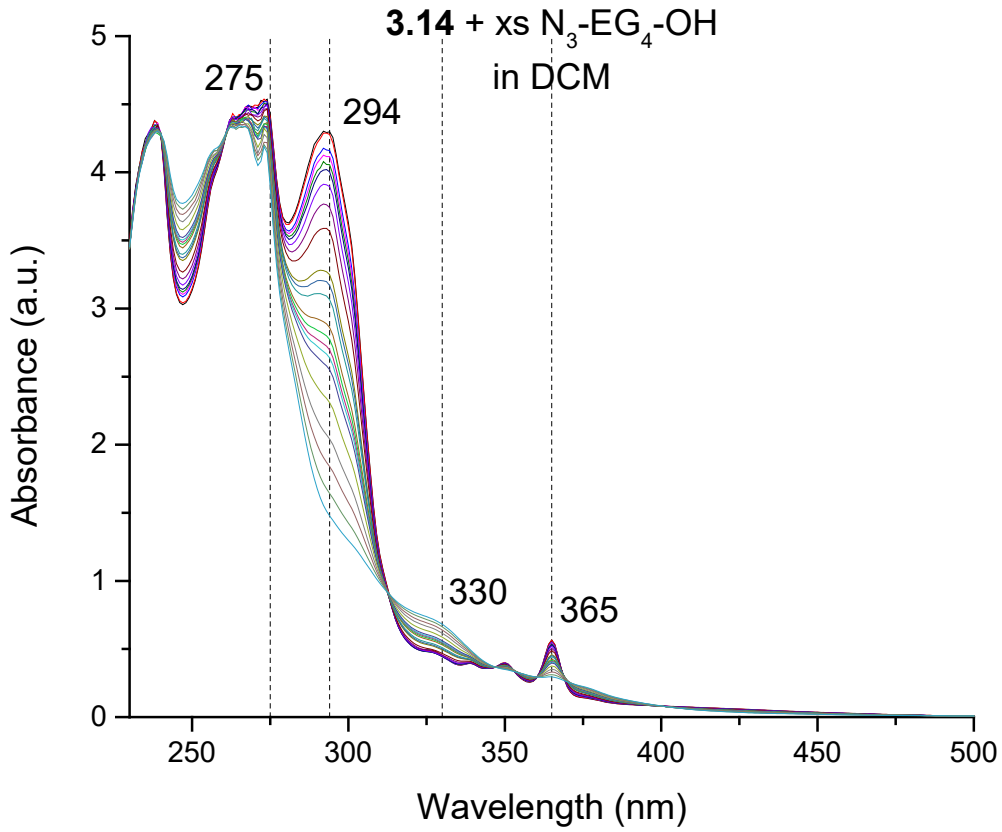

Figure 3.2 Scanning kinetics spectra for the reaction of **3.12** with an excess of azide in DCM. Absorbance bands that experience the greatest change are highlighted by dashed vertical lines.

3.3 Synthesis and Characterization of Water Soluble DIBOD Derivative WS-BC-DIBOD-2

We start analogously to WS-DIBOD-1 until the deprotection of the methoxy group of the anisole. At this stage, we perform the Wittig-Horner cyclization to give the 8-membered ring intermediate with methoxy substitution on the aromatic rings. From here, the synthesis was split into two pathways: Pathway A and B.

Pathway A (Scheme 3.3)

From the bis-methoxy intermediate, deprotection of the methoxy groups using BBr_3 gives a bis-phenol. The bis-phenol is then subjected to potassium carbonate and 1,2-dibromoethane to give the bis-ethylbromide intermediate. Substitution of the bromines for morpholine and acidifying the product gives the morpholine salt. From here, the same methods employed in chapter 2 can lead to the bis-cyclopropenone. Currently, we have a small amount of the morpholine salt, 3.17.

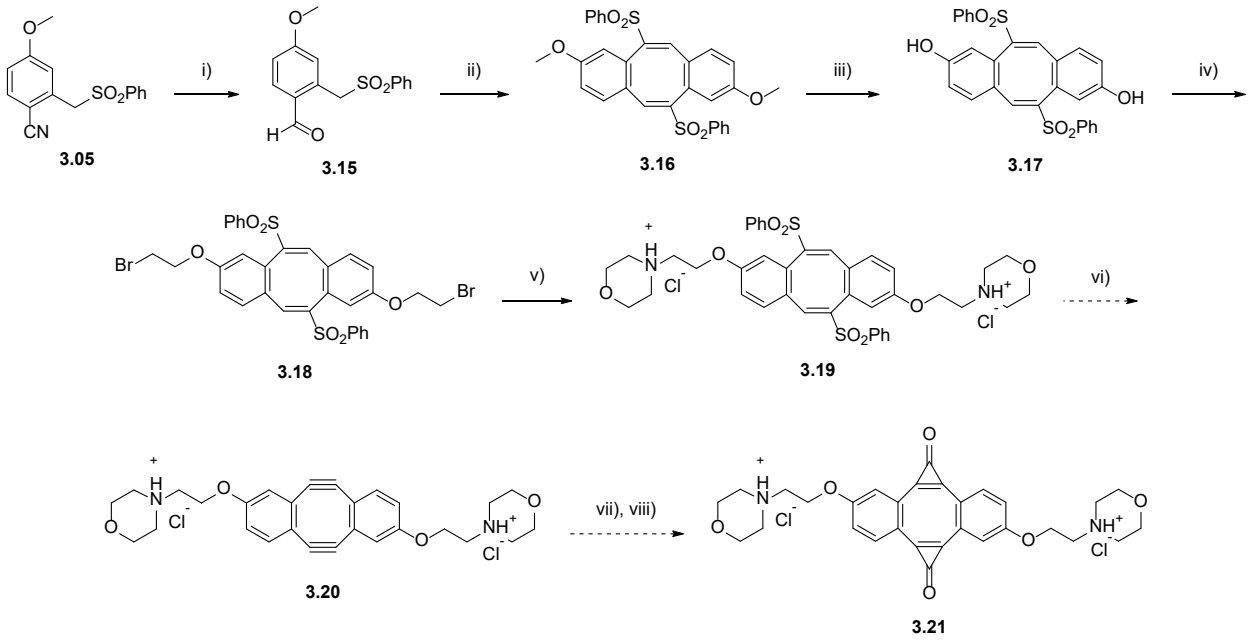

Scheme 3.3 Proposed synthesis of WS-BC-DIBOD-2 via Pathway A starting from 3.05. Reagents and conditions: i) DIBAL, DCM, -78 °C, 2 h. ii) LiHMDS, $ClOP(OEt)_2$, THF, -78 °C, 2h. iii) BBr_3, DCM, 0 °C – rt, 4 d. iv) K_2CO_3, 1,2-dibromoethane, DMF, 75 °C, 12 h. v) Morpholine, 95 °C, 4 h, HCl. vi) LDA, -78 °C, 2h. vii) NaI, $TMSCF_3$, THF, 110 °C, 2 h. viii) wet silica gel, 1 d.

Pathway B (Scheme 3.4)

From the bis-methoxy intermediate, we can use the same methods employed in chapter 2 to get to the bis-cyclopropenone. Then, the same chemistries described in Pathway A can lead to the desired product.

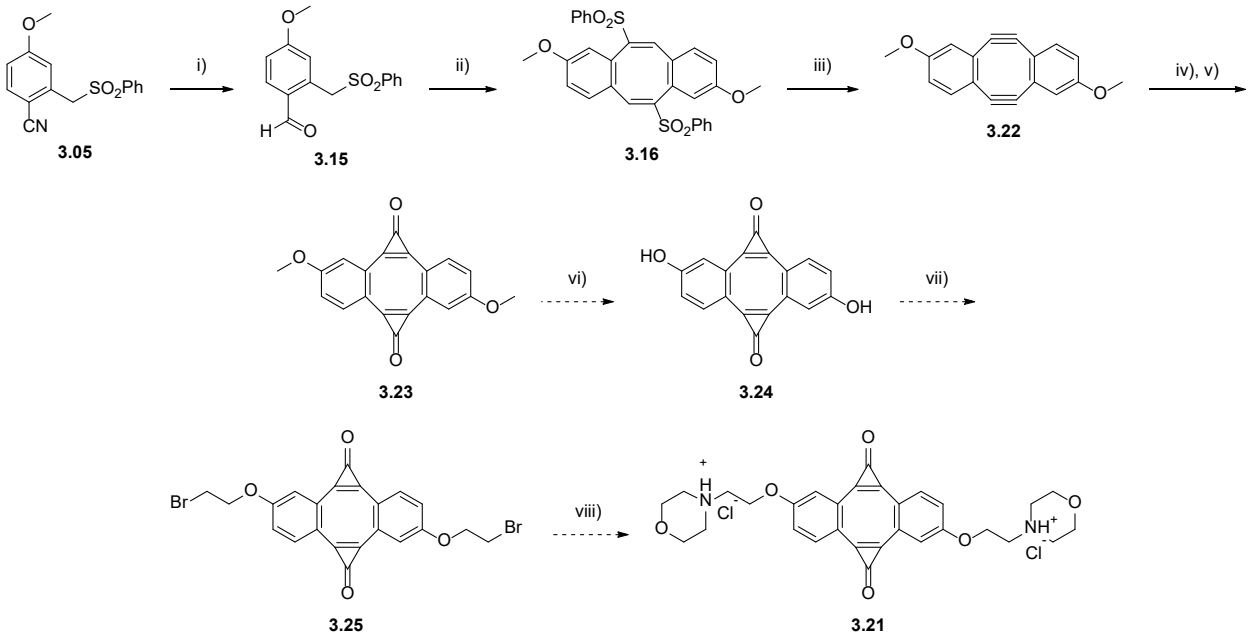

Scheme 3.4 Proposed synthesis of WS-BC-DIBOD-2 via Pathway B starting from 3.05. Reagents and conditions: i) DIBAL, DCM, -78 °C, 2 h. ii) LiHMDS, $ClOP(OEt)_2$, THF, -78 °C – rt, 2 h. iii) LDA, THF, -78 °C, 2 h. iv) NaI, $TMSCF_3$, THF, 110 °C, 2 h. v) wet silica gel, 1 d. vi) BBr_3, DCM, 0 °C – rt, 4 d. vii) K_2CO_3, 1,2-dibromoethane, DMF, 75 °C, 12 h. viii) Morpholine, 95 °C, 4 h, HCl.

Many challenges are encountered with Pathway B, starting with the bis-methoxy-bis-cyclopropenone intermediate. This compound is extremely insoluble in aqueous solvents and all organic solvents tested. Therefore, purification of the compound is incredibly challenging by standard chromatographic methods. However, it can be isolated, but in very low yields. This is only the first hurdle that must be overcome.

The next challenge encountered in Pathway B is the substitution reactions. As described in section 2.3, the cyclopropenone group is sensitive to weak bases and nucleophiles. Thus, the step at which the bromoethane is installed would likely decompose the cyclopropenones. However, even if this decomposition could be circumvented, the substitution of bromine for morpholine requires heating the compound in morpholine. Morpholine is a secondary amine, thus it could potentially cause decomposition by adding to the cyclopropenone under these conditions.

We, therefore, decided it would be best to test the stability of photo-DIBOD in the presence of secondary (morpholine) and tertiary (triethylamine) amines under reflux conditions. As anticipated, refluxing photo-DIBOD in the presence of morpholine leads to mono- and bis-adducts. However, refluxing photo-DIBOD in the presence of triethylamine did not induce any change and the photo-DIBOD was completely recovered.

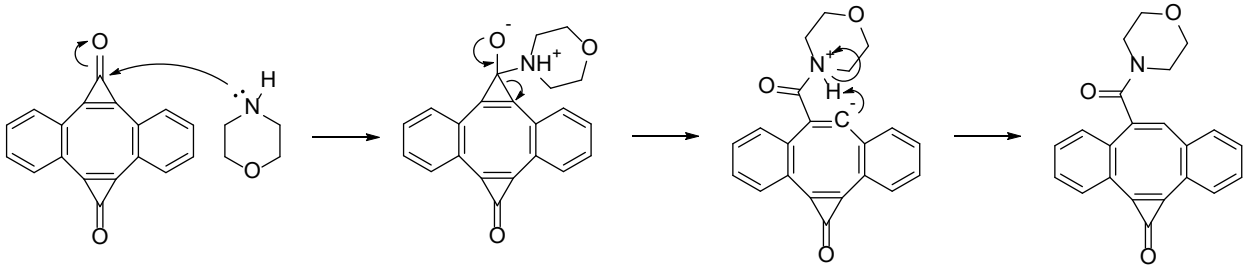

Scheme 3.5 Mechanism of morpholine addition to photo-DIBOD. Mono- and bis-adducts are observed by GC-MS.

3.4 Summary and Future Directions

Regardless the outcome, the results of this study are promising and indicate that some amount of the desired WS-BC-DIBOD-1 may have been synthesized. Attempting to synthesize WS-BC-DIBOD-2 via multiple pathways reveals the challenges involved and why the order in which the reactions are performed is crucial to obtaining the correct product. These experiments give a better understanding of how to approach the cyclopropenone protection of DIBOD derivatives. Attempting to make modifications to the aromatic sidechains can cause too many undesired reactions on the cyclopropenone, which makes Pathway B obsolete. It seems that the methodology of Pathway A is ideal as the substitution on the aromatic rings is accomplished before cyclopropenation.

3.5 Experimental Procedures

All solvents used for reactions were purified and dried using an MBRAUN SPS-5 solvent purification system. All reagents were purchased from Sigma Aldrich, VWR, or Fischer Scientific and used as received unless otherwise noted. Flash chromatography was performed using 40-63 μm silica gel. Electronic spectra and scanning kinetics data were collected using a Cary 300 Bio UV-Vis spectrophotometer. Photolyses of samples were conducted using a Rayonet photoreactor equipped with sixteen 4W 350 nm fluorescent lamps. GC-MS data were collected on a Shimadzu GCMS-QP2010 SE. All NMR spectra were recorded on a 400MHz Bruker Ascend^{TM} 400 spectrometer using deuterochloroform or DMSO-d_6.

Synthetic Procedures

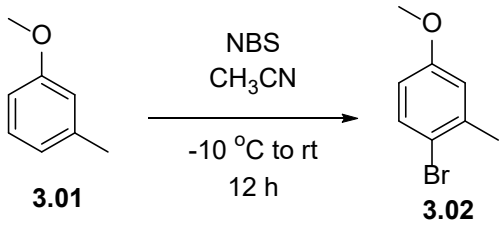

3.01 **3.02**

1-bromo-4-methoxy-2-methylbenzene (3.02). 3.01 (13.07 g, 107 mmol) was dissolved in acetonitrile (535 mL) and the mixture was cooled to -10 °C. Next, NBS (19.10 g, 107 mmol) was added to the solution. The mixture was stirred for 30 min at -10 °C and then allowed to warm to room temperature and stirred for an additional 20 hours. After this, the acetonitrile was removed under vacuum and the resulting oil was diluted in ethyl acetate and washed with water and brine. The resulting organic layer was dried with $MgSO_4$ and the ethyl acetate was removed under vacuum to give 18.90 g (88%) of the product as a clear oil. ^{1}H NMR: 7.43 (d, J = 8.7 Hz, 1H), 6.82 (d, J = 3.1 Hz, 1H), 6.63 (dd, J = 8.7 Hz, 3.1 Hz, 1H), 3.77 (s, 3H), 2.41 (s, 3H). ^{13}C NMR: 158.88, 138.73, 132.80, 116.56, 115.40, 112.93, 55.24, 23.14.

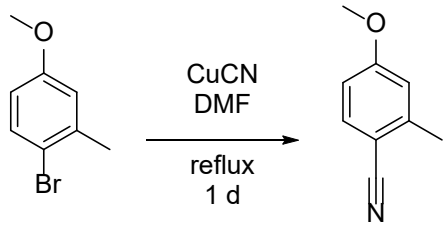

3.02 **3.03**

4-methoxy-2-methylbenzonitrile (3.03). 3.02 (10.05 g, 50 mmol) was dissolved in DMF (250 mL) and CuCN (8.76 g, 100 mmol) was added. The mixture was refluxed at 160 °C overnight. Then, a 1:1 mixture of water/diethylamine was added, and the mixture was stirred for 2 h. The product mixture was then extracted with ether and washed with NaCN in water and brine. The resulting organic extracts were dried, concentrated under vacuum, and the product was purified via flash chromatography (10% EtOAc/hexanes) to give 6.17 g (84%) of the product as a light-yellow oil. ^{1}H NMR: 7.52 (d, J = 8.5 Hz, 1H), 6.83 – 6.73 (m, 2H), 3.84 (s, 3H) 2.51 (s, 3H) ^{13}C NMR: 162.54, 143.67, 133.82, 118.28, 115.50, 111.93, 104.10, 55.25, 20.26.

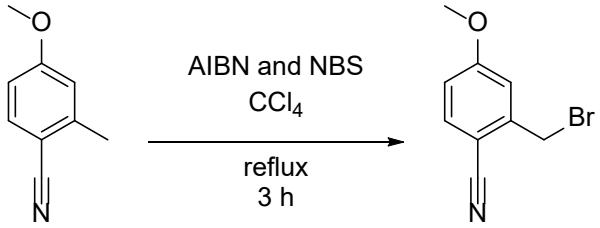

3.03 **3.04**

2-(bromomethyl)-4-methoxybenzonitrile (3.04). 3.03 (6.17 g, 42 mmol) was dissolved in CCl_4 (210 mL) and NBS (7.46 g, 42 mmol) and AIBN (1.38 g, 8.4 mmol) were added. The mixture was refluxed at 90 °C for 3 h. The reaction mixture was then worked up with sodium thiosulfate and washed with water and brine. The organic layer was concentrated under vacuum and purified via flash chromatography (20% EtOAc/hexanes) to give 4.73 g (50%) of the product as a white solid. ^{1}H NMR: 7.58 (d, J = 8.6 Hz, 1H), 7.03 (d, J = 2.5 Hz, 1H), 6.89 (dd, J = 8.7, 2.5 Hz, 1H), 4.58 (s,

2H), 3.87 (s, 3H). ^{13}C NMR: 163.11, 143.21, 135.00, 117.31, 116.12, 114.83, 104.07, 55.85, 29.59, 25.28.

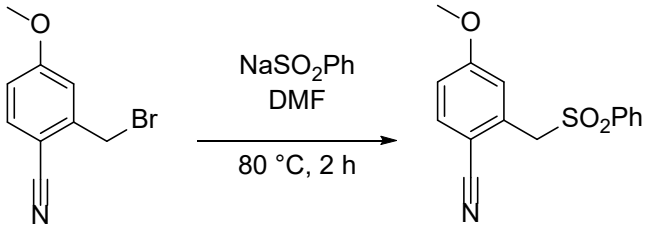

3.04 **3.05**

4-methoxy-2-((phenylsulfonyl)methyl)benzonitrile (3.05). 3.04 (4.73 g, 21 mmol) was dissolved in DMF (50 mL) and sodium benzene sulfinate (7.24 g, 25 mmol) was added. The mixture was heated to 80 °C and stirred for 2 hours. Then, the mixture was diluted with DCM, and washed with water and brine. The organic extracts were dried over $MgSO_4$ and the solvent was removed under vacuum. The crude product was recrystallized from EtOAc/hexanes to give 5.41 g (90 %) of the product as a white solid. ^{1}H NMR: 7.70 (d, J = 7.0 Hz, 2H), 7.64 (t, J = 7.5 Hz, 1H), 7.48 (t, J = 7.8 Hz, 2H), 7.43 (d, J = 8.7 Hz, 1H), 7.04 (d, J = 2.6 Hz, 1H), 6.91 (dd, J = 8.7, 2.6 Hz, 1H), 4.50 (s, 2H), 3.83 (s, 3H). ^{13}C NMR: 162.70, 137.51, 134.35, 133.58, 129.31, 128.69, 117.42, 117.06, 115.57, 105.84, 60.51, 55.83.

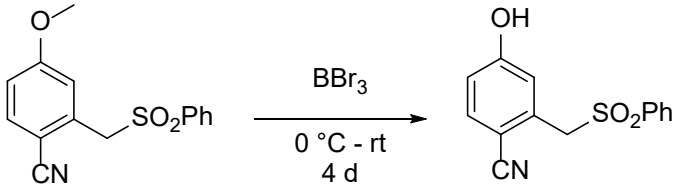

3.05 **3.06**

4-hydroxy-2-((phenylsulfonyl)methyl)benzonitrile (3.06). 3.05 (5.41 g, 19 mmol) was dissolved in DCM and cooled to 0 °C. Then, BBr_3 (9.00 mL, 95 mmol) was added and the solution was allowed to warm to room temperature. The mixture was stirred for 4 days. After this time, the reaction was quenched by pouring into distilled water. The mixture was diluted in DCM and

washed with sodium bicarbonate, water, and brine. The organic extracts were dried over Na_2SO_4 and the solvent was removed under vacuum. The crude product was purified by column chromatography (20% EtOAc/hexanes – 40% EtOAc/hexanes) and then recrystallized (chloroform/hexanes) to give 4.27 g (83%) of the product as a white solid. ^{1}H NMR: (DMSO-d6) 10.77 (s, 1H), 7.77 (t, J = 7.3 Hz, 1H), 7.72 (d, J = 7.0 Hz, 2H), 7.62 (dd, J = 15.8, 7.8 Hz, 3H), 6.88 (dd, J = 8.5, 2.4 Hz, 1H), 6.79 (d, J = 2.4 Hz, 1H), 4.72 (s, 2H). ^{13}C NMR: (DMSO-d6) 161.09, 137.90, 134.88, 134.37, 133.61, 129.48, 128.15, 119.38, 117.65, 116.59, 103.55, 59.45.

3.L1

5-((tert-butyldiphenylsilyl)oxy)pentan-1-ol (3.L1). 1,5-pentanediol (5.21 g, 50 mmol), imidazole (3.74 g, 55 mmol), and TBDPSCl (13.74 g, 50 mmol) were dissolved in DCM (250 mL) and stirred for 12 hours at room temperature. After this time, the solvent was removed under vacuum and the crude product was purified by chromatography (20% EtOAc/hexanes) to give 6.12 g (36%) of the product as a clear viscous oil. ^{1}H NMR: 7.68 (dd, J = 7.8, 1.6 Hz, 4H), 7.47 – 7.35 (m, 6H), 3.68 (t, J = 6.4 Hz, 2H), 3.62 (t, J = 6.5 Hz, 2H), 1.65 – 1.51 (m, 4H), 1.49 – 1.41 (m, 2H), 1.39 (s, 1H), 1.06 (s, 9H).

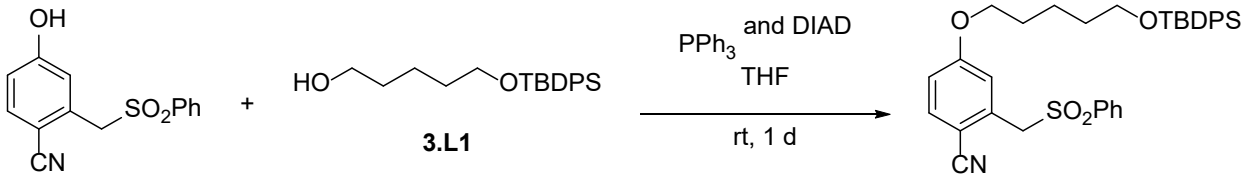

3.06 **3.L1** **3.07**

4-((5-((tert-butyldiphenylsilyl)oxy)pentyl)oxy)-2-((phenylsulfonyl)methyl)benzonitrile (3.07). 3.06 (4.27 g, 16 mmol), 3.L1 (5.35 g, 16 mmol), and triphenyl phosphine (4.92 g, 19 mmol) were dissolved in THF. Then, DIAD (3.07 mL, 16 mmol) was added dropwise to the solution,

which was then stirred for 1 day. The mixture was concentrated under vacuum then diluted in EtOAc and washed with water and brine. The organic extracts were purified by column chromatography (20% EtOAc/hexanes) to yield 3.12 g (33 %) of the product as a viscous oil. ^{1}H NMR: 7.73 (d, J = 6.9 Hz, 2H), 7.70 – 7.62 (m, 5H), 7.50 (t, J = 7.8 Hz, 2H), 7.46 – 7.34 (m, 7H), 7.09 (d, J = 2.5 Hz, 1H), 6.89 (dd, J = 8.7, 2.5 Hz, 1H), 4.51 (s, 2H), 3.99 (t, J = 6.4 Hz, 2H), 3.70 (t, J = 6.1 Hz, 2H), 1.80 (p, J = 6.7 Hz, 2H), 1.63 (q, J = 6.7 Hz, 2H), 1.55 (t, J = 7.7 Hz, 2H), 1.06 (s, 9H). ^{13}C NMR: 162.43, 137.66, 135.70, 134.43, 134.37, 134.09, 133.70, 129.73, 129.41, 128.86, 127.77, 117.82, 117.19, 116.18, 105.67, 68.72, 63.70, 60.67, 32.26, 28.76, 27.01, 22.34, 19.37.

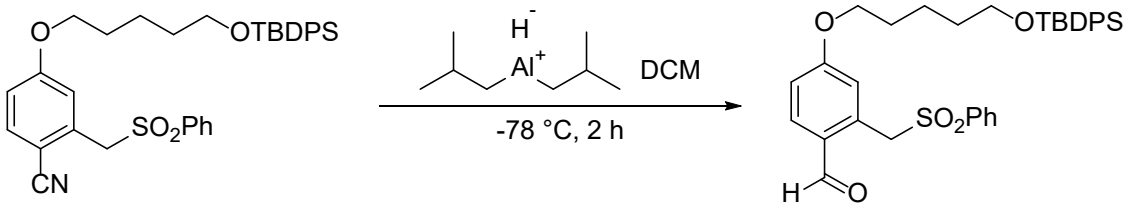

3.07 **3.08**

4-((5-((tert-butyldiphenylsilyl)oxy)pentyl)oxy)-2-((phenylsulfonyl)methyl)benzaldehyde (3.08). 3.07 (3.12 g, 5.2 mmol) was dissolved in DCM (25 mL) and the solution was cooled to -78 °C. Then, DIBAL (1 M in cyclohexane, 11.5 mL, 11.5 mmol) was added dropwise via addition funnel. The mixture was stirred at low temperature for 2 hours. After this time, the reaction was quenched with ammonium chloride and 1 M HCl was added and the resulting mixture was stirred for 30 minutes. The solution was then diluted with DCM, and washed with 1 M HCl and brine. The resulting organic layer dried over Na_2SO_4 and the solvent was evaporated under vacuum. The crude product was purified by flash chromatography (20% EtOAc/hexanes) to give 2.05 g (65%) of the product as a white solid. ^{1}H NMR: 9.63 (s, 1H), 7.75 – 7.64 (m, 7H), 7.63 – 7.55 (m, 2H), 7.47 – 7.36 (m, 9H), 7.00 – 6.94 (m, 2H), 5.04 (s, 2H), 4.01 (t, J = 6.4 Hz, 2H), 3.71 (t, J = 6.1 Hz, 2H), 1.80 (p, J = 6.7 Hz, 2H), 1.68 – 1.61 (m, 2H), 1.58 – 1.52 (m, 2H), 1.06 (s, 9H). ^{13}C NMR:

190.81, 163.03, 138.45, 137.43, 135.70, 134.93, 134.11, 133.89, 131.32, 129.79, 129.72, 128.91, 128.86, 127.85, 127.79, 127.76, 119.87, 115.03, 68.64, 63.73, 57.72, 32.27, 28.82, 27.01, 22.35, 19.37.

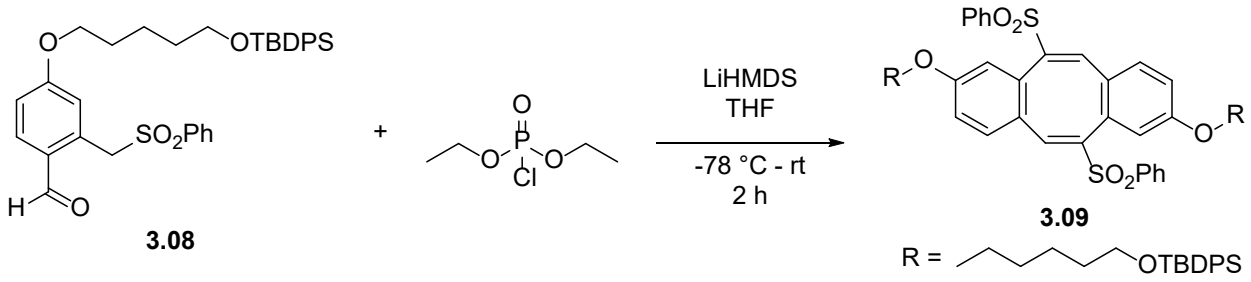

(((((5E,11E)-6,12-bis(phenylsulfonyl)dibenzo[a,e][8]annulene-2,8-diyl)bis(oxy))bis(pentane-5,1-diyl))bis(oxy))bis(tert-butyldiphenylsilane) (3.09). 3.08 (2.05 g, 3.4 mmol) and diethyl chlorophosphate (0.592 mL, 4.1 mmol) were dissolved in THF (100 mL) and cooled to -78 °C. Then, LiHMDS (1.1 M in THF, 6.2 mL, 6.8 mmol) was added to the mixture. The mixture was stirred at low temperature for 30 minutes, then allowed to warm to room temperature for 1.5 hours. After this time, the reaction was quenched with saturated ammonium chloride solution. The resulting mixture was diluted with EtOAc and washed with water and brine. The organic layer was then dried over $MgSO_4$ and the solvent was removed under vacuum. The crude product was purified by chromatography (20% EtOAc/hexanes) to give 740 mg (25%) of the product as a white solid. ^{1}H NMR: 7.67 – 7.63 (m, 8H), 7.63 – 7.57 (m, 2H), 7.48 – 7.42 (m, 8H), 7.40 – 7.32 (m, 14H), 6.96 (d, J = 2.5 Hz, 2H), 6.86 (d, J = 8.6 Hz, 2H), 6.78 (dd, J = 8.6, 2.5 Hz, 2H), 3.88 – 3.77 (m, 4H), 3.66 (t, J = 6.3 Hz, 4H), 1.71 (p, J = 6.7 Hz, 4H), 1.63 – 1.57 (m, 4H), 1.52 – 1.44 (m, 4H), 1.03 (s, 18H).

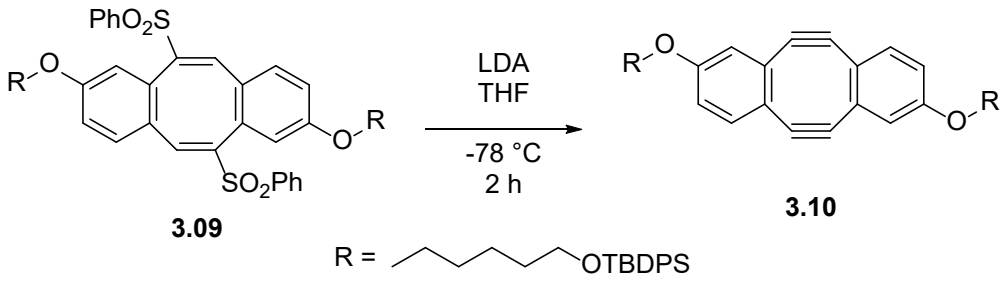

5,6,11,12-tetradehydro-2,8-bis((5-((tert-butyldiphenylsilyl)oxy)pentyl)oxy)dibenzo[a,e][8] annulene (3.10). LDA was prepared in situ by dissolving diisopropylamine (0.935 mL, 6.7 mmol) in THF (65 mL) and cooling the solution to -78 °C. Then, n-butyllithium (1.6 M in hexanes, 4.07 mL, 6.5 mmol) was added dropwise to the solution via addition funnel. The mixture was allowed to stir for 30 minutes. After this time, 3.09 (760 mg, 0.65 mmol) dissolved in THF (1 mL) was added to the mixture and the reaction was allowed to progress for 2 hours. After this time, the reaction was quenched with saturated ammonium chloride solution. The mixture was then poured into a separatory funnel and the organic layer was separated and the solvent was removed under vacuum. The crude product was diluted with DCM and washed with water and brine. The organic extracts were dried over Na_2SO_4 and the solvent was removed under vacuum. The crude product was then purified by chromatography (20% EtOAc/hexanes – 20% DCM/hexanes) to give 180 mg (31%) of the product as a yellow solid. ^{1}H NMR: 7.70 – 7.64 (m, 8H), 7.45 – 7.35 (m, 12H), 6.66 (d, J = 8.4 Hz, 2H), 6.39 – 6.30 (m, 4H), 3.82 (t, J = 6.4 Hz, 4H), 3.68 (t, J = 6.2 Hz, 4H), 1.71 (p, J = 6.8 Hz, 4H), 1.64 – 1.57 (m, 4H), 1.54 – 1.45 (m, 4H), 1.05 (s, 18H). ^{13}C NMR: 159.93, 135.71, 134.99, 134.15, 129.70, 127.95, 127.75, 123.73, 115.08, 112.63, 110.31, 107.48, 68.12, 63.75, 32.26, 28.86, 27.01, 22.33, 19.36.

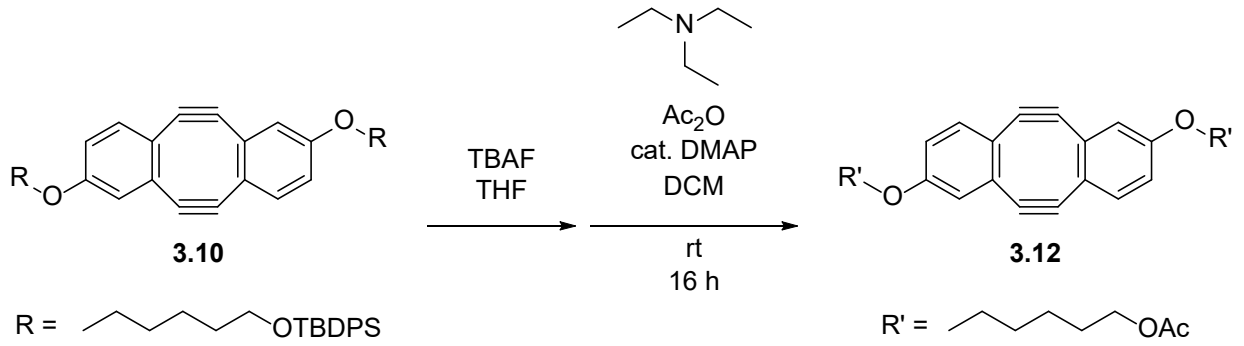

(((5,6,11,12-tetradehydrodibenzo[a,e][8]annulene-2,8-diyl)bis(oxy))bis(pentane-5,1-diyl) diacetate (3.12). 3.10 (170 mg, 0.20 mmol) was dissolved in THF (2 mL). Next, TBAF (1 M in THF, 1 mL, 1 mmol) was added. The mixture was stirred at room temperature for 2 hours. Then, DOWEX and $CaCO_2$ (excess) were added to the mixture and a precipitate formed. The solution was gravity filtered and the solvent was removed under vacuum. The intermediate (3.11) was used in the next step without further purification. 3.11 (70 mg, 0.17 mmol) was dissolved in triethylamine (1 mL) along with DMAP (4 mg, 0.03 mmol). Then, acetic anhydride (0.064 mL, 0.68 mmol) was added to the mixture and the mixture was stirred for 3 hours. After this time, the mixture was diluted with DCM and washed with water and brine. The organic extracts were dried over Na_2SO_4 and the solvent was removed under vacuum. The crude product was purified by chromatography (1% MeOH/DCM) to give 41 mg (49%) of the product as a bright yellow solid. ^{1}H NMR: 6.66 (d, J = 8.4 Hz, 2H), 6.37 (dd, J = 8.4, 2.6 Hz, 2H), 6.32 (d, J = 2.6 Hz, 2H), 4.08 (t, J = 6.6 Hz, 4H), 3.86 (t, J = 6.3 Hz, 4H), 2.05 (s, 6H), 1.80 – 1.73 (m, 4H), 1.71 – 1.64 (m, 4H), 1.53 – 1.45 (m, 4H). ^{13}C NMR: 159.71, 134.89, 127.85, 114.94, 112.50, 110.18, 107.33, 77.35, 77.03, 76.72, 67.79, 64.30, 28.70, 28.33, 22.54, 21.03.

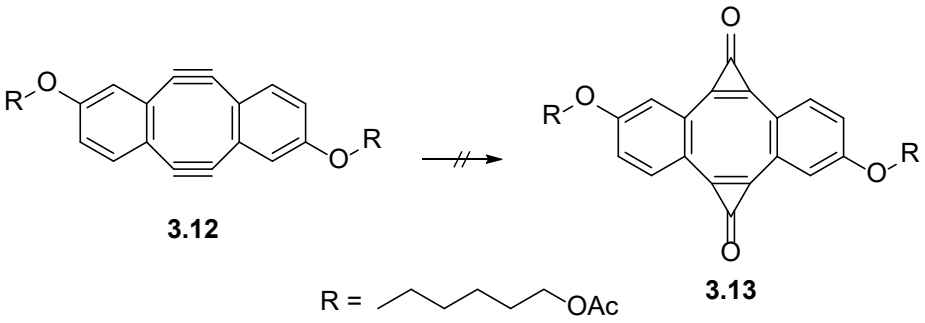

((1,6-dioxo-1,6-dihydrodibenzo[a,e]dicyclopropa[c,g][8]annulene-3,8-diyl)bis(oxy))bis (pentane-5,1-diyl) diacetate (3.13) (attempted). **3.12** (200 mg, 0.41 mmol) was dissolved in THF (4 mL) in a pressure vessel and NaI (258 mg, 1.72 mmol) was added. The mixture was degassed and $TMSCF_3$ (0.243 mL, 1.64 mmol) was added. Then, the mixture was heated to 110 °C for 2 hours. After this time, the reaction was quenched with sodium bicarbonate and diluted with DCM. The organic layer was washed with water and brine and dried over anhydrous K_2CO_3. The organic solvent was removed under vacuum and the crude product was added to a wet silica gel column (1% H_2O in 50% DCM/hexanes). The column was incubated overnight and the product was eluted (50% acetone/hexanes) to give 54 mg of a bright yellow solid product. It was determined by MS that a mixture of products was formed from this reaction.

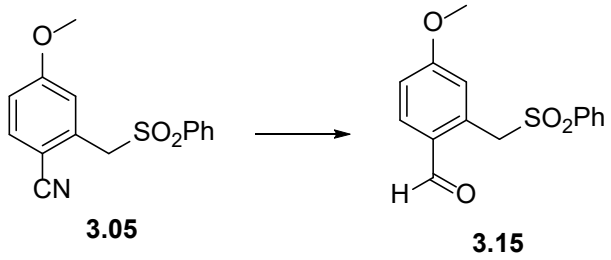

4-methoxy-2-((phenylsulfonyl)methyl)benzaldehyde (3.15). The nitrile reduction was carried out analogously to compound **3.08** starting with **3.05** (10 g, 34.8 mmol) in DCM (175 mL) with DIBAL (1.1 M in hexanes, 66.4 mL) and yielding 6.62 g (66%) of the product as a white solid. ^1H NMR: 9.64 (s, 1H), 7.69 (d, J = 7.1 Hz, 2H), 7.65 – 7.55 (m, 2H), 7.43 (t, J = 7.8 Hz, 2H), 6.99

(dd, J = 8.5, 2.6 Hz, 1H), 6.92 (d, J = 2.5 Hz, 1H), 5.02 (s, 2H), 3.85 (s, 3H). ^{13}C NMR: 190.74, 163.33, 138.33, 137.28, 133.87, 131.30, 128.87, 128.75, 127.96, 119.44, 114.48, 57.63, 55.82.

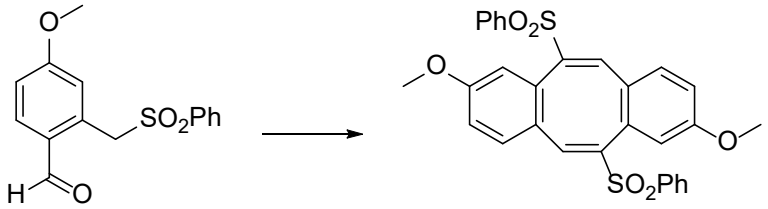

3.15 **3.16**

(5E,11E)-2,8-dimethoxy-6,12-bis(phenylsulfonyl)dibenzo[a,e][8]annulene (3.16). The Wittig-Horner cyclization was carried out analogously to compound **3.09** starting with **3.15** (4 g, 13.8 mmol) and diethyl chlorophosphate (2.42 mL, 16.6 mmol) dissolved in THF (415 mL) and adding LiHMDS (1.3 M in THF, 21.23 mL) to yield 1.97 g (26%) of the product as a white solid. ^{1}H NMR: 7.63 (tt, J = 6.9, 1.8 Hz, 2H), 7.51 – 7.41 (m, 8H), 7.34 (s, 2H), 6.98 (d, J = 2.6 Hz, 2H), 6.89 (d, J = 8.6 Hz, 2H), 6.82 (dd, J = 8.6, 2.6 Hz, 2H), 3.73 (s, 6H). ^{13}C NMR: 159.41, 144.08, 139.42, 139.20, 133.90, 130.65, 129.09, 128.45, 128.20, 127.87, 116.34, 115.31, 55.50.

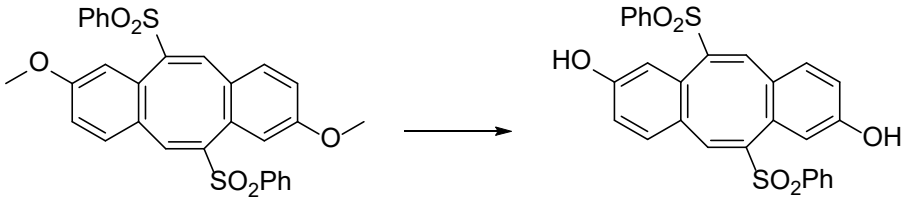

3.16 **3.17**

(5E,11E)-6,12-bis(phenylsulfonyl)dibenzo[a,e][8]annulene-2,8-diol (3.17). The methoxy deprotection was carried out analogously to compound **3.06** starting with **3.16** (545 mg, 1 mmol) dissolved in DCM (10 mL) and adding BBr_3 (0.612 mL, 5 mmol) to give 403 mg (78%) of the product as a white solid. ^{1}H NMR: (DMSO-d6) 9.93 (s, 2H), 7.76 (t, J = 7.5 Hz, 2H), 7.62 (t, J = 7.8 Hz, 4H), 7.35 (d, J = 7.0 Hz, 4H), 7.17 (s, 2H), 7.02 – 6.95 (m, 2H), 6.79 – 6.70 (m, 4H).

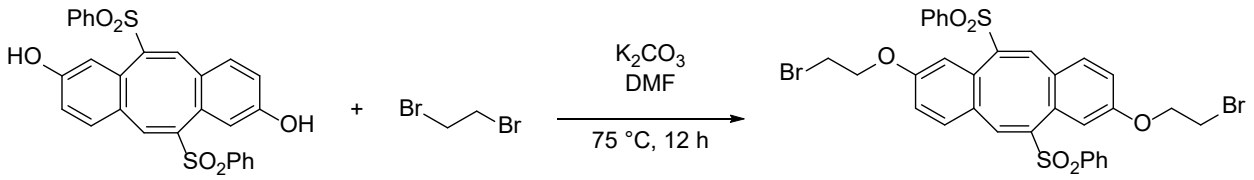

3.17 **3.18**

(5E,11E)-2,8-bis(2-bromoethoxy)-6,12-bis(phenylsulfonyl)dibenzo[a,e][8]annulene (3.18). **3.17** (300 mg, 0.58 mmol) was dissolved in DMF (6 mL). Then, K_2CO_3 (2.40 g, 17.4 mmol) and 1,2-dibromoethane (1.63 g, 8.7 mmol) were added. The mixture was heated to 75 °C and stirred for 12 hours. After this time, the crude product was allowed to cool and diluted with EtOAc. The crude product was then washed with water and brine and the organic extracts were dried over Mg_2SO_4. The solvent was then removed under vacuum and the product was purified by chromatography (15% EtOAc/hexanes – 20% EtOAc/hexanes) to give 110 mg (26%) of the product as a white solid. ^{1}H NMR: 7.67 – 7.60 (m, 2H), 7.51 – 7.42 (m, 8H), 7.33 (s, 2H), 6.97 (d, J = 2.5 Hz, 2H), 6.91 (d, J = 8.6 Hz, 2H), 6.85 (dd, J = 8.6, 2.5 Hz, 2H), 4.21 (qt, J = 10.8, 6.3 Hz, 4H), 3.59 (t, J = 6.1 Hz, 4H). ^{13}C NMR: 157.96, 144.19, 139.30, 139.13, 134.00, 130.76, 129.15, 128.63, 128.57, 128.21, 117.08, 115.93, 67.95, 28.82.

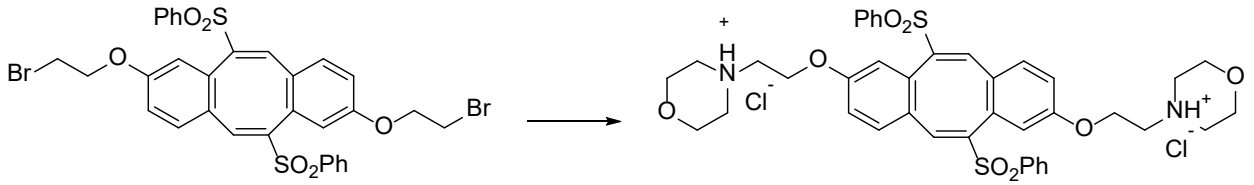

3.18 **3.19**

4,4'-((((5E,11E)-6,12-bis(phenylsulfonyl)dibenzo[a,e][8]annulene-2,8-diyl)bis(oxy))bis (ethane-2,1-diyl))bis(morpholin-4-ium) chloride (3.19). **3.18** (110 mg, 0.15 mmol) was dissolved in morpholine (3 mL, 34.8 mmol). The solution was heated to 95 °C and stirred for 4 hours. After this time, the mixture was diluted with saturated sodium bicarbonate solution. The aqueous layer was extracted with chloroform and the organic extracts were washed with 1 M HCl.

Then, NaOH was added to the aqueous acid layer and tested with pH paper until alkaline. This alkaline aqueous layer was extracted with chloroform. The organic extracts were combined and washed with brine, dried over $MgSO_4$, and the solvent was evaporated under vacuum. The crude product was subjected to HCl (1 M, 0.30 mL, 0.30 mmol) and purified by recrystallization from EtOAc/hexanes and to give 59 mg (48%) of the product as a white solid. ^{1}H NMR: 7.65 – 7.58 (m, 2H), 7.49 – 7.38 (m, 8H), 7.30 (s, 2H), 7.00 (d, J = 2.4 Hz, 2H), 6.88 – 6.80 (m, 4H), 4.07 – 3.96 (m, 4H), 3.69 (t, J = 4.7 Hz, 8H), 2.74 (t, J = 5.7 Hz, 4H), 2.53 (t, J = 4.7 Hz, 8H). ^{13}C NMR: 158.58, 144.12, 139.34, 139.22, 133.89, 130.65, 129.06, 128.41, 128.15, 128.04, 116.82, 116.01, 66.97, 66.07, 57.52, 54.18.

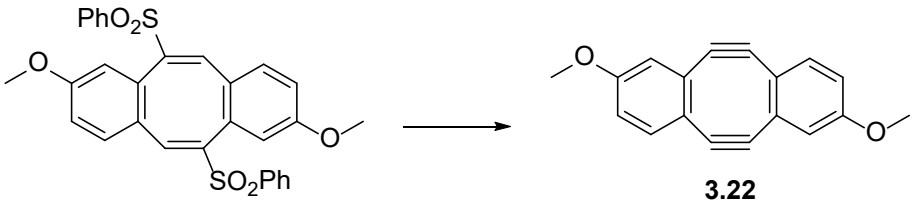

3.16 **3.22**

5,6,11,12-tetradehydro-2,8-dimethoxydibenzo[a,e][8]annulene (3.22). The double sulfone elimination was carried out analogously to compound **3.10** starting with LDA (0.28 M in THF prepared in situ) and adding **3.16** (1 g, 1.95 mmol) to yield 500 mg (98%) of the product as a bright yellow solid.

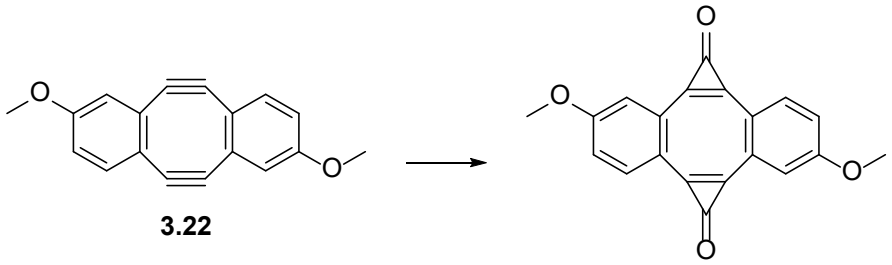

3.22 **3.23**

3,8-dimethoxydibenzo[a,e]dicyclopropa[c,g][8]annulene-1,6-dione (3.23). The cyclopropenation was carried out analogously to compound **3.13** starting with **3.22** (500 mg, 1.92

mmol), NaI (1.21 g, 8.1 mmol), and $TMSCF_3$ (1.14 mL, 7.7 mmol) dissolved in THF (15 mL), hydrolyzed on wet silica gel (1% H_2O in 20% methanol/chloroform) to give 63 mg (10%) of the product as the bright yellow solid. Characterization was not performed for this compound due to the extremely limited solubility.

3.6 References

1. Xu, F.; Peng, L.; Shinohara, K.; Morita, T.; Yoshida, S.; Hosoya, T.; Orita, A.; Otera, J. Substituted 5,6,11,12-Tetradehydrodibenzo[a,e]cyclooctenes: Syntheses, Properties, and DFT Studies of Substituted Sondheimer–Wong Diynes. *The Journal of Organic Chemistry* **2014**, *79* (23), 11592-11608.

2. Tera, M.; Harati Taji, Z.; Luedtke, N. W. Intercalation-enhanced "Click" Crosslinking of DNA. *Angewandte Chemie International Edition* **2018**, *57* (47), 15405-15409.

3. Sharma, K.; Strizhak, A. V.; Fowler, E.; Wang, X.; Xu, W.; Hatt Jensen, C.; Wu, Y.; Sore, H. F.; Lau, Y. H.; Hyvönen, M.; et al. Water-soluble, stable and azide-reactive strained dialkynes for biocompatible double strain-promoted click chemistry. *Organic & Biomolecular Chemistry* **2019**, *17* (34), 8014-8018.

CHAPTER 4

CONCLUSIONS

This work outlines the design and synthesis of a variety of hydrophilic mono- and bis-cyclopropenone caged dibenzocyclooctadiyne compounds that possess properties amenable to bioorthogonal chemistry and click reactions.

Chapter 1 includes a discussion of current click chemical reactions that consist of 1,3-dipolar cycloadditions (CuAAC and SPAAC), Staudinger ligation, and IEDDA reactions. Along with the summary of each technique and the progress that has been made in developing each, the pitfalls are also discussed. Lastly, the goals of the project are proposed which aim to circumvent the problematic aspects of current cyclooctyne click reagents.

Chapter 2 describes the synthesis and chemistry of MC-DIBOT. The reactions and photochemical properties of this unique cyclopropenone-caged dibenzocyclooctyne reagent are discussed. The investigation into the effect of water on the SPAAC reaction using DIBOT and data from this analysis are provided. These kinetics data can be used to extrapolate to the rate constant of the SPAAC reaction in neat aqueous conditions, which appears to be at least 10-fold higher than for organic solvents. Additionally, the kinetics of the IEDDA reaction of DIBOT with pyTz in organic media is described. Lastly, some potential alternative uses for MC-DIBOT derivatives are given.

Finally, chapter 3 desribes the attempted synthesis of a water soluble bis-cyclopropenone caged dibenzocyclooctadiyne compound (WS-BC-DIBOD). The various routes that have been

attempted to achieve the desired product and the challenges that need to be overcome are outlined. Some evidence that points toward the successful synthesis of one such derivative is provided.

APPENDIX A

^{1}H NMR AND ^{13}C NMR SPECTRA OF ESSENTIAL COMPOUNDS

^{1}H NMR (400 MHz, $CDCl_3$) δ 7.54 (dd, *J* = 7.5, 1.4 Hz, 2H), 7.25 – 7.15 (m, 4H), 6.90 (dd, *J* = 7.5, 1.3 Hz, 2H).

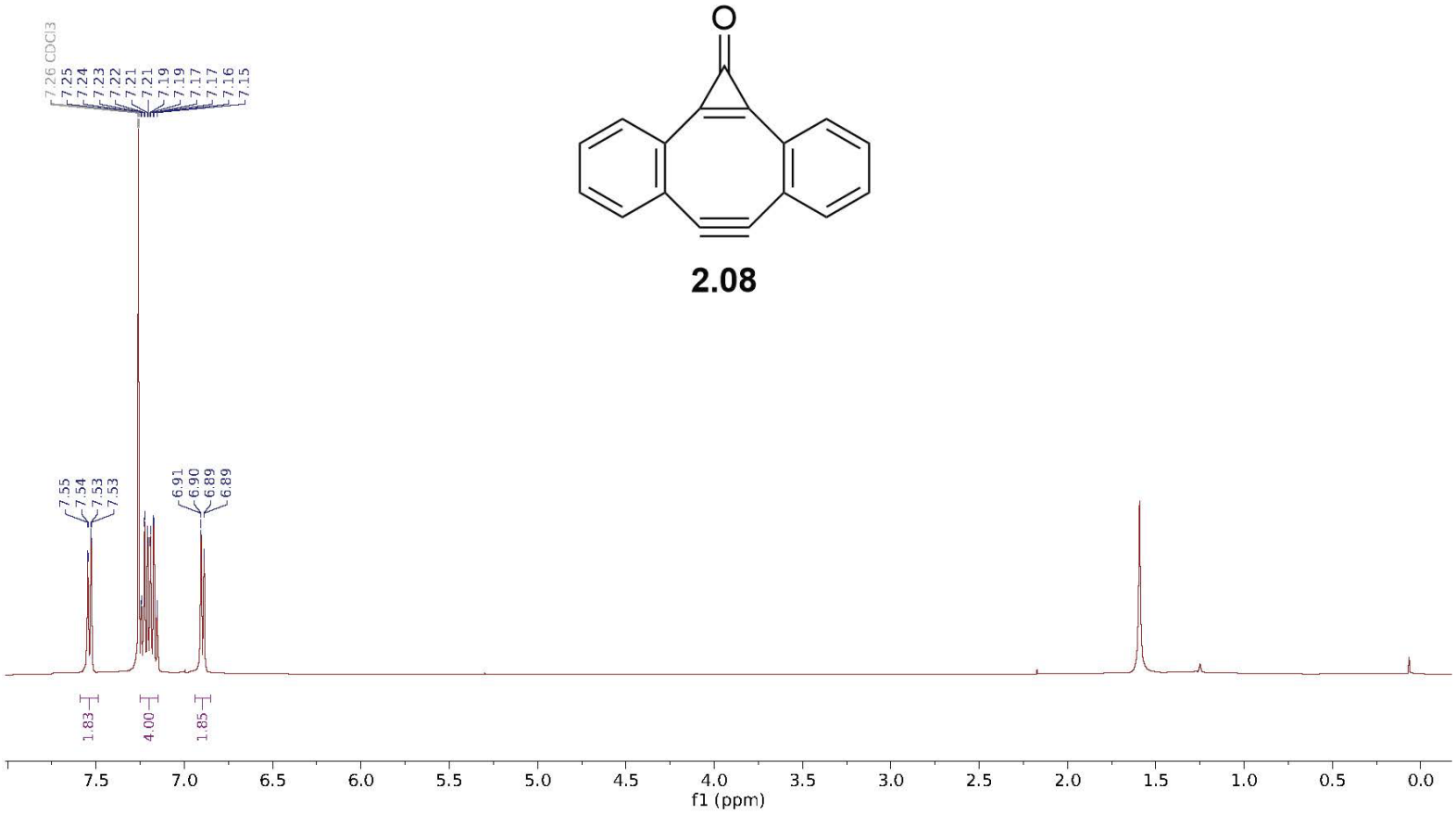

2.08

^{13}C NMR (101 MHz, $CDCl_3$) δ 150.76, 135.35, 133.84, 132.24, 130.24, 127.35, 125.33, 106.93.

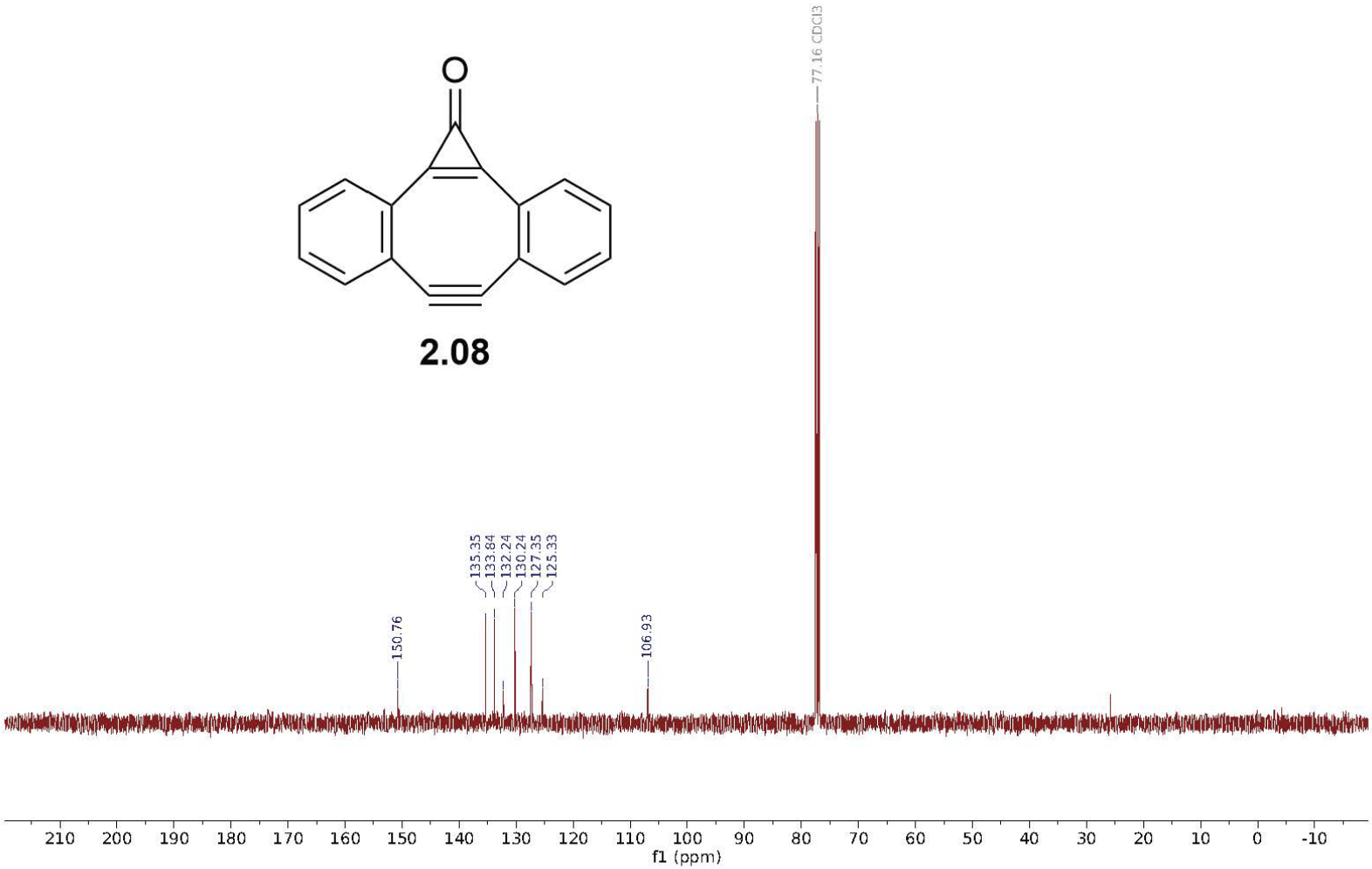

^{1}H NMR (400 MHz, Chloroform-*d*) δ 7.89 (d, *J* = 7.7 Hz, 1H), 7.71 (d, *J* = 7.8 Hz, 1H), 7.68 – 7.52 (m, 5H), 7.47 (t, *J* = 7.5 Hz, 1H), 4.46 (ddd, *J* = 14.1, 6.6, 4.4 Hz, 1H), 4.31 (ddd, *J* = 14.2, 6.2, 4.3 Hz, 1H), 3.96 (ddd, *J* = 10.7, 6.6, 4.3 Hz, 1H), 3.87 (ddd, *J* = 10.4, 6.2, 4.4 Hz, 1H), 3.73 – 3.67 (m, 2H), 3.64 – 3.49 (m, 10H), 3.13 (s, 1H).

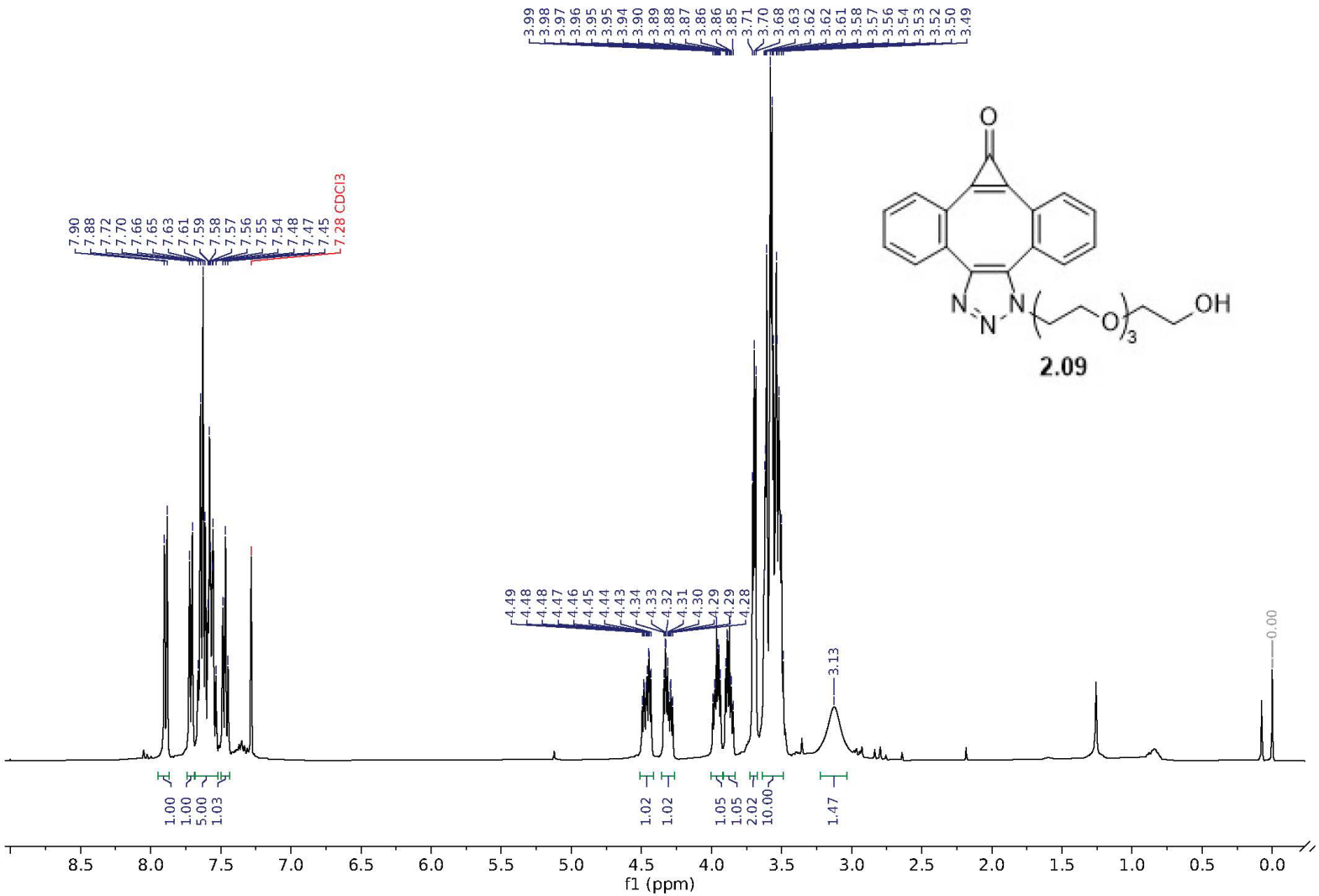

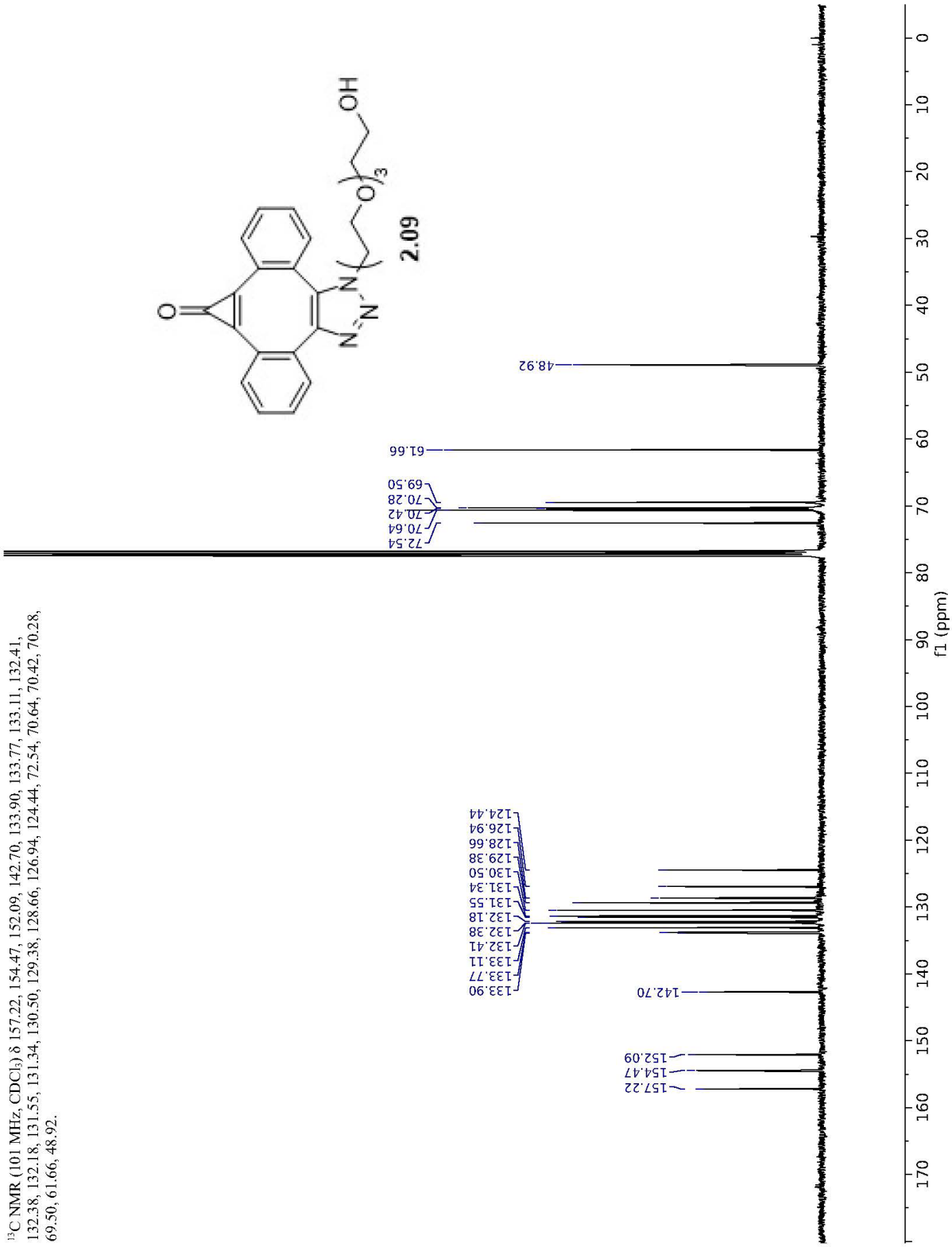

^{13}C NMR (101 MHz, $CDCl_3$) δ 157.22, 154.47, 152.09, 142.70, 133.90, 133.77, 133.11, 132.41, 132.38, 132.18, 131.55, 131.34, 130.50, 129.38, 128.66, 126.94, 124.44, 72.54, 70.64, 70.42, 70.28, 69.50, 61.66, 48.92.

^{1}H NMR (400 MHz, $CDCl_3$) δ 8.68 (d, *J* = 4.9 Hz, 1H), 8.21 (d, *J* = 4.8 Hz, 1H), 8.08 (d, *J* = 7.8 Hz, 1H), 7.83 7.72 (m, 1H), 7.56 (t, *J* = 8.5 Hz, 2H), 7.44 (d, *J* = 7.7 Hz, 1H), 7.35 7.27 (m, 2H), 7.23 (t, *J* = 6.4 Hz, 1H), 7.14 (dd, *J* = 7.7, 5.0 Hz, 1H), 7.05 (dt, *J* = 7.6, 3.8 Hz, 1H), 6.98 (t, *J* = 7.7 Hz, 1H), 6.86 (d, *J* = 7.8 Hz, 1H), 6.75 (d, *J* = 7.9 Hz, 1H), 4.79 4.68 (m, 1H), 4.66 4.54 (m, 1H), 4.31 4.20 (m, 1H), 4.12 4.03 (m, 1H), 3.71 3.53 (m, 12H).

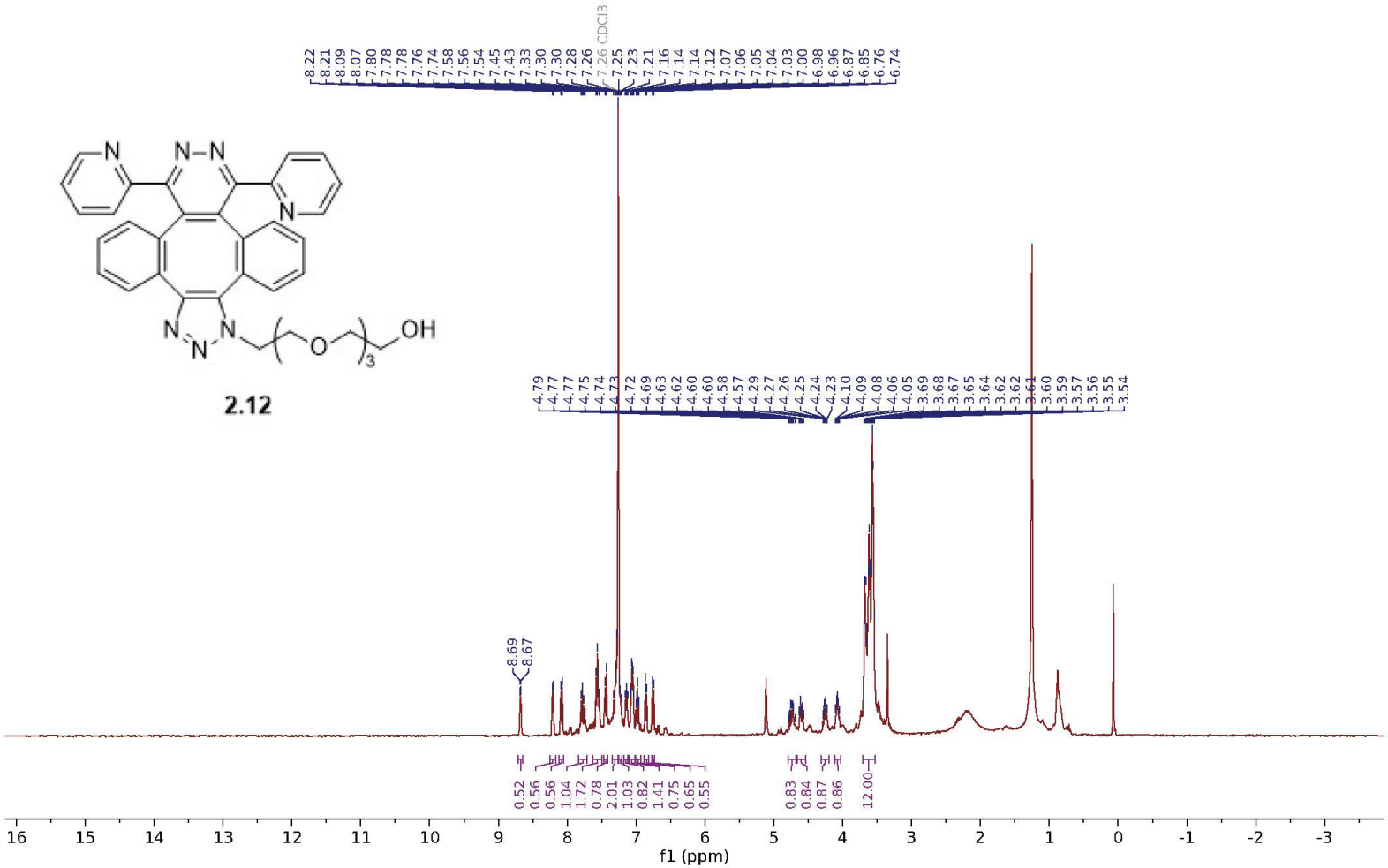

^{1}H NMR (400 MHz, $CDCl_3$) δ 7.90 – 7.83 (m, 2H), 7.69 – 7.65 (m, 2H), 7.63 – 7.49 (m, 10H), 7.45 (tt, *J* = 7.6, 1.5 Hz, 2H), 4.45 – 4.37 (m, 2H), 4.31 – 4.22 (m, 2H), 3.99 – 3.92 (m, 2H), 3.82 (dt, *J* = 10.4, 5.3 Hz, 2H), 3.52 – 3.43 (m, 8H).

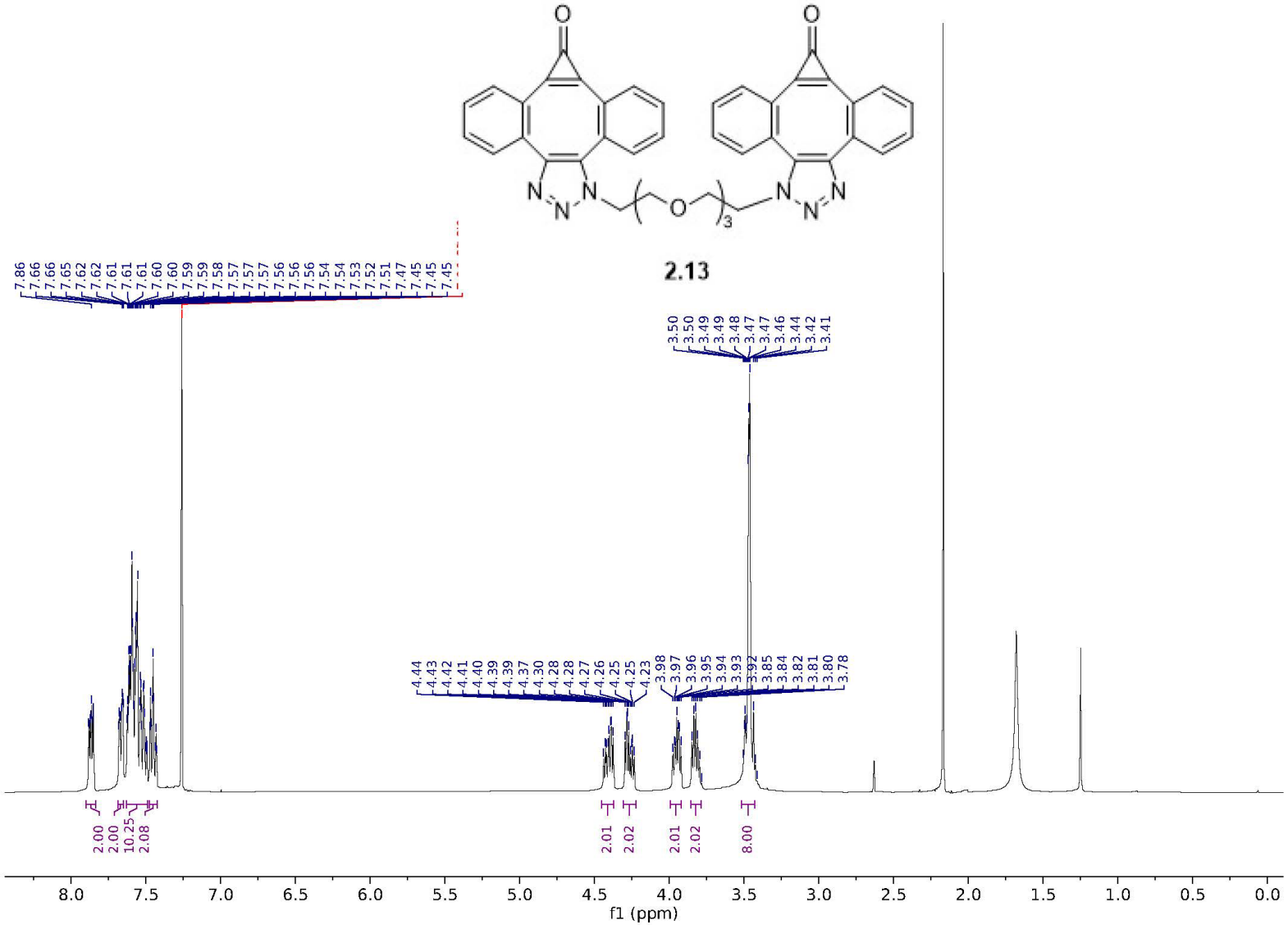

^{13}C NMR (101 MHz, $CDCl_3$) δ 157.49, 154.67, 152.04, 142.83, 133.93, 133.87, 133.18, 132.53, 132.38, 132.28, 131.58, 131.41, 130.58, 129.47, 128.71, 127.11, 124.59, 70.74, 70.58, 69.60, 48.96.

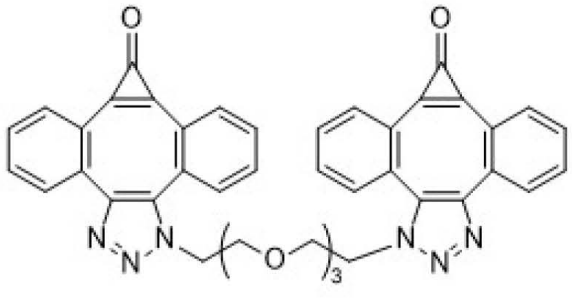

2.13

^{1}H NMR (400 MHz, CDCl$_3$) δ 7.58 (d, J = 8.6 Hz, 1H), 7.03 (d, J = 2.5 Hz, 1H), 6.89 (dd, J = 8.7, 2.5 Hz, 1H), 4.58 (s, 2H), 3.87 (s, 3H).

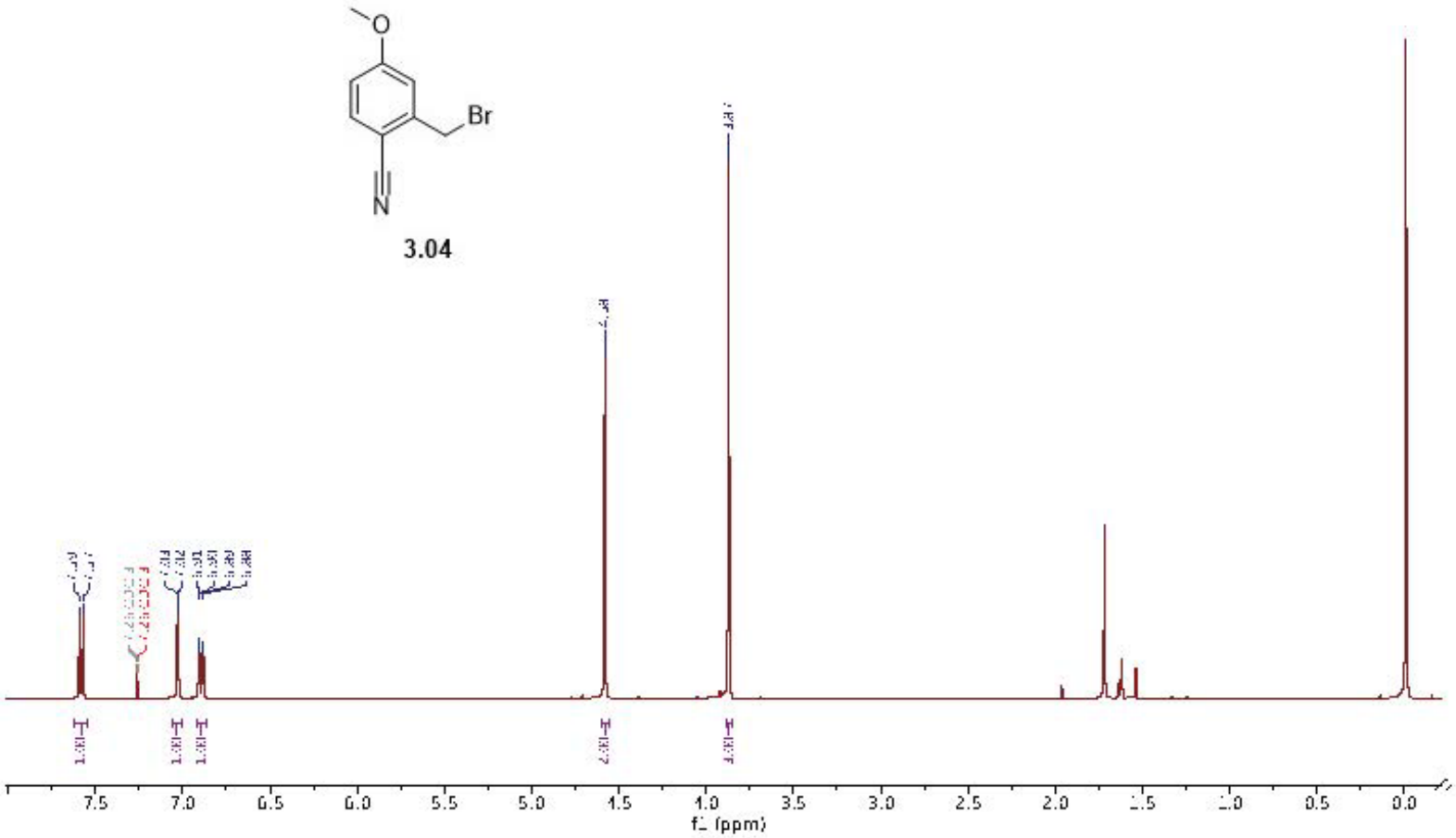

^{13}C NMR (101 MHz, $CDCl_3$) δ 163.11, 143.21, 135.00, 117.31, 116.12, 114.83, 104.07, 55.85, 29.59, 25.28.

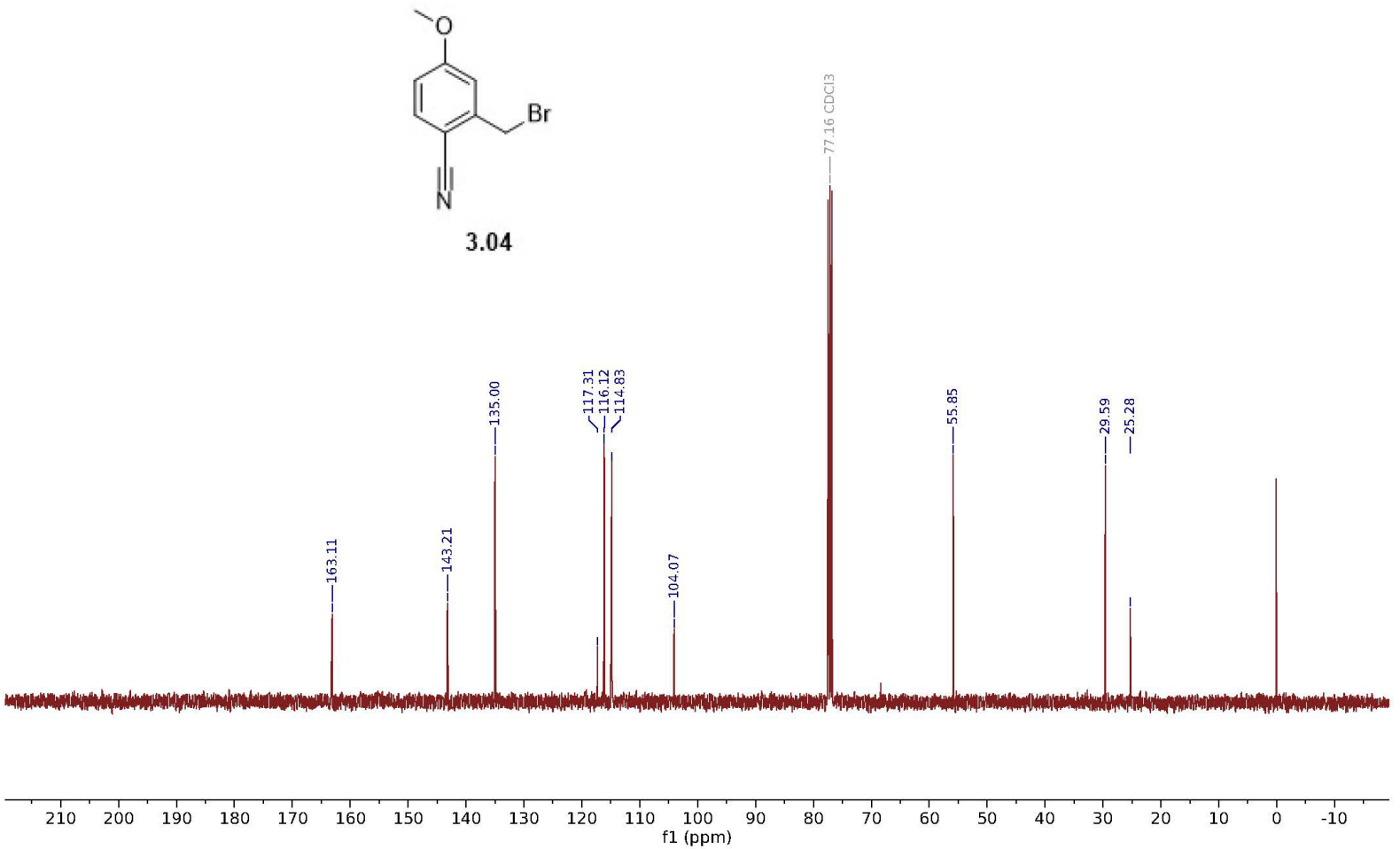

^{1}H NMR (400 MHz, $CDCl_3$) δ 7.70 (d, J = 7.0 Hz, 2H), 7.64 (t, J = 7.5 Hz, 1H), 7.48 (t, J = 7.8 Hz, 2H), 7.43 (d, J = 8.7 Hz, 1H), 7.04 (d, J = 2.6 Hz, 1H), 6.91 (dd, J = 8.7, 2.6 Hz, 1H), 4.50 (s, 2H), 3.83 (s, 3H).

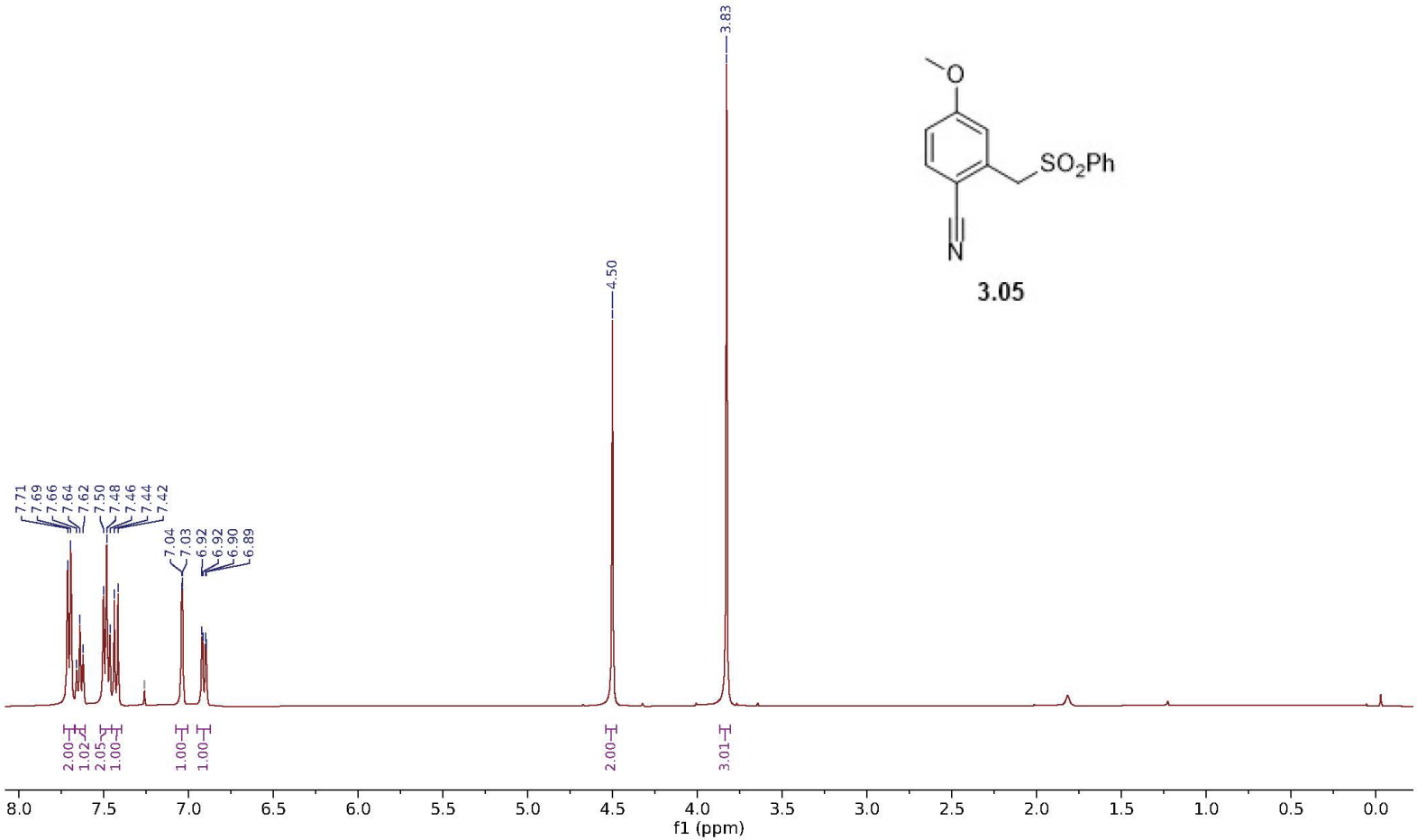

3.05

^{13}C NMR (101 MHz, $CDCl_3$) δ 162.70, 137.51, 134.35, 133.58, 129.31, 128.69, 117.42, 117.06, 115.57, 105.84, 60.51, 55.83.

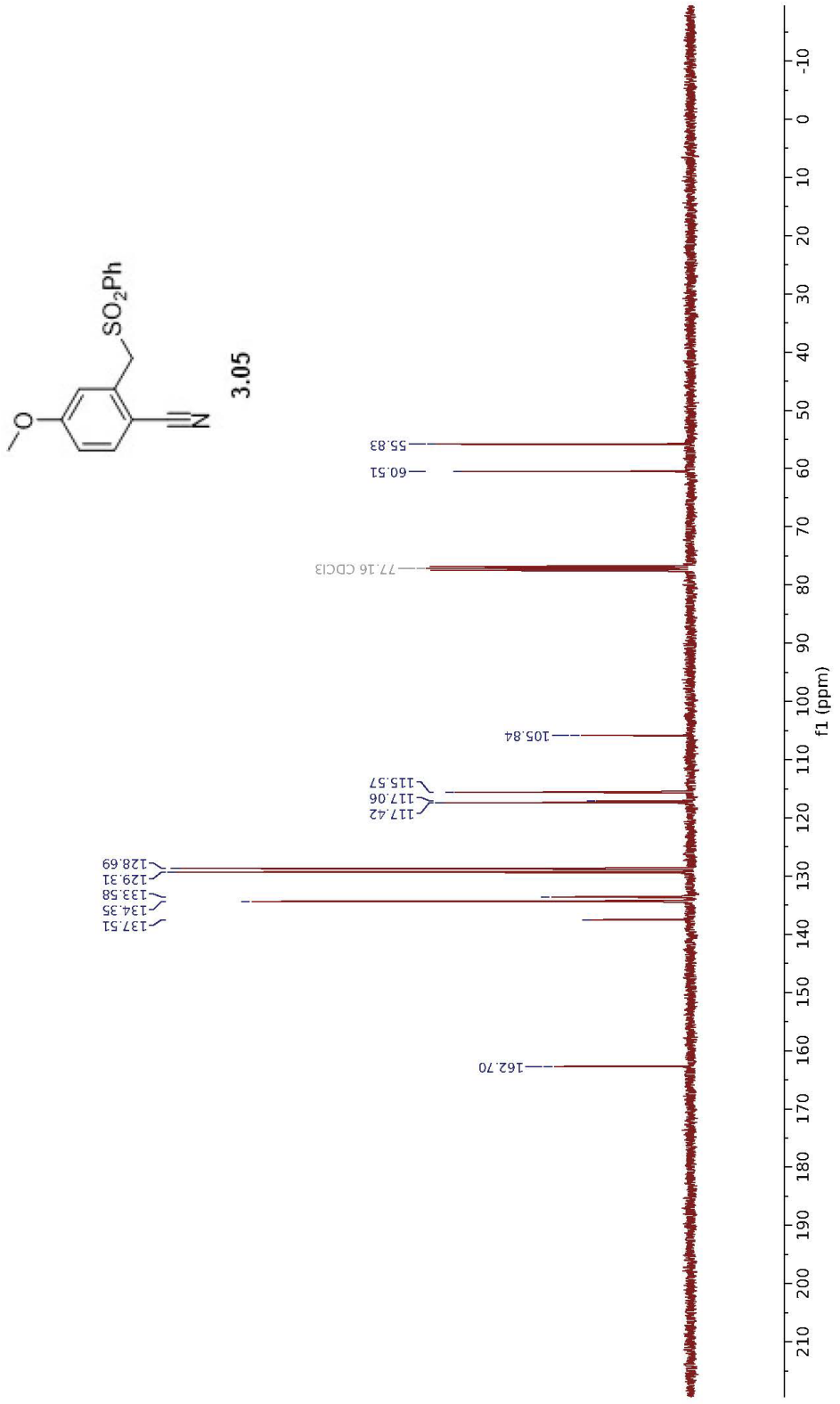

^{1}H NMR (500 MHz, DMSO) δ 10.27 (s, 1H), 7.77 (s, J = 7.5 Hz, 1H), 7.72 (d, J = 7.0 Hz, 2H), 7.62 (dd, J = 15.8, 7.8 Hz, 3H), 6.88 (dd, J = 8.5, 2.7 Hz, 1H), 6.79 (d, J = 2.7 Hz, 1H), 4.72 (s, 2H).

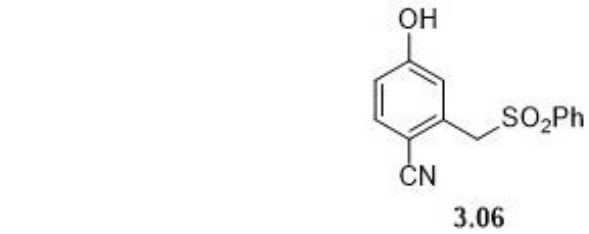

3.06

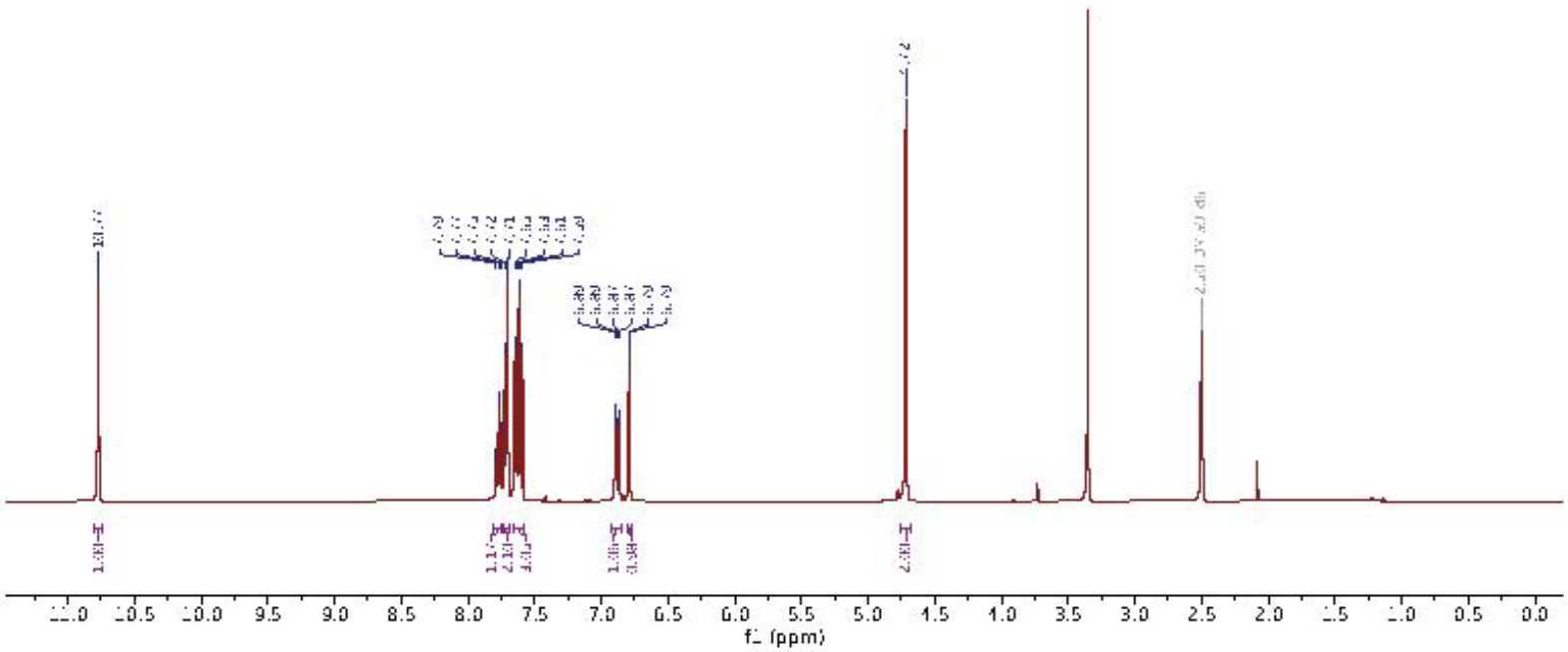

^{13}C NMR (101 MHz, DMSO) δ 161.09, 137.90, 134.88, 134.37, 133.61, 129.48, 128.15, 119.38, 117.65, 116.59, 103.55, 59.45.

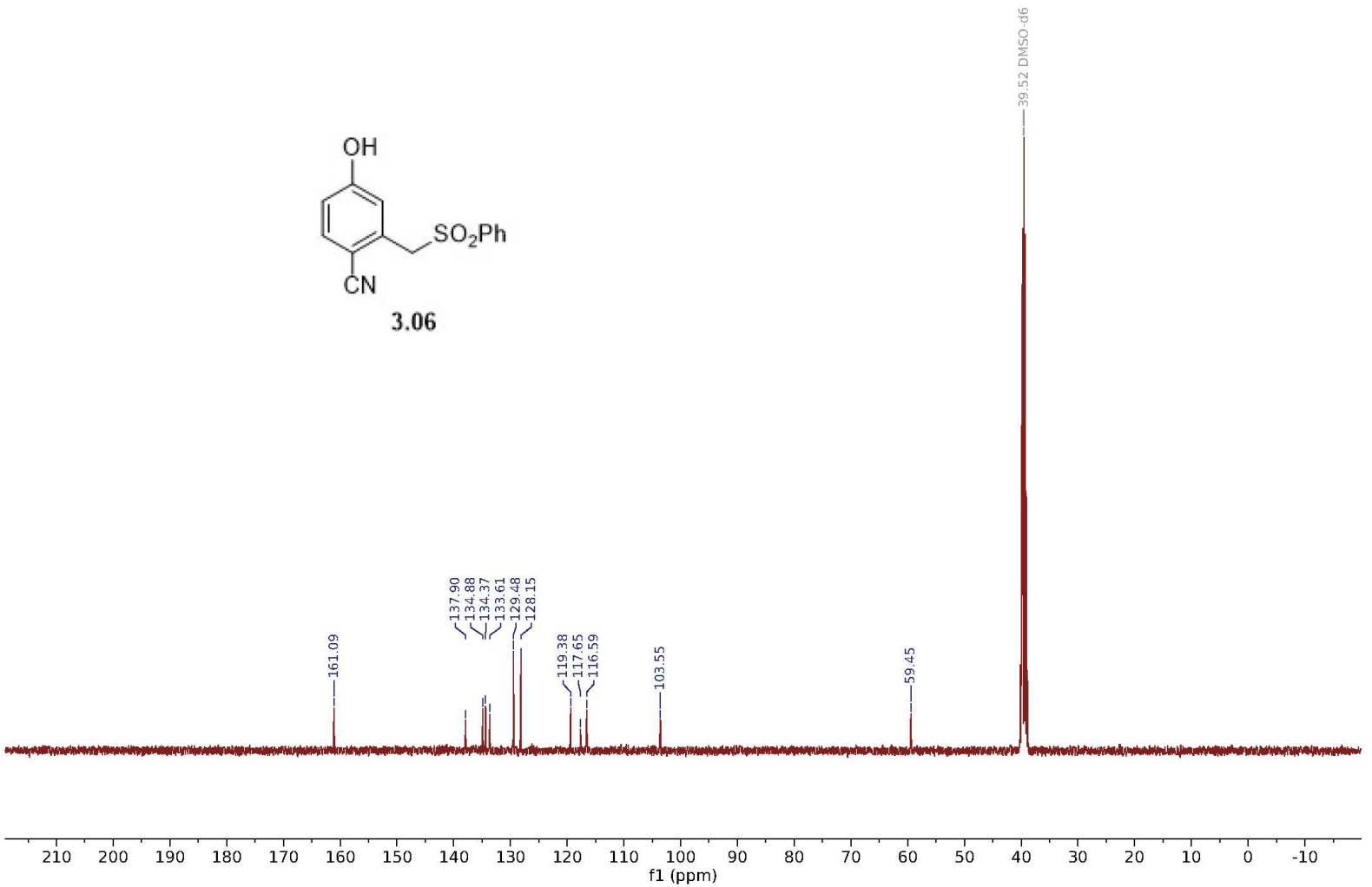

^{1}H NMR (400 MHz, $CDCl_3$) δ 7.73 (d, *J* = 6.9 Hz, 2H), 7.70 – 7.62 (m, 5H), 7.50 (t, *J* = 7.8 Hz, 2H), 7.46 – 7.34 (m, 7H), 7.09 (d, *J* = 2.5 Hz, 1H), 6.89 (dd, *J* = 8.7, 2.5 Hz, 1H), 4.51 (s, 2H), 3.99 (t, *J* = 6.4 Hz, 2H), 3.70 (t, *J* = 6.1 Hz, 2H), 1.80 (p, *J* = 6.7 Hz, 2H), 1.63 (q, *J* = 6.7 Hz, 2H), 1.55 (t, *J* = 7.7 Hz, 2H), 1.06 (s, 9H).

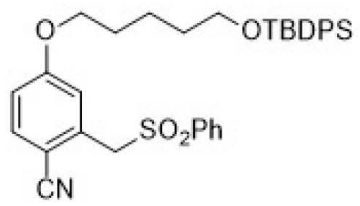

3.07

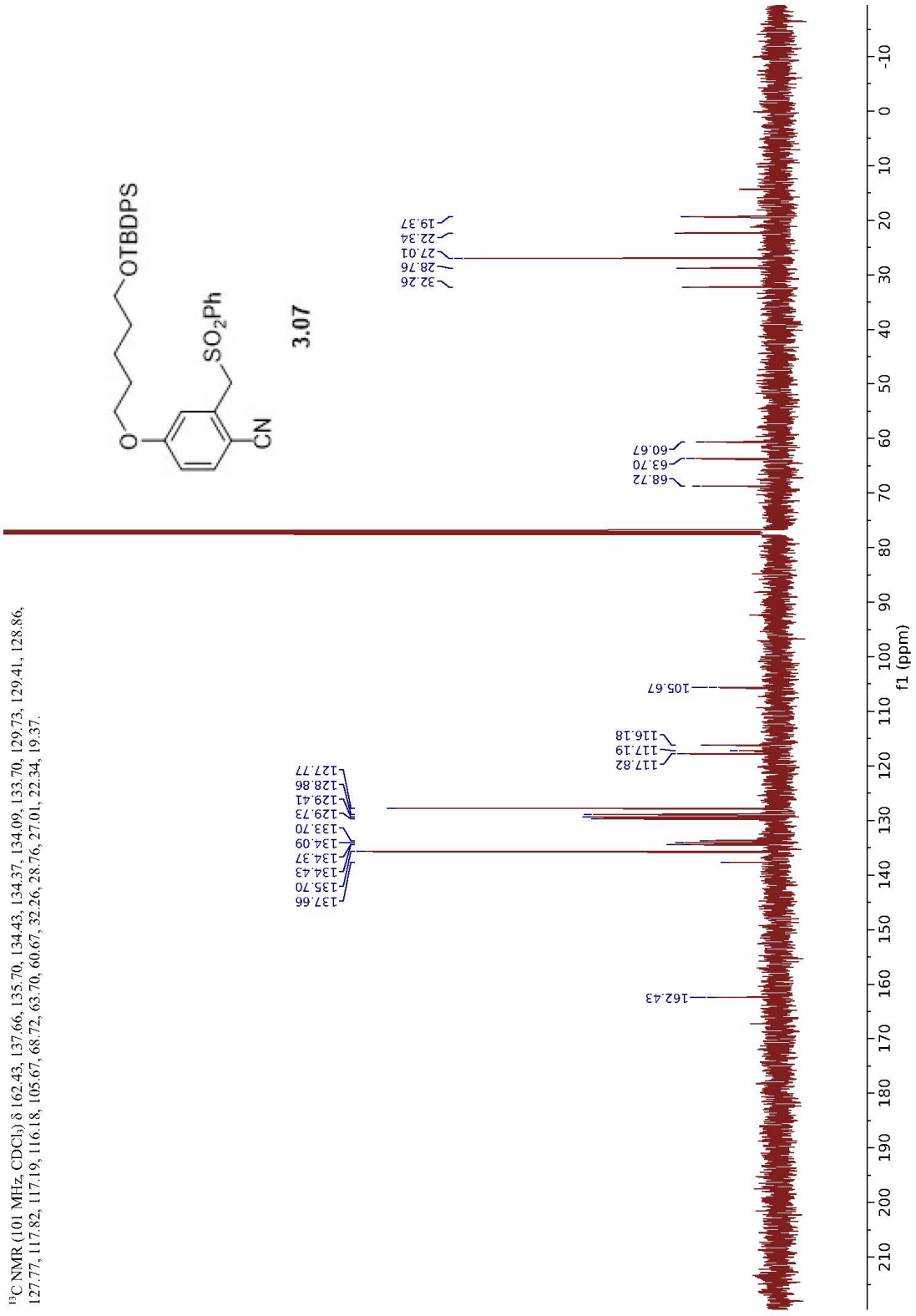

^{13}C NMR (101 MHz, $CDCl_3$) δ 162.43, 137.66, 135.70, 134.43, 134.37, 134.09, 133.70, 129.73, 129.41, 128.86, 127.77, 117.82, 117.19, 116.18, 105.67, 68.72, 63.70, 60.67, 32.26, 28.76, 27.01, 22.34, 19.37.

^{1}H NMR (400 MHz, $CDCl_3$) δ 9.63 (s, 1H), 7.75 – 7.64 (m, 7H), 7.63 – 7.55 (m, 2H), 7.47 – 7.36 (m, 9H), 7.00 – 6.94 (m, 2H), 5.04 (s, 2H), 4.01 (t, J = 6.4 Hz, 2H), 3.71 (t, J = 6.1 Hz, 2H), 1.80 (p, J = 6.7 Hz, 2H), 1.68 – 1.61 (m, 2H), 1.58 – 1.52 (m, 2H), 1.06 (s, 9H).

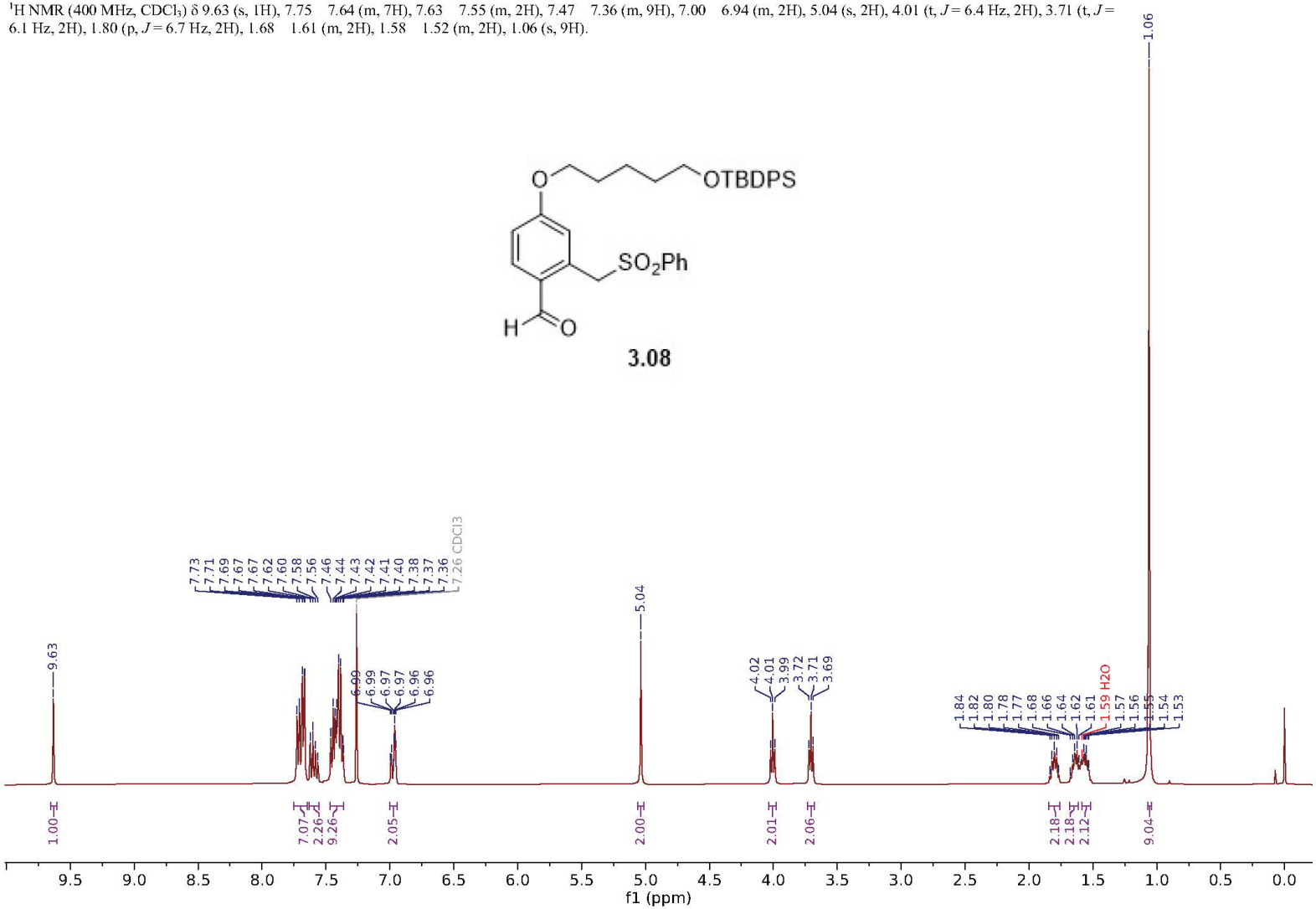

^{13}C NMR (101 MHz, $CDCl_3$) δ 190.81, 163.03, 138.45, 137.43, 135.70, 134.93, 134.11, 133.89, 131.32, 129.79, 129.72, 128.91, 128.86, 127.85, 127.79, 127.76, 119.87, 115.03, 68.64, 63.73, 57.72, 32.27, 28.82, 27.01, 22.35, 19.37.

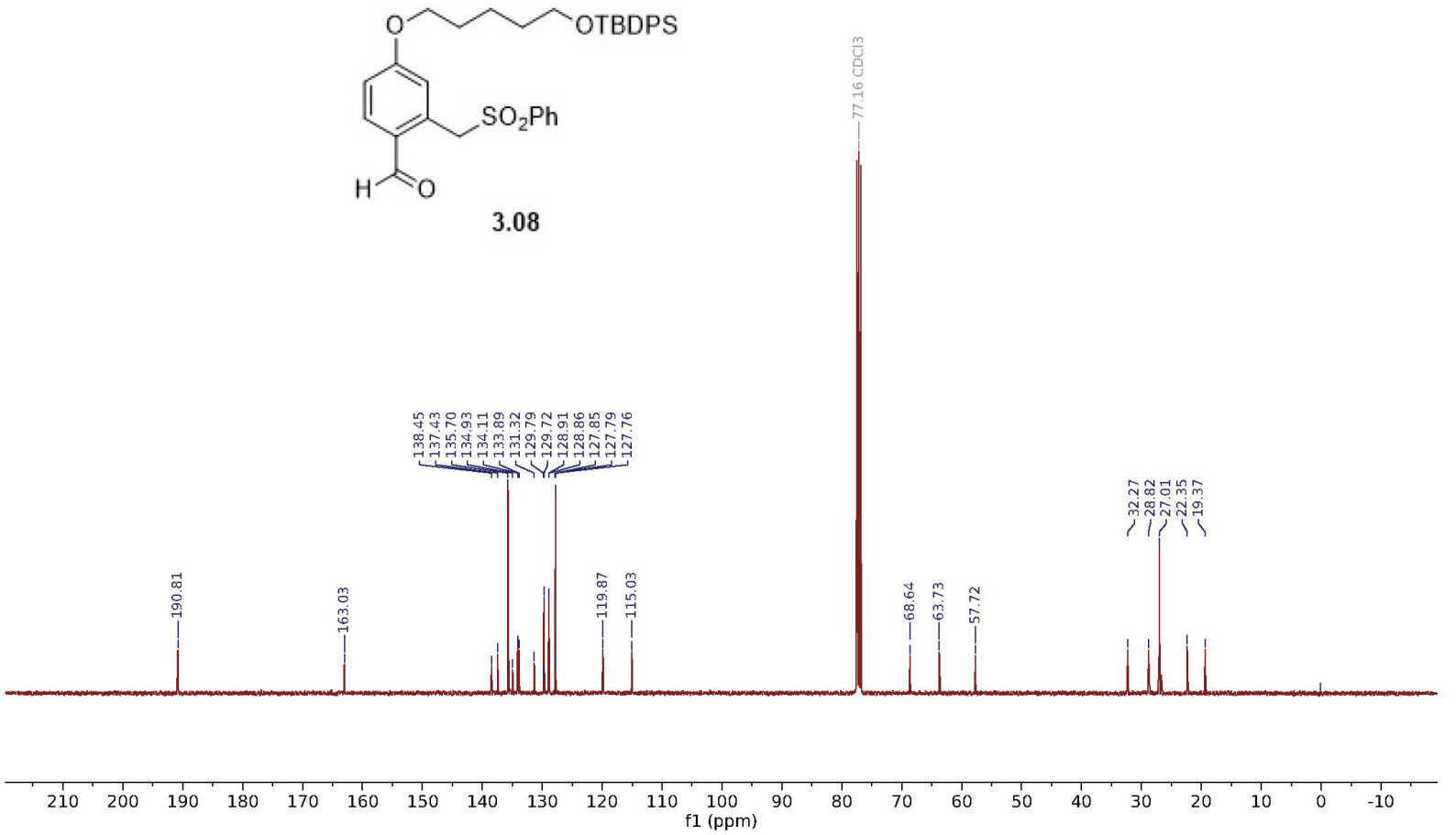

^{1}H NMR (400 MHz, $CDCl_3$) δ 7.67 7.63 (m, 8H), 7.63 7.57 (m, 2H), 7.48 7.42 (m, 8H), 7.40 7.32 (m, 14H), 6.96 (d, J = 2.5 Hz, 2H), 6.86 (d, J = 8.6 Hz, 2H), 6.78 (dd, J = 8.6, 2.5 Hz, 2H), 3.88 3.77 (m, 4H), 3.66 (t, J = 6.3 Hz, 4H), 1.71 (p, J = 6.7 Hz, 4H), 1.63 1.57 (m, 4H), 1.52 1.44 (m, 4H), 1.03 (s, 18H).

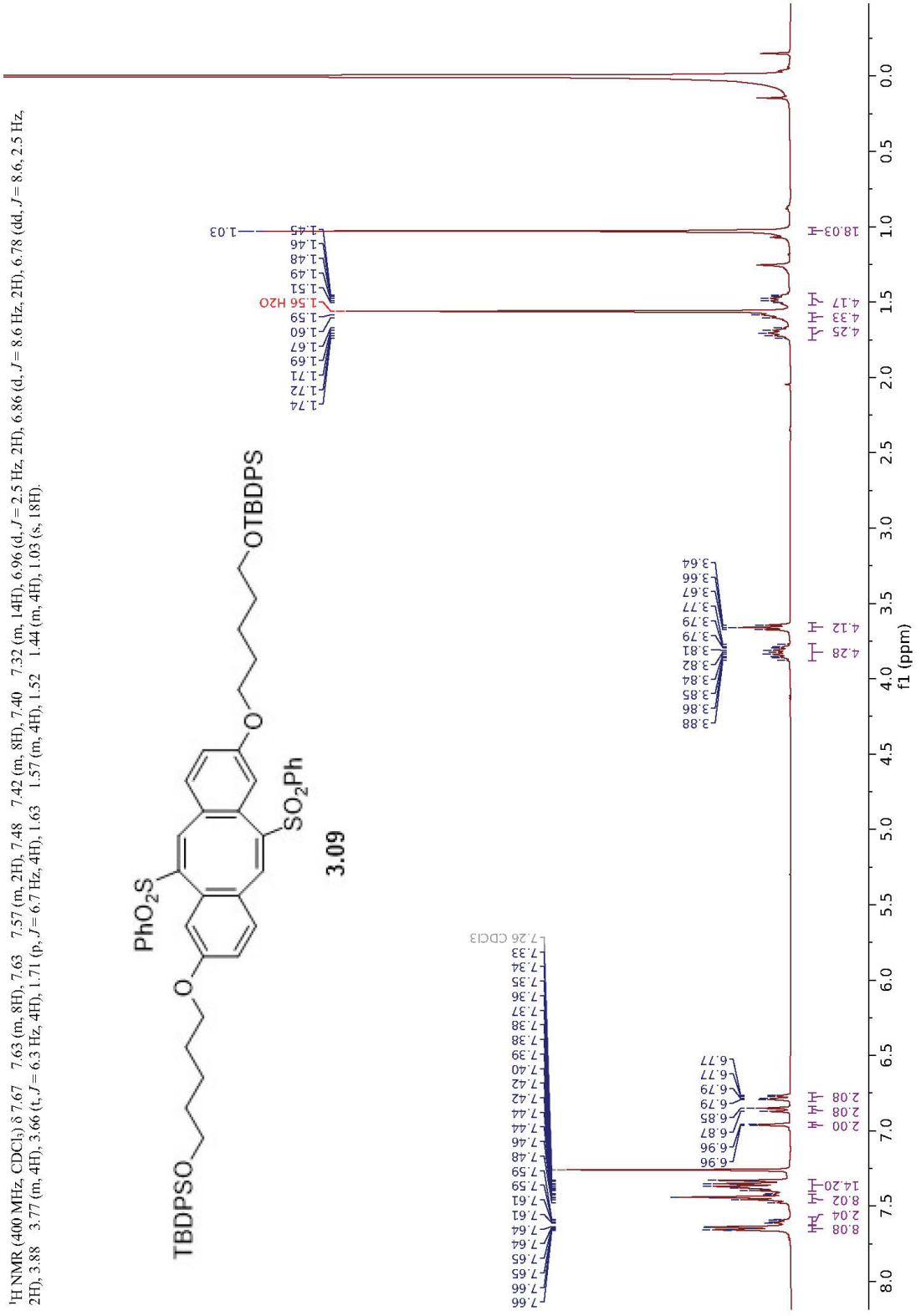

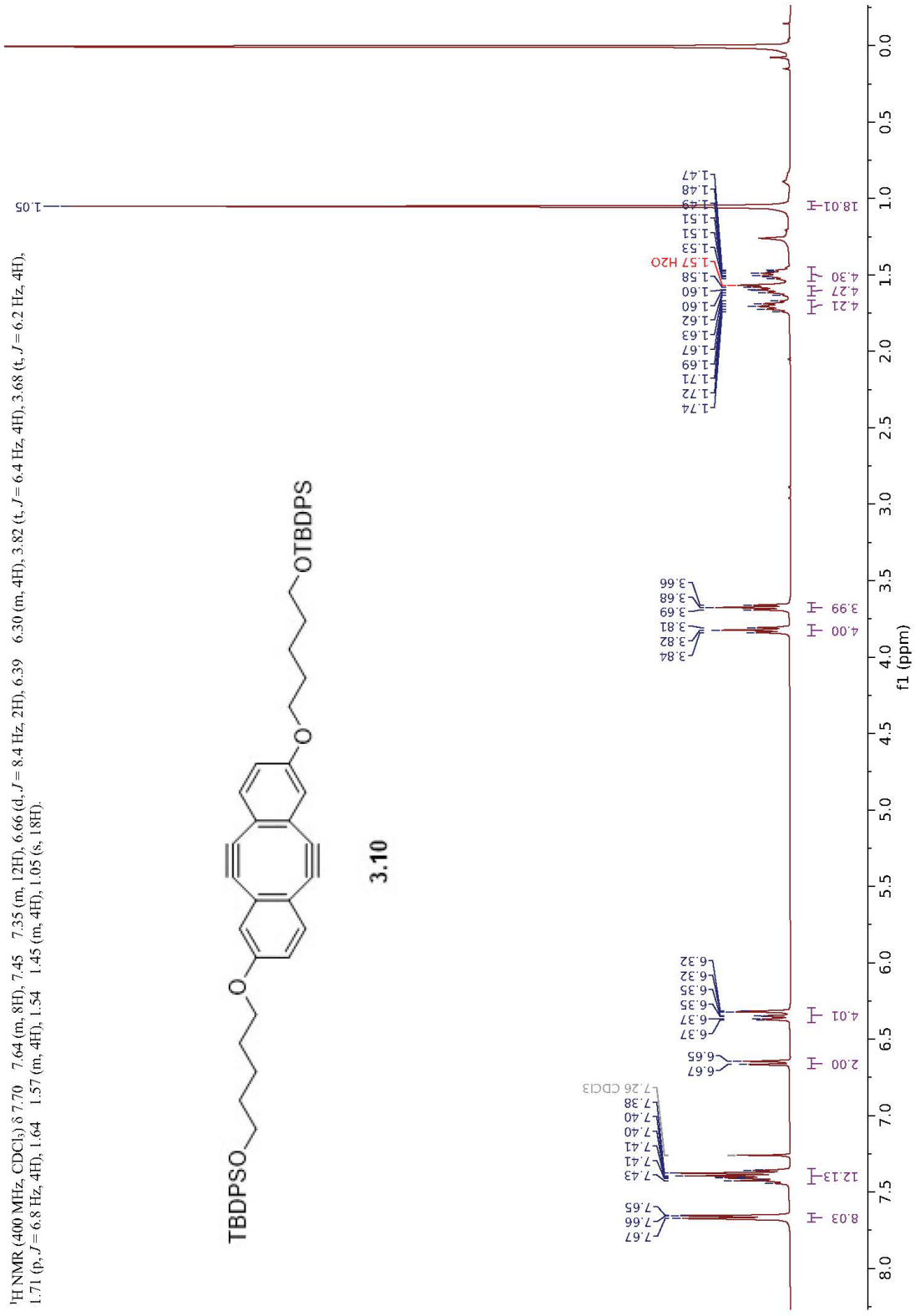

^{1}H NMR (400 MHz, $CDCl_3$) δ 7.70 7.64 (m, 8H), 7.45 7.35 (m, 12H), 6.66 (d, J = 8.4 Hz, 2H), 6.39 6.30 (m, 4H), 3.82 (t, J = 6.4 Hz, 4H), 3.68 (t, J = 6.2 Hz, 4H), 1.71 (p, J = 6.8 Hz, 4H), 1.64 1.57 (m, 4H), 1.54 1.45 (m, 4H), 1.05 (s, 18H).

^{13}C NMR (101 MHz, $CDCl_3$) δ 159.93, 135.71, 134.99, 134.15, 129.70, 127.95, 127.75, 123.73, 115.08, 112.63, 110.31, 107.48, 68.12, 63.75, 32.26, 28.86, 27.01, 22.33, 19.36.

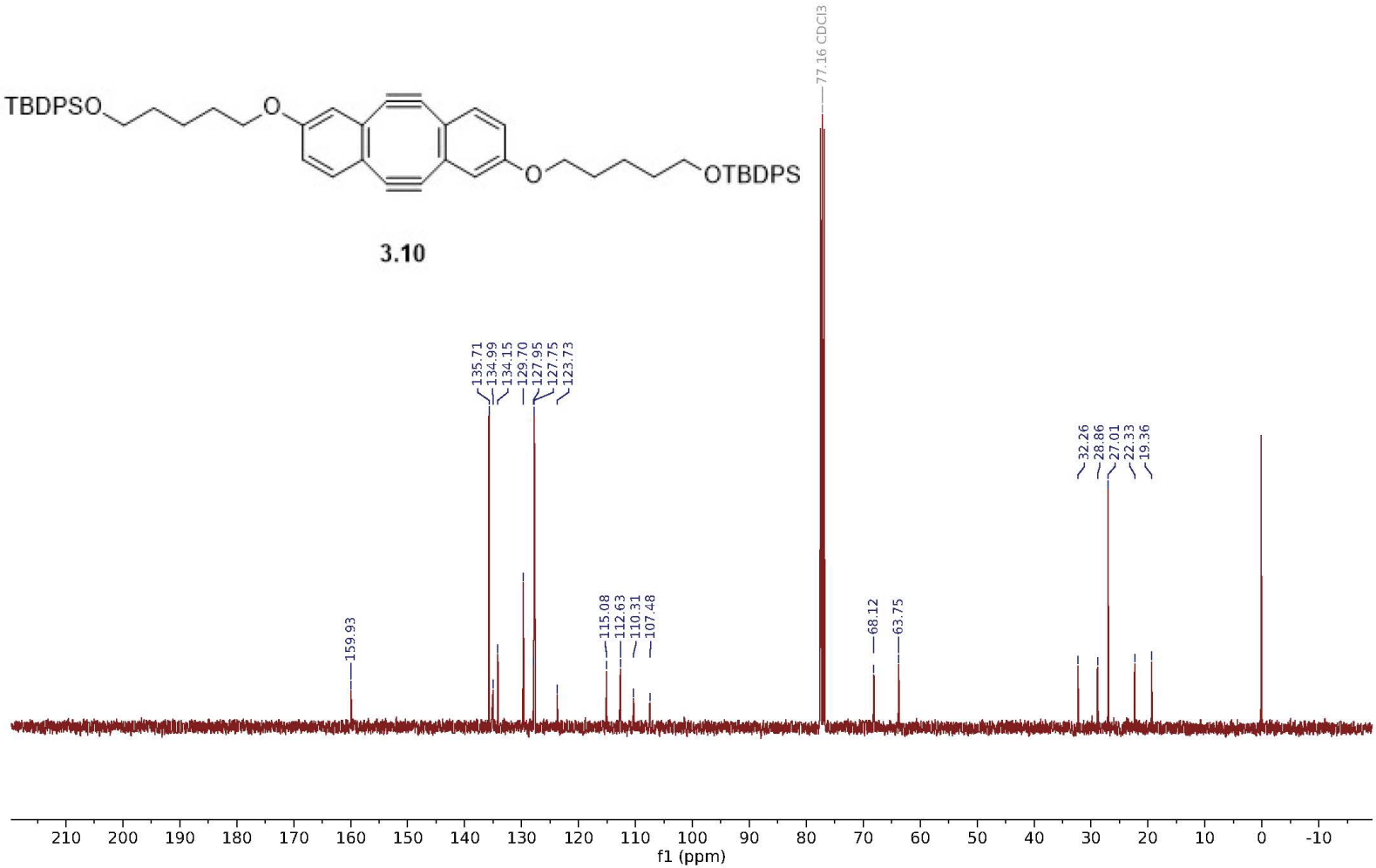

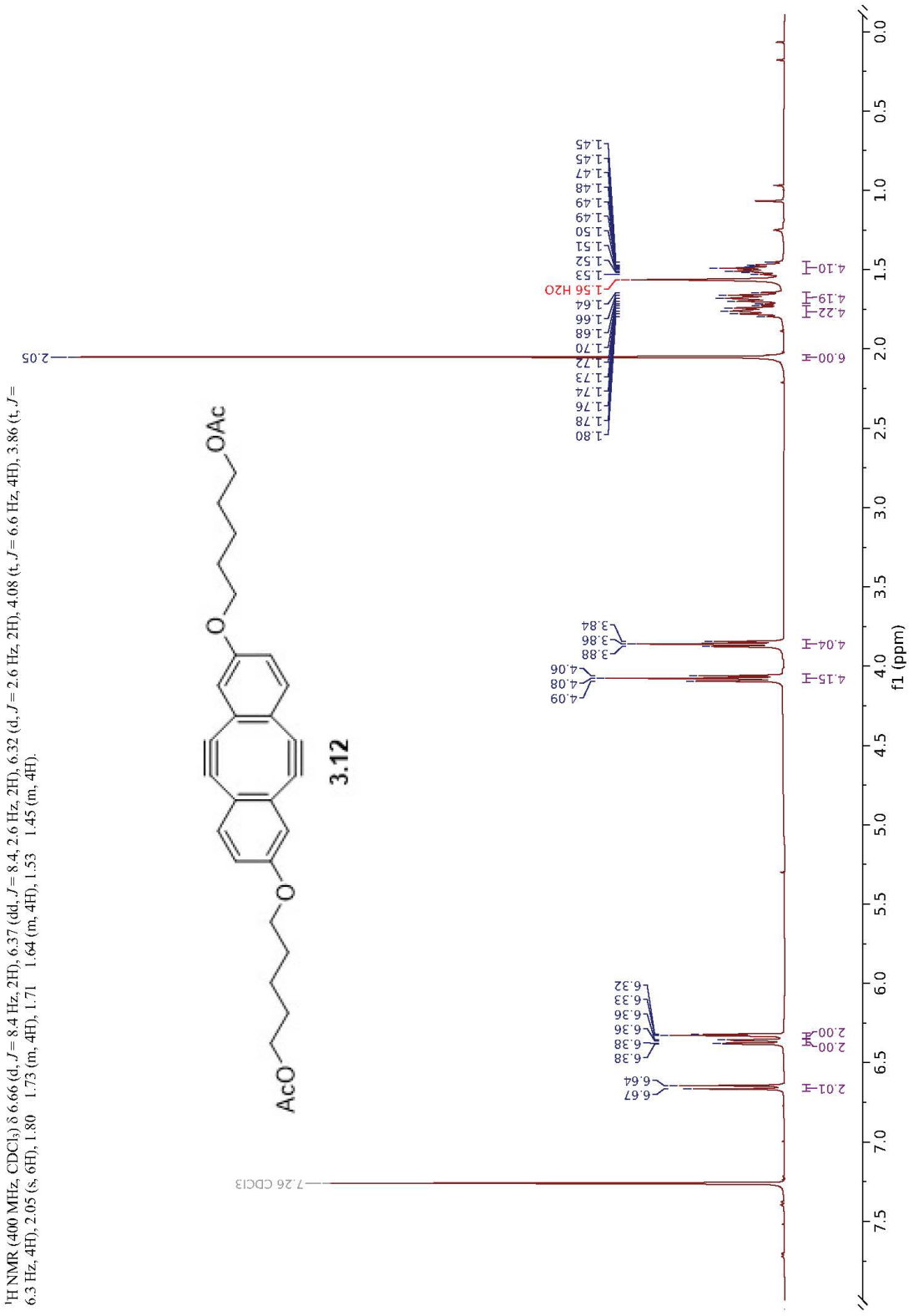

^{1}H NMR (400 MHz, $CDCl_3$) δ 6.66 (d, J = 8.4 Hz, 2H), 6.37 (dd, J = 8.4, 2.6 Hz, 2H), 6.32 (d, J = 2.6 Hz, 2H), 4.08 (t, J = 6.6 Hz, 4H), 3.86 (t, J = 6.3 Hz, 4H), 2.05 (s, 6H), 1.80 1.73 (m, 4H), 1.71 1.64 (m, 4H), 1.53 1.45 (m, 4H).

^{13}C NMR (101 MHz, $CDCl_3$) δ 159.71, 134.89, 127.85, 114.94, 112.50, 110.18, 107.33, 77.35, 77.03, 76.72, 67.79, 64.30, 28.70, 28.33, 22.54, 21.03.

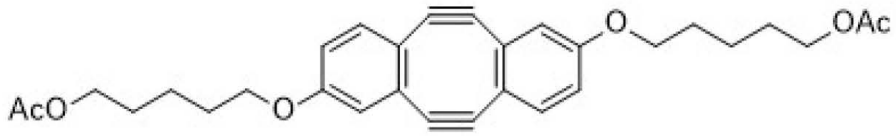

3.12

^{1}H NMR (400 MHz, $CDCl_3$) δ 9.64 (s, 1H), 7.69 (d, J = 7.1 Hz, 2H), 7.65 – 7.55 (m, 2H), 7.43 (t, J = 7.8 Hz, 2H), 6.99 (dd, J = 8.5, 2.6 Hz, 1H), 6.92 (d, J = 2.5 Hz, 1H), 5.02 (s, 2H), 3.85 (s, 3H).

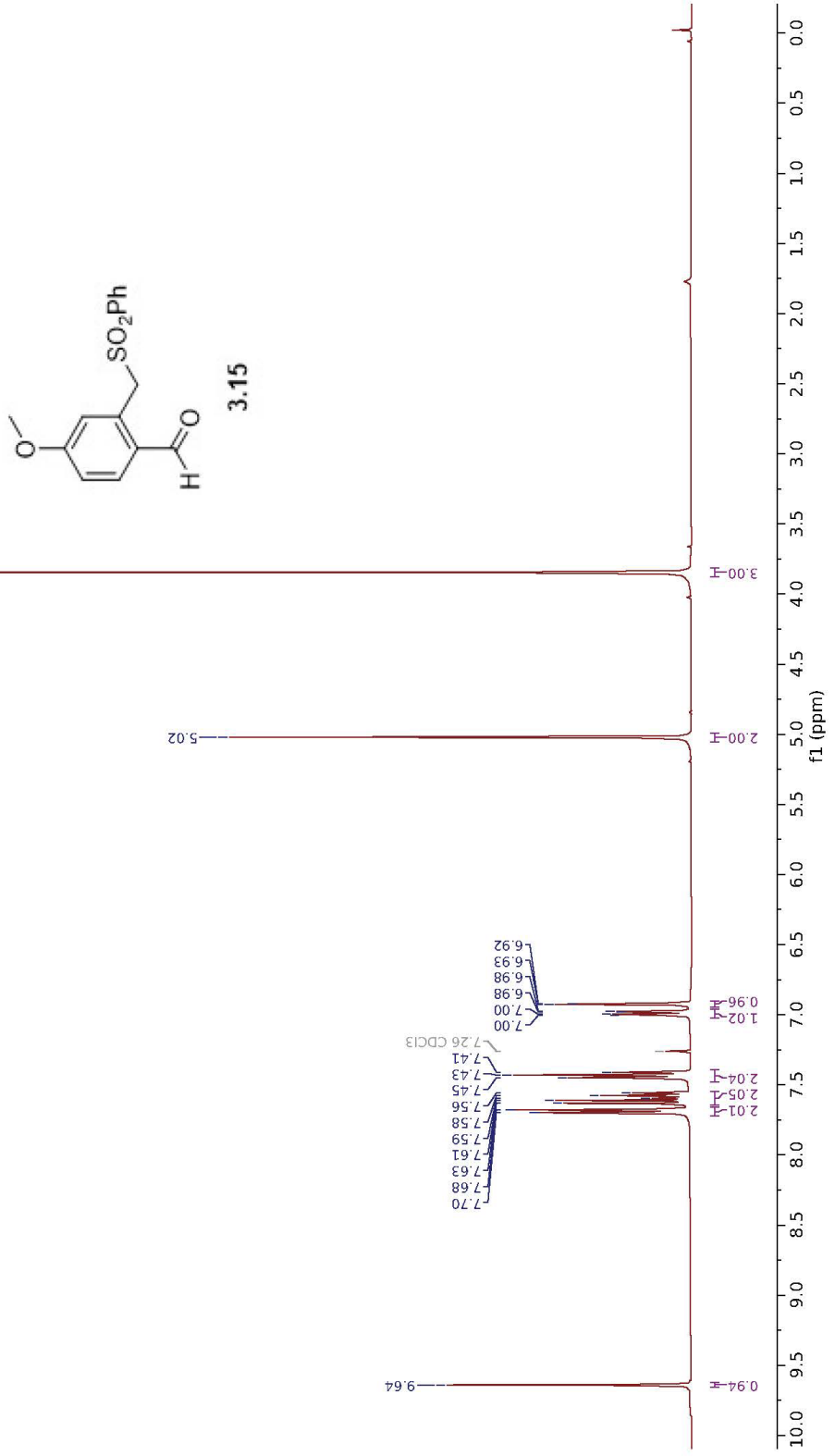

^{13}C NMR (101 MHz, $CDCl_3$) δ 190.74, 163.33, 138.33, 137.28, 133.87, 131.30, 128.87, 128.75, 127.96, 119.44, 114.48, 57.63, 55.82.

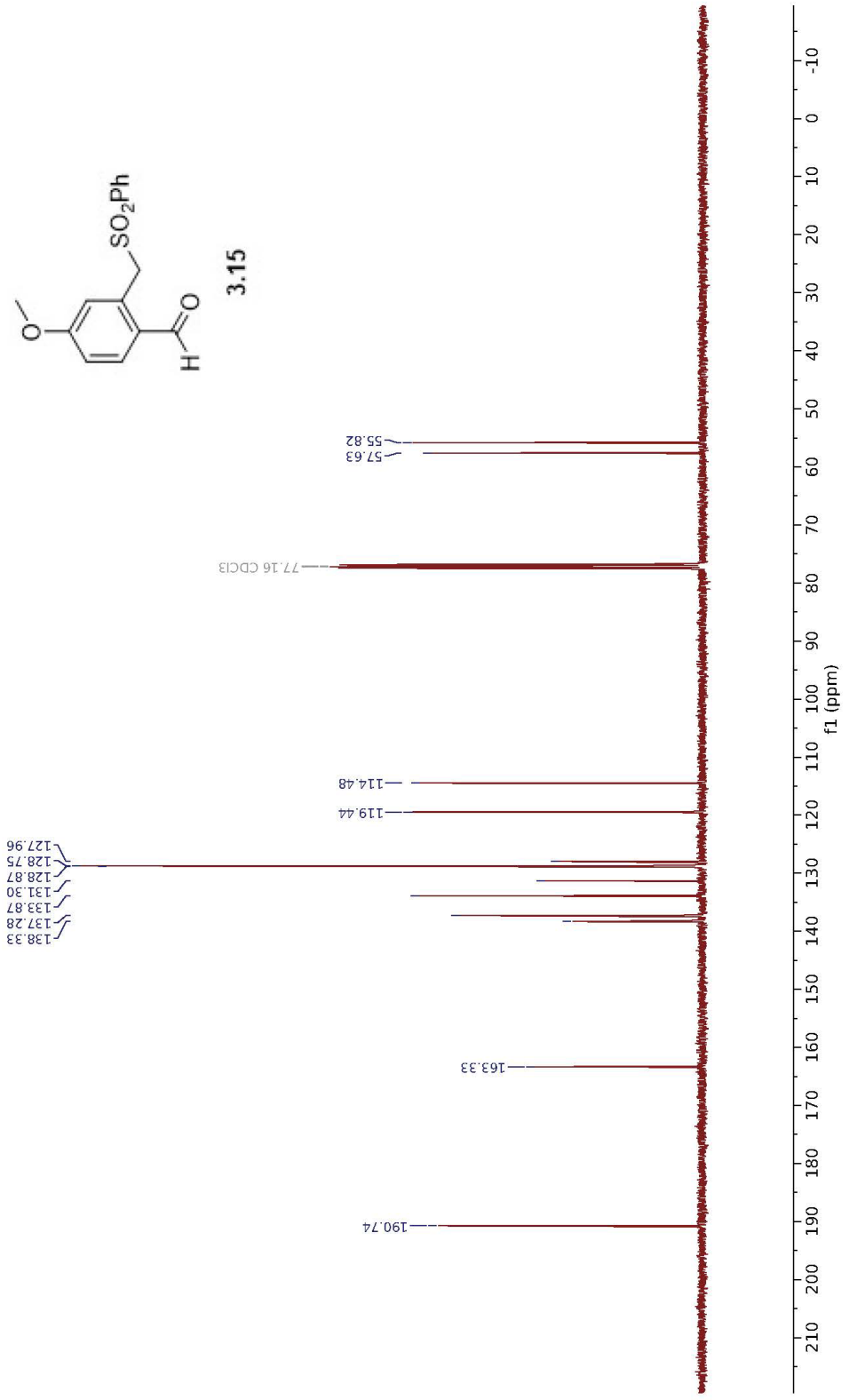

^{1}H NMR (400 MHz, $CDCl_3$) δ 7.63 (tt, J = 6.9, 1.8 Hz, 2H), 7.51 7.41 (m, 8H), 7.34 (s, 2H), 6.98 (d, J = 2.6 Hz, 2H), 6.89 (d, J = 8.6 Hz, 2H), 6.82 (dd, J = 8.6, 2.6 Hz, 2H), 3.73 (s, 6H).

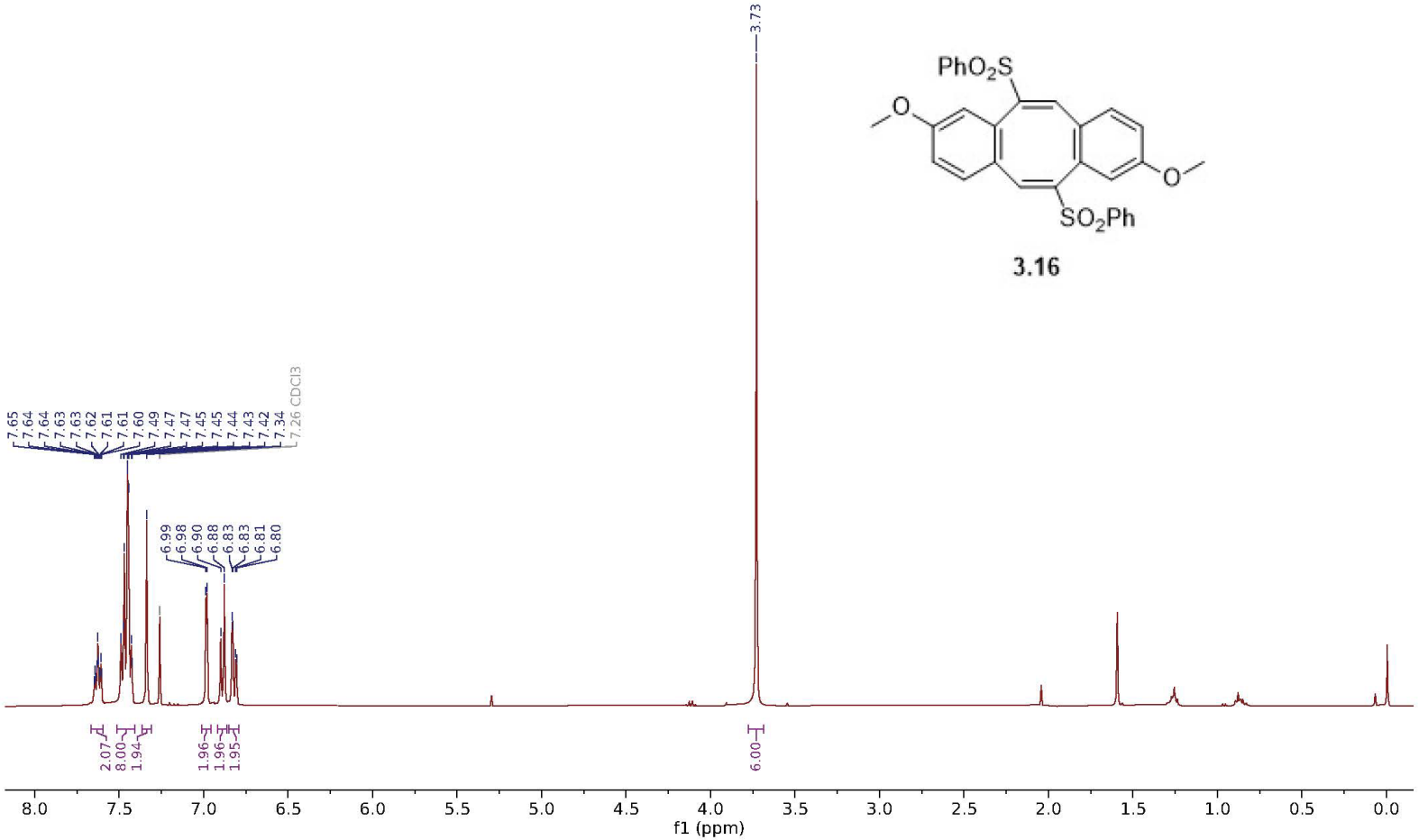

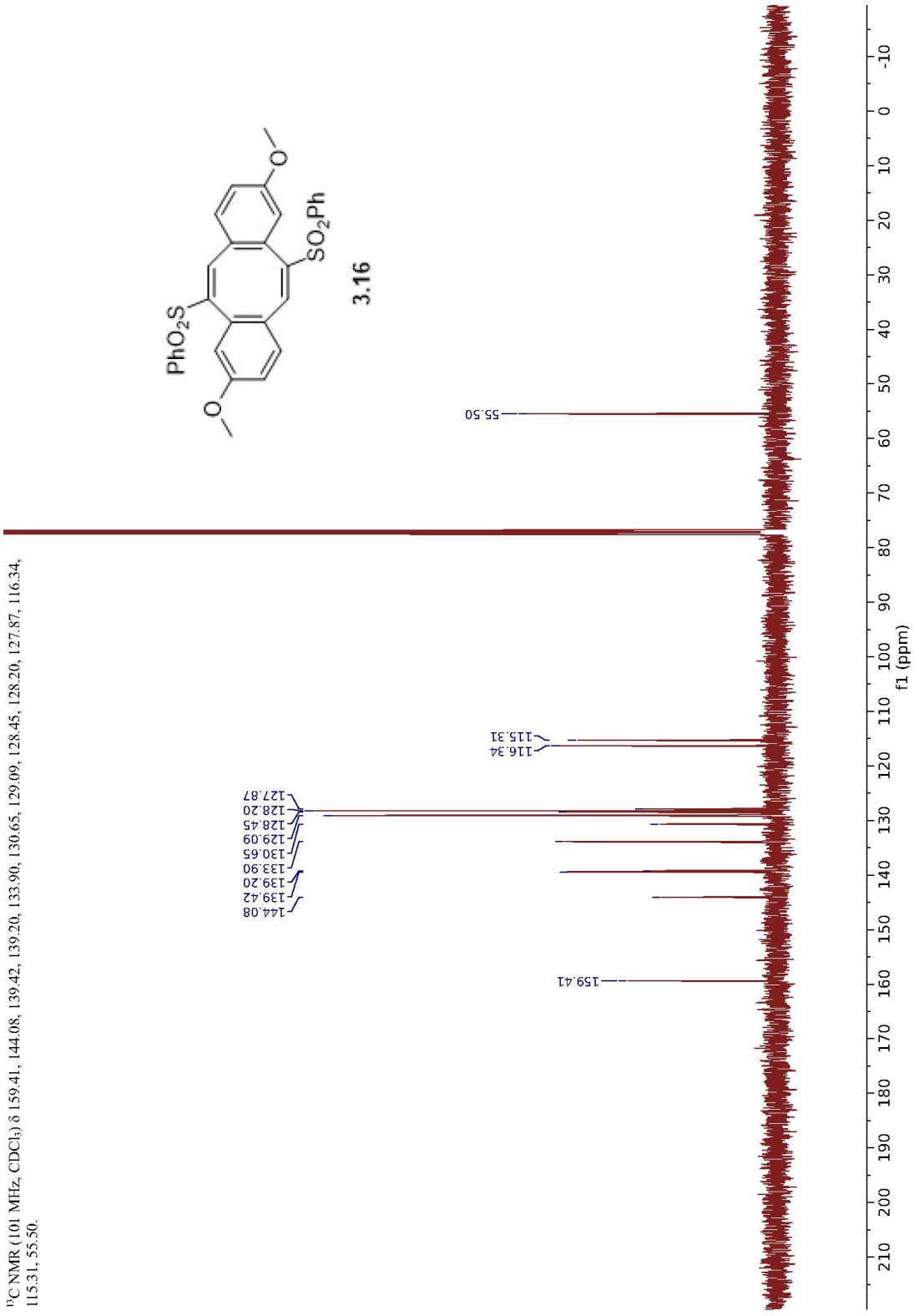

^{13}C NMR (101 MHz, $CDCl_3$) δ 159.41, 144.08, 139.42, 139.20, 133.90, 130.65, 129.09, 128.45, 128.20, 127.87, 116.34, 115.31, 55.50.

^{1}H NMR (400 MHz, DMSO-d_6) δ 9.93 (s, 2H), 7.76 (t, J = 7.5 Hz, 2H), 7.62 (t, J = 7.8 Hz, 4H), 7.35 (d, J = 7.0 Hz, 4H), 7.17 (s, 2H), 7.02 6.95 (m, 2H), 6.79 6.70 (m, 4H).

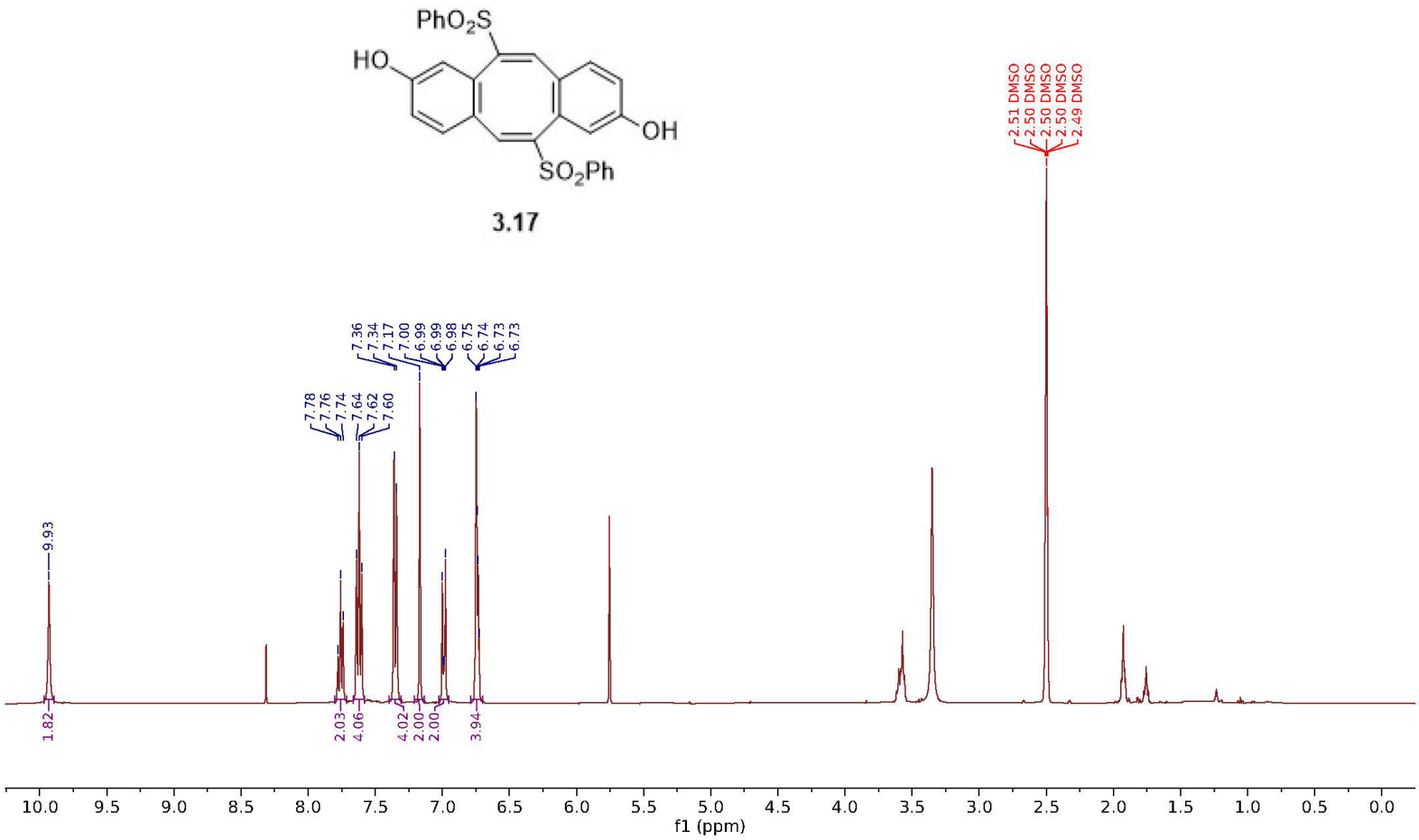

^{1}H NMR (400 MHz, Chloroform-*d*) δ 7.67 7.60 (m, 2H), 7.51 7.42 (m, 8H), 7.33 (s, 2H), 6.97 (d, *J* = 2.5 Hz, 2H), 6.91 (d, *J* = 8.6 Hz, 2H), 6.85 (dd, *J* = 8.6, 2.5 Hz, 2H), 4.21 (qt, *J* = 10.8, 6.3 Hz, 4H), 3.59 (t, *J* = 6.1 Hz, 4H).

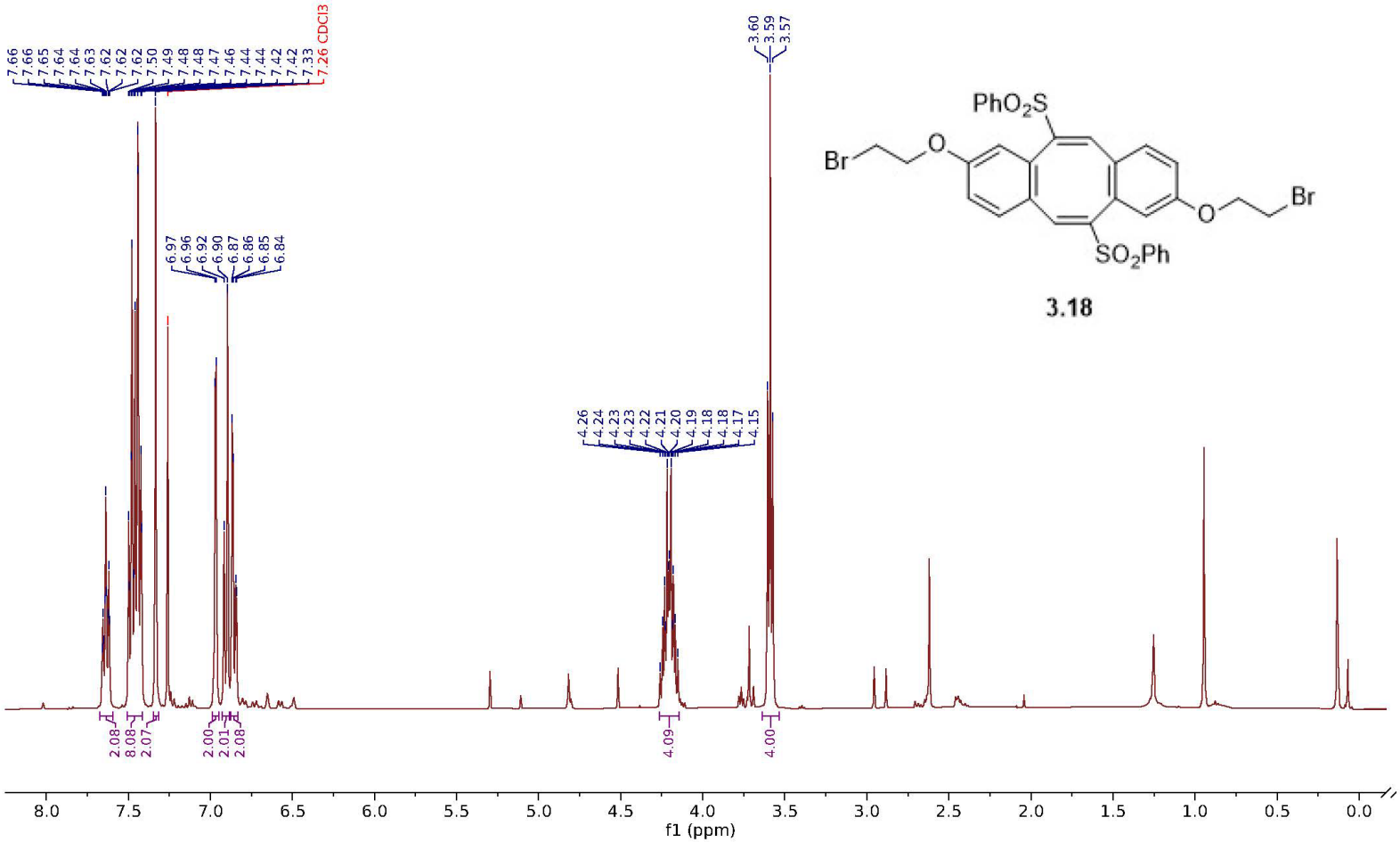

3.18

^{13}C NMR (101 MHz, $CDCl_3$) δ 157.96, 144.19, 139.30, 139.13, 134.00, 130.76, 129.15, 128.63, 128.57, 128.21, 117.08, 115.93, 67.95, 28.82.

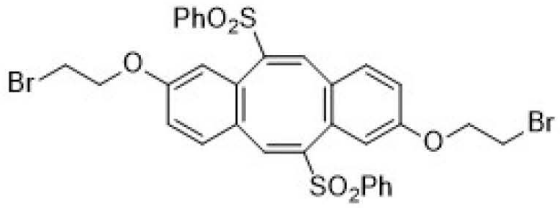

3.18

^{1}H NMR (400 MHz, Chloroform-*d*) δ 7.65 7.58 (m, 2H), 7.49 7.38 (m, 8H), 7.30 (s, 2H), 7.00 (d, *J* = 2.4 Hz, 2H), 6.88 6.80 (m, 4H), 4.07 3.96 (m, 4H), 3.69 (t, *J* = 4.7 Hz, 8H), 2.74 (t, *J* = 5.7 Hz, 4H), 2.53 (t, *J* = 4.7 Hz, 8H).

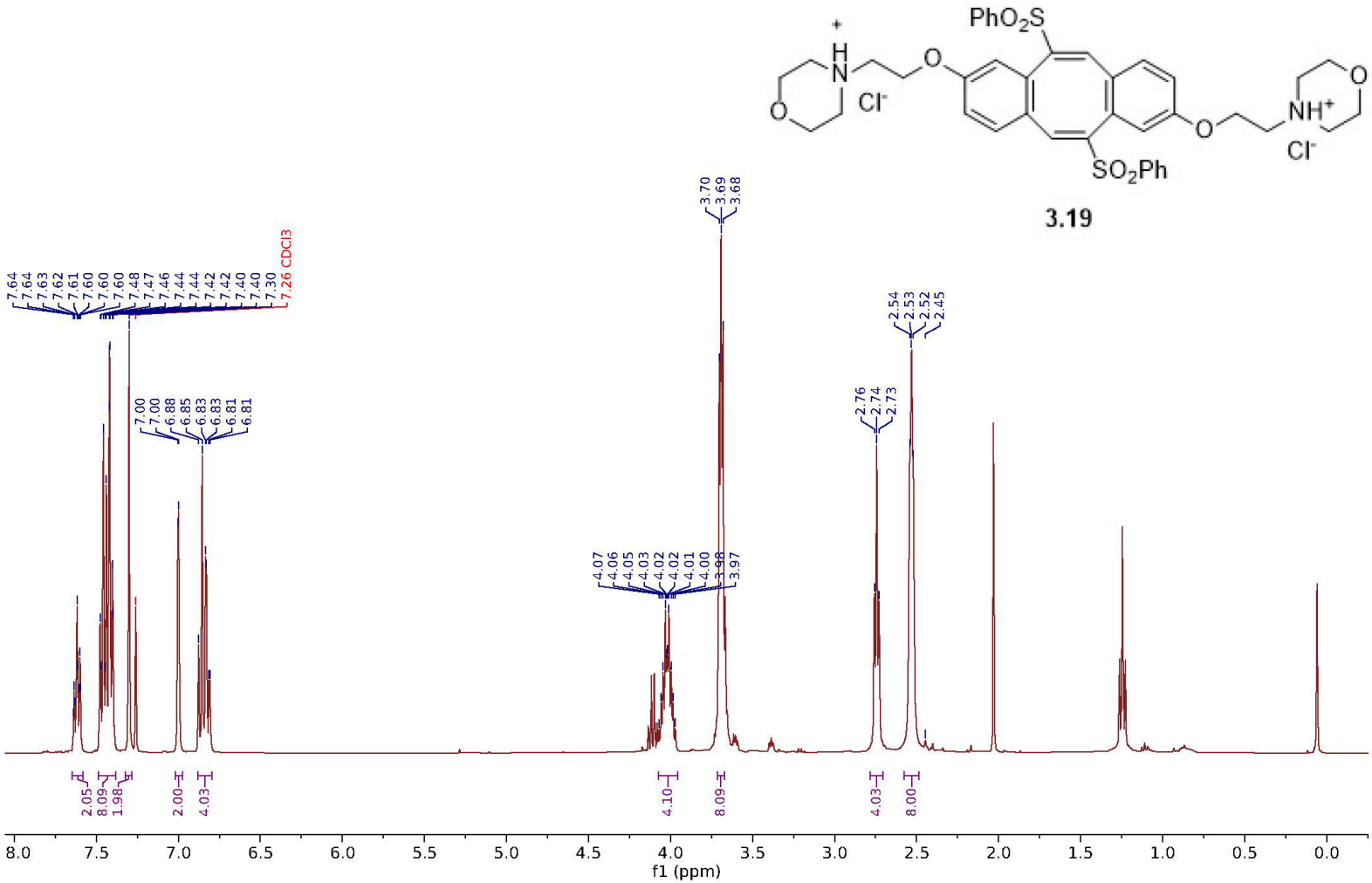

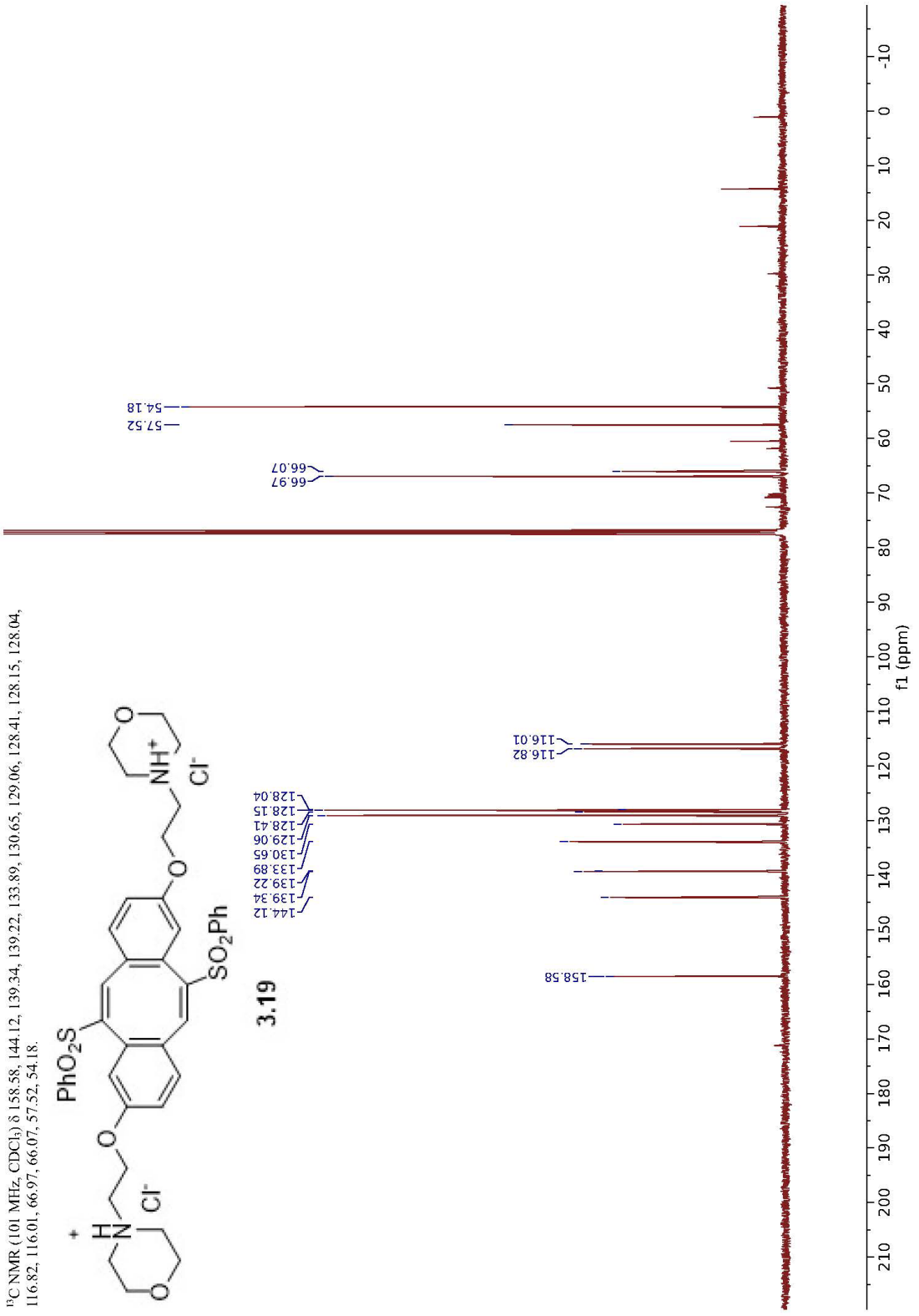
^{13}C NMR (101 MHz, $CDCl_3$) δ 158.58, 144.12, 139.34, 139.22, 133.89, 130.65, 129.06, 128.41, 128.15, 128.04, 116.82, 116.01, 66.97, 66.07, 57.52, 54.18.
3.19
PhO_2S
SO_2Ph
Cl⁻
Cl⁻
158.58
144.12
139.34
139.22
133.89
130.65
129.06
128.41
128.15
128.04
116.82
116.01
66.97
66.07
57.52
54.18
f1 (ppm)

^{1}H NMR (400 MHz, $CDCl_3$) δ 7.68 (dd, *J* = 7.8, 1.6 Hz, 4H), 7.47 7.35 (m, 6H), 3.68 (t, *J* = 6.4 Hz, 2H), 3.62 (t, *J* = 6.5 Hz, 2H), 1.65 1.51 (m, 4H), 1.49 1.41 (m, 2H), 1.39 (s, 1H), 1.06 (s, 9H).

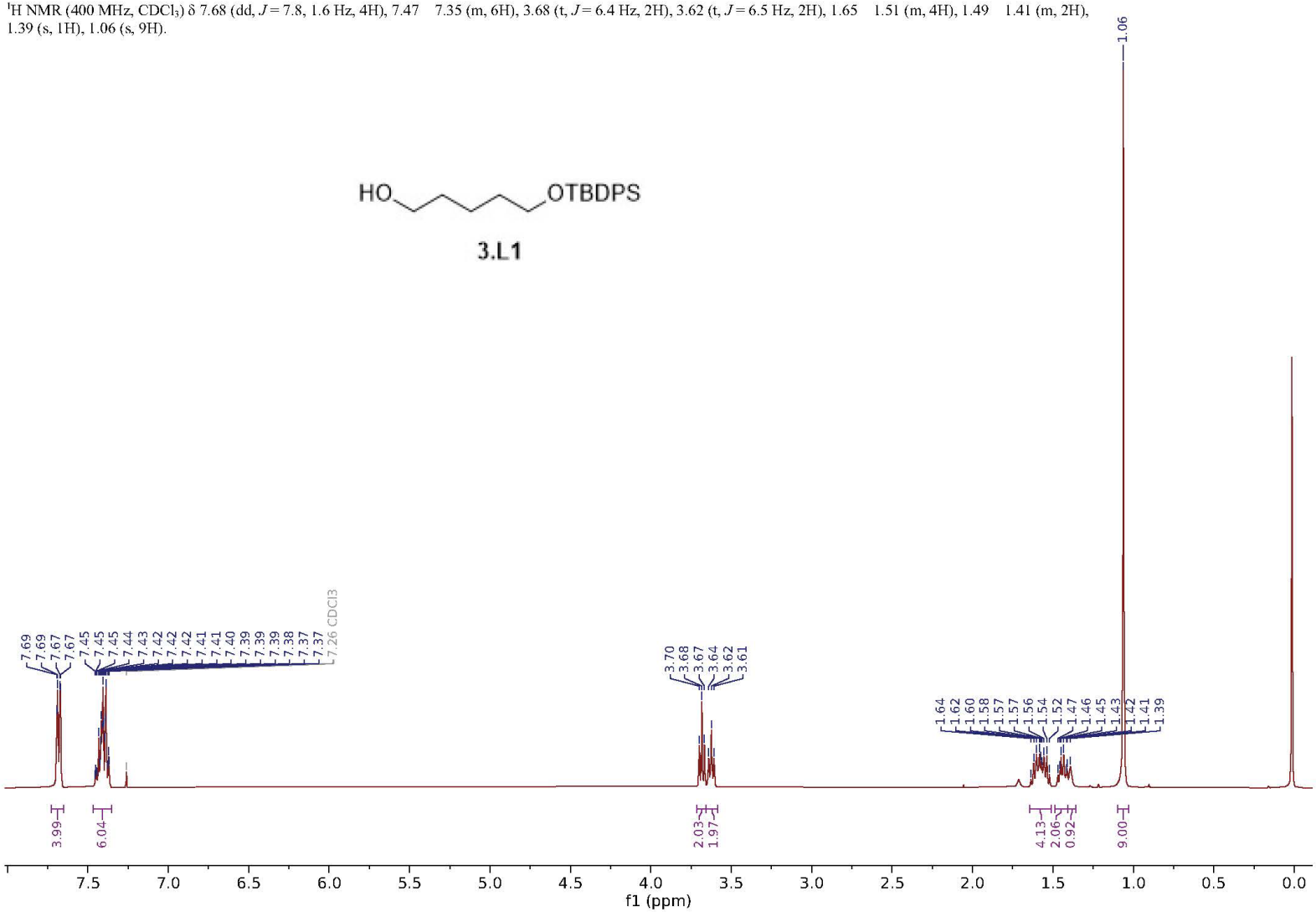

APPENDIX B

MASS SPECTRA

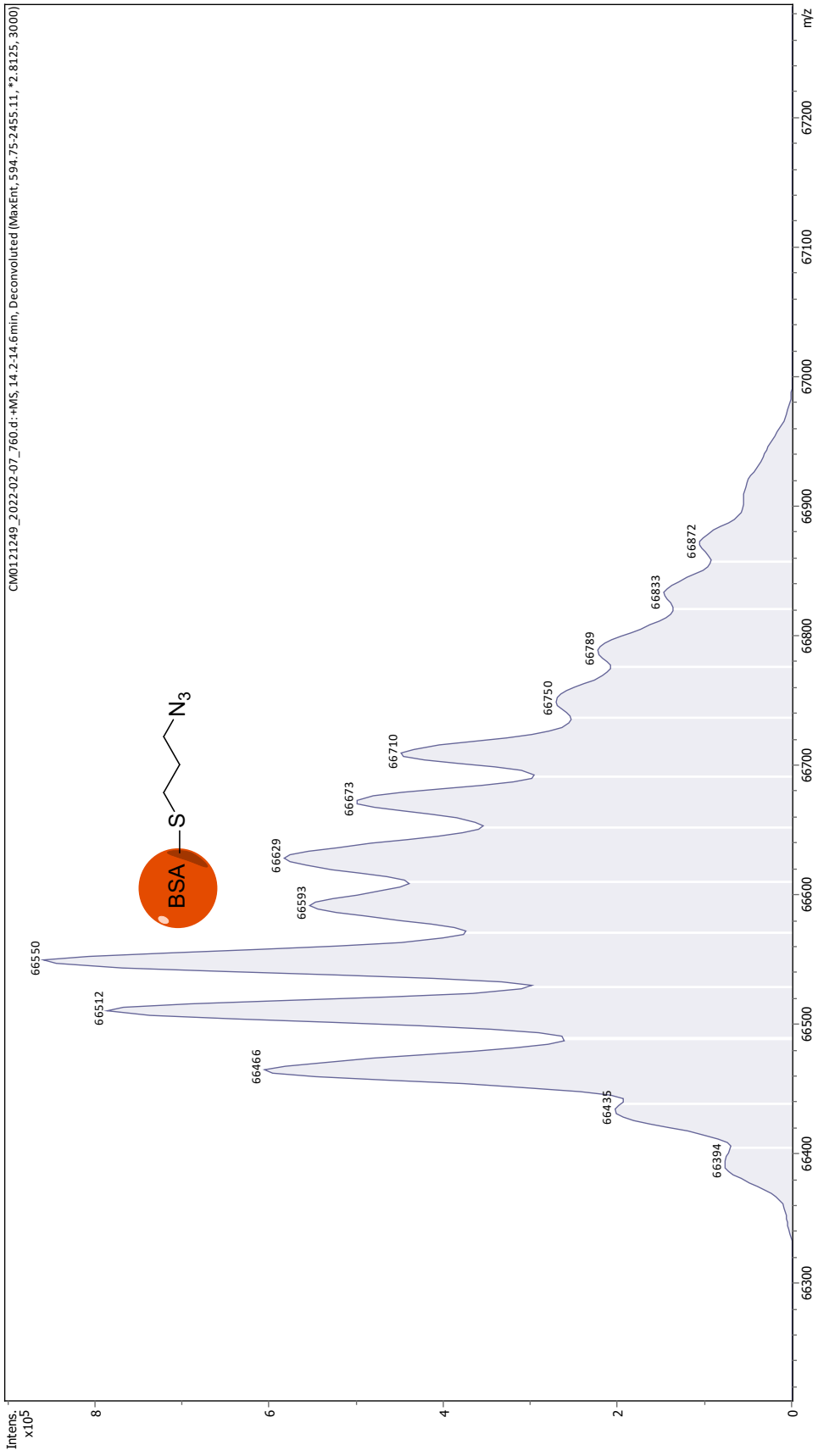
CM0121249_2022-02-07_760.d: +MS, 14.2-14.6 min, Deconvoluted (MaxEnt, 594.75-2455.11, *2.8125, 3000)
Intens.
x10^5
m/z
BSA
S
N3
66550
66512
66466
66435
66394
66629
66593
66673
66710
66750
66789
66833
66872

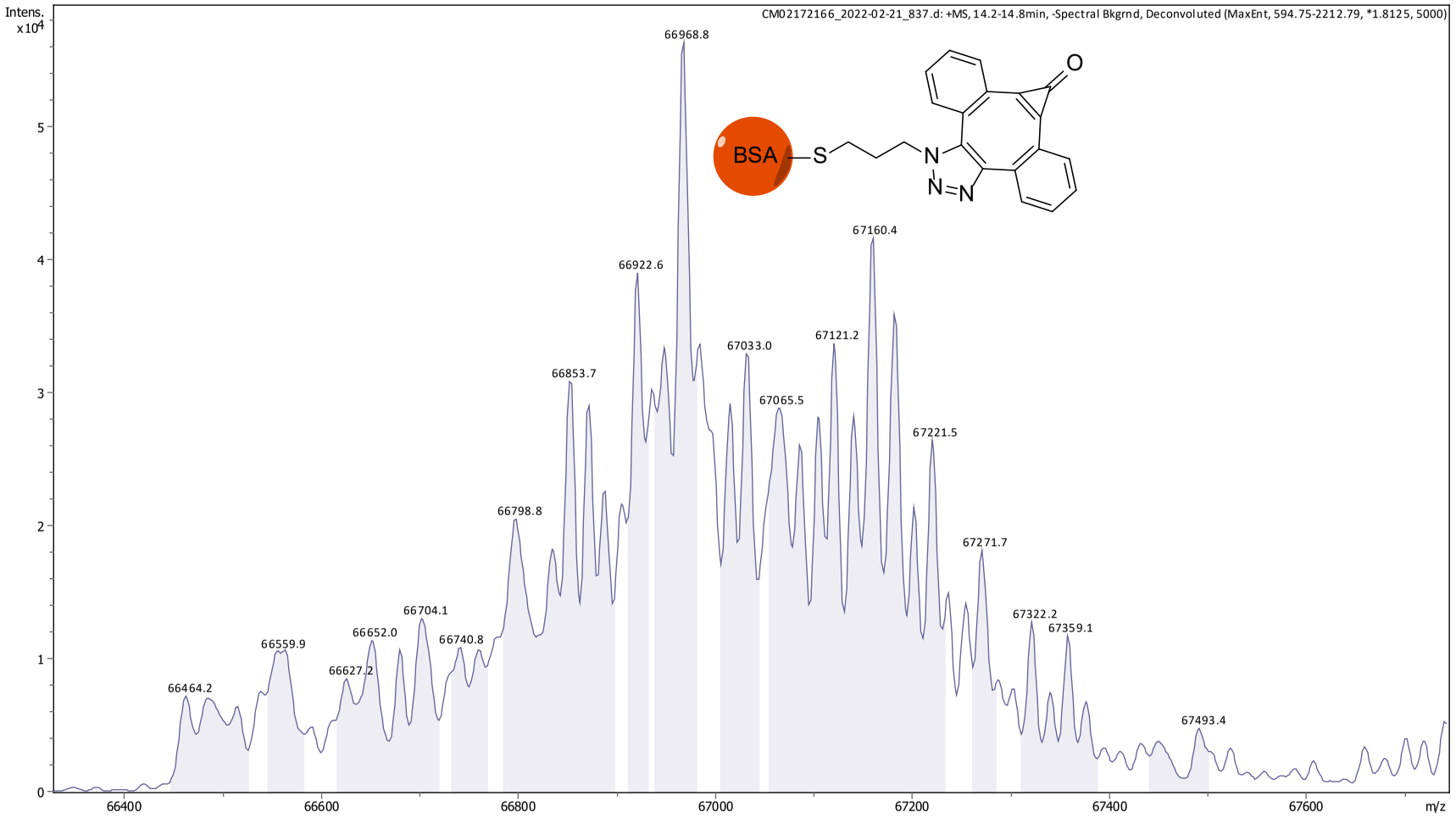
Intens.
x10^4
CM02172166_2022-02-21_837.d: +MS, 14.2-14.8min, -Spectral Bkgrnd, Deconvoluted (MaxEnt, 594.75-2212.79, *1.8125, 5000)
BSA
S
N
N
N
O
66968.8
67160.4
66922.6
67121.2
67033.0
66853.7
67065.5
67221.5
66798.8
67271.7
66704.1
66652.0
66740.8
67322.2
67359.1
66559.9
66627.2
66464.2
67493.4
0
1
2
3
4
5
66400
66600
66800
67000
67200
67400
67600
m/z

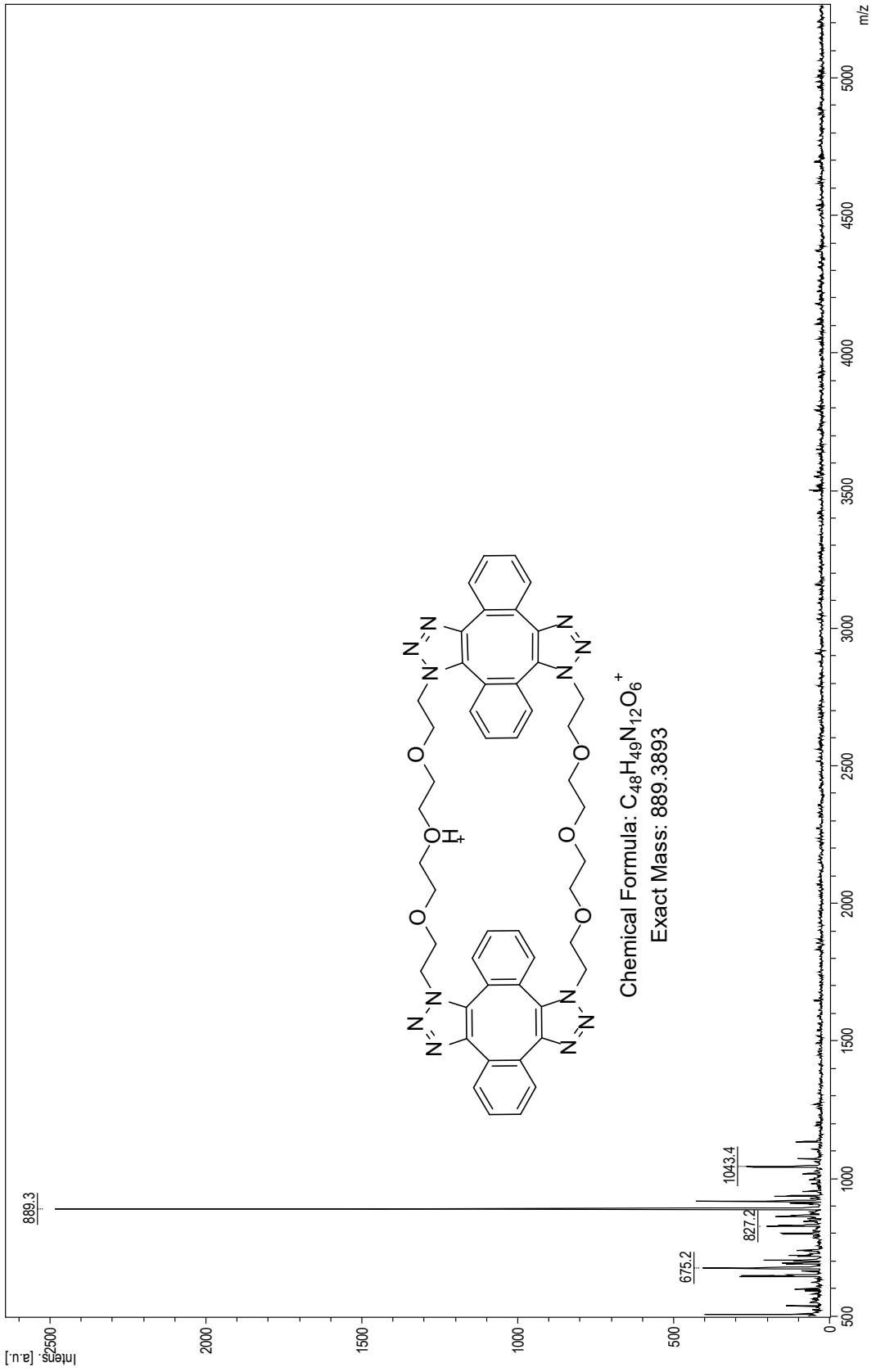
Intens. [a.u.]
2500
2000
1500
1000
500
0
500
1000
1500
2000
2500
3000
3500
4000
4500
5000
m/z
889.3
1043.4
827.2
675.2
Chemical Formula: $C_{48}H_{49}N_{12}O_6^+$
Exact Mass: 889.3893

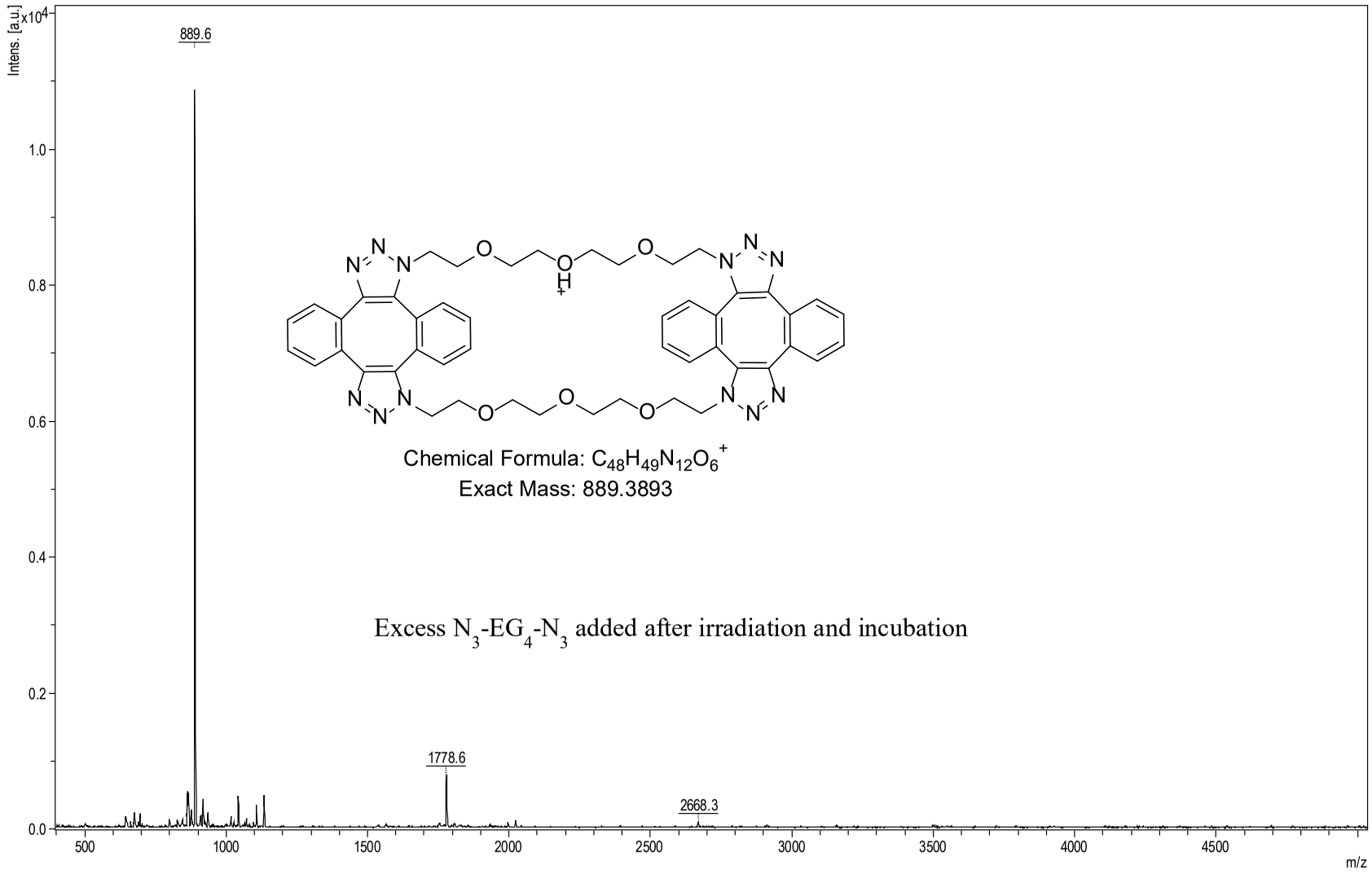
Intens. [a.u.]
x10^4
1.0
0.8
0.6
0.4
0.2
0.0
889.6
1778.6
2668.3
500
1000
1500
2000
2500
3000
3500
4000
4500
m/z
Chemical Formula: C48H49N12O6+
Exact Mass: 889.3893
Excess N3-EG4-N3 added after irradiation and incubation

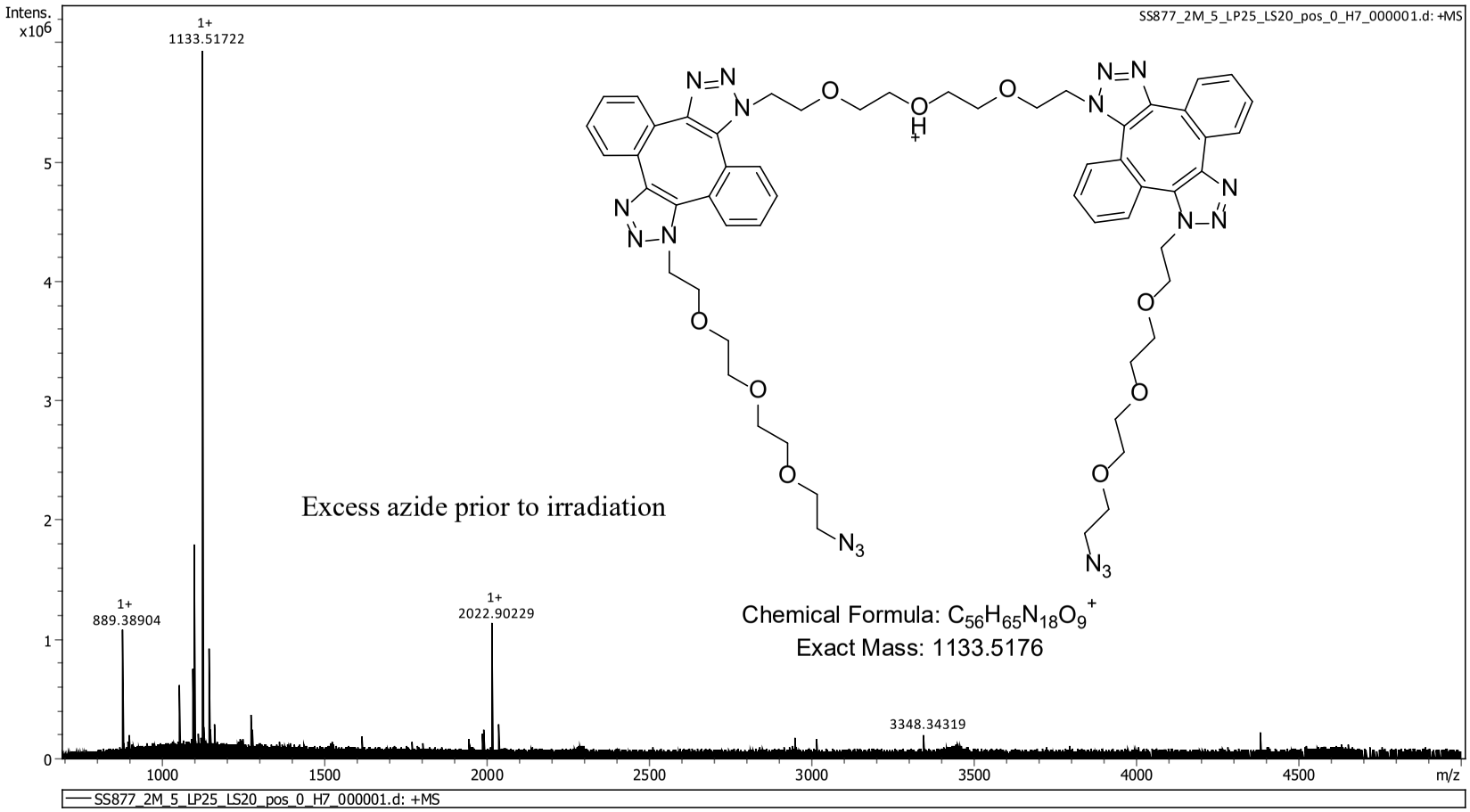
Intens.
x10^6
SS877_2M_5_LP25_LS20_pos_0_H7_000001.d: +MS
1+
1133.51722
1+
889.38904
1+
2022.90229
3348.34319
Excess azide prior to irradiation
Chemical Formula: C56H65N18O9+
Exact Mass: 1133.5176
m/z
SS877_2M_5_LP25_LS20_pos_0_H7_000001.d: +MS

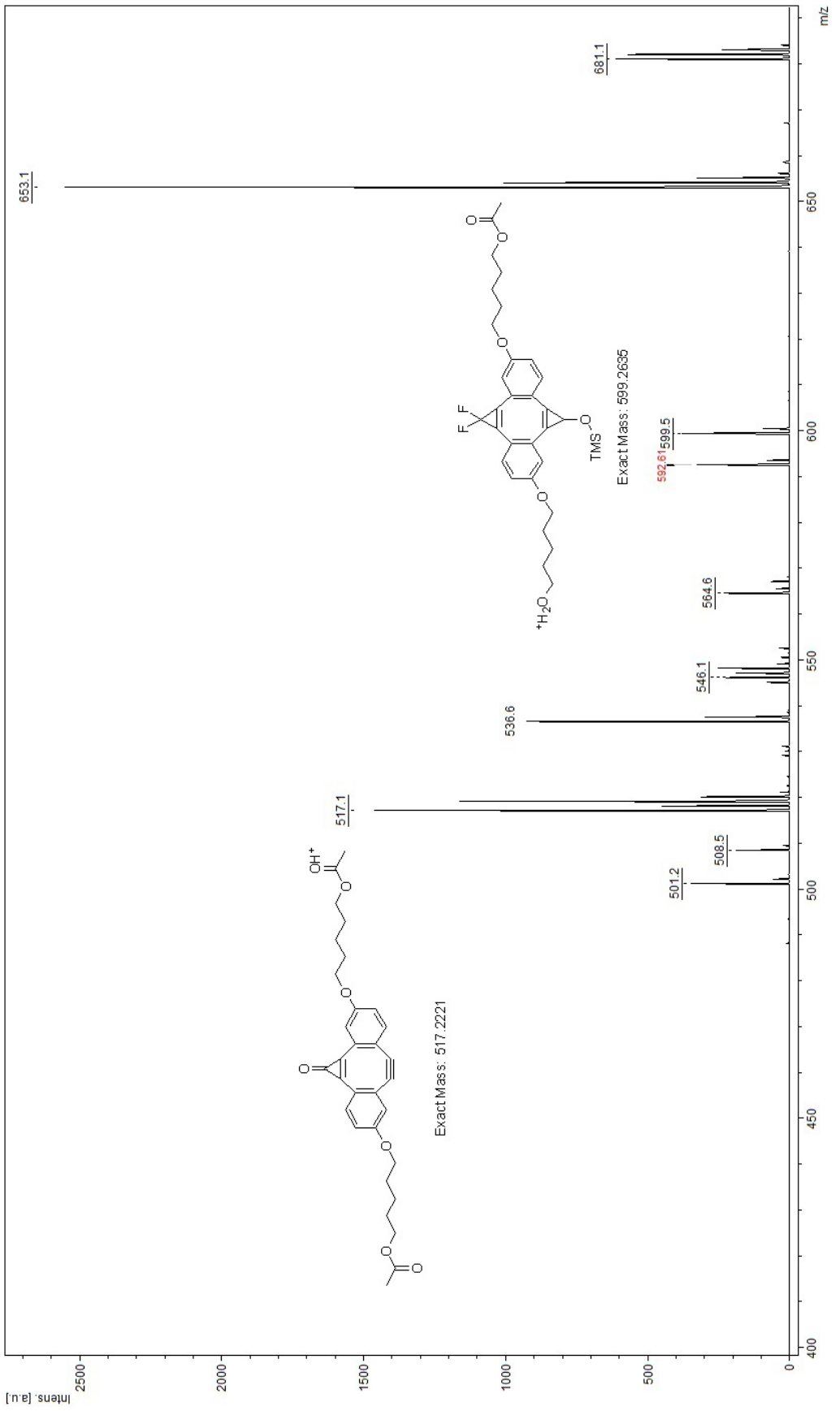
Intens. [a.u.]
2500
2000
1500
1000
500
0
m/z
400
450
500
550
600
650
653.1
681.1
599.5
592.61
564.6
546.1
536.6
517.1
508.5
501.2
Exact Mass: 599.2635
Exact Mass: 517.2221

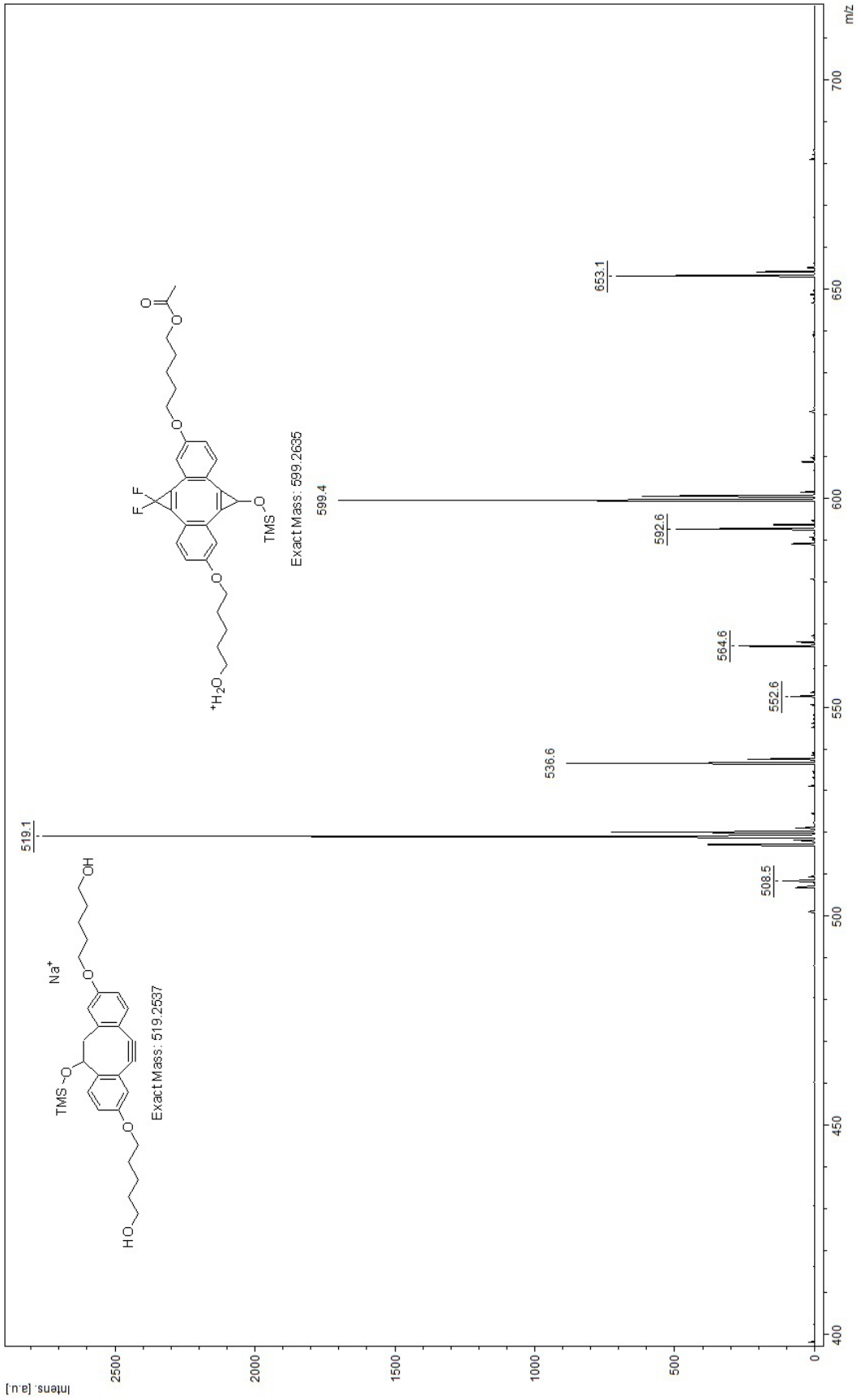
Intens. [a.u.]
2500
2000
1500
1000
500
0
400
450
500
550
600
650
700
m/z
519.1
508.5
536.6
552.6
564.6
592.6
599.4
653.1
Exact Mass: 599.2635
Exact Mass: 519.2537
TMS
Na+
F
F
+H2O

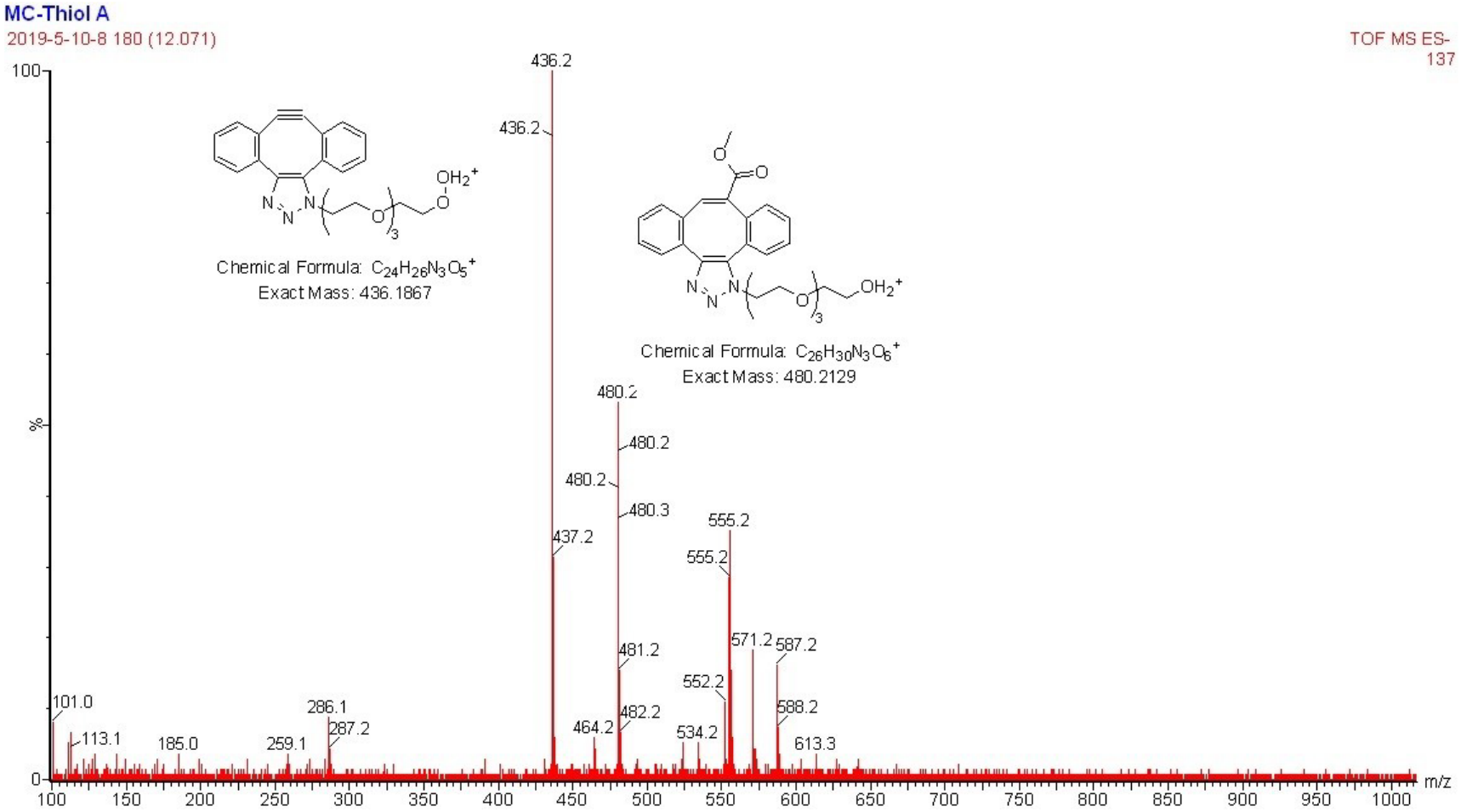
MC-Thiol A
2019-5-10-8 180 (12.071)
TOF MS ES-
137
Chemical Formula: C24H26N3O5+
Exact Mass: 436.1867
Chemical Formula: C26H30N3O6+
Exact Mass: 480.2129
%
m/z
436.2
480.2
555.2
571.2
587.2
481.2
552.2
588.2
482.2
464.2
534.2
613.3
437.2
480.3
101.0
113.1
185.0
259.1
286.1
287.2

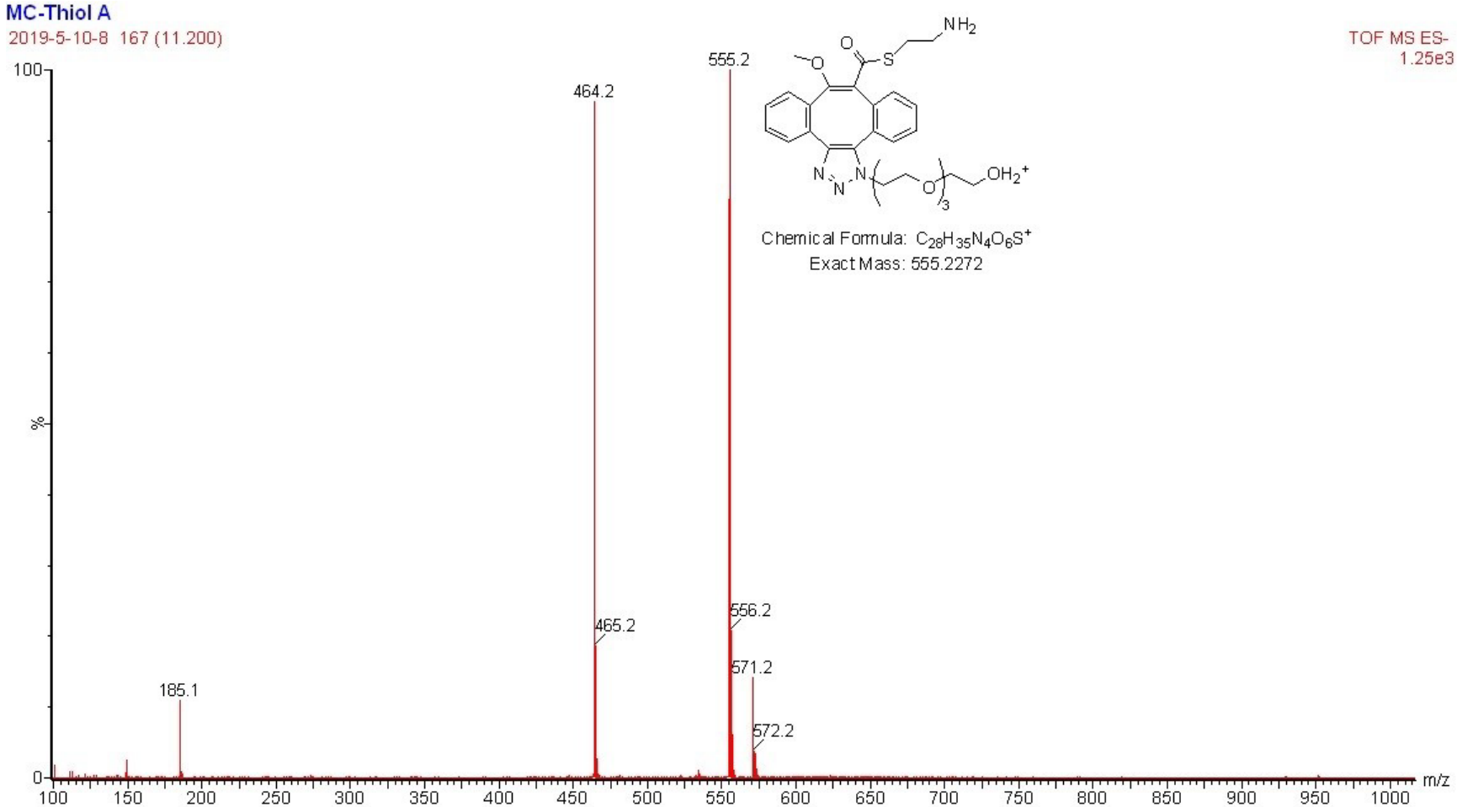
MC-Thiol A
2019-5-10-8 167 (11.200)
TOF MS ES-
1.25e3
100
%
0
464.2
555.2
465.2
556.2
571.2
572.2
185.1
Chemical Formula: C28H35N4O6S+
Exact Mass: 555.2272
100 150 200 250 300 350 400 450 500 550 600 650 700 750 800 850 900 950 1000
m/z

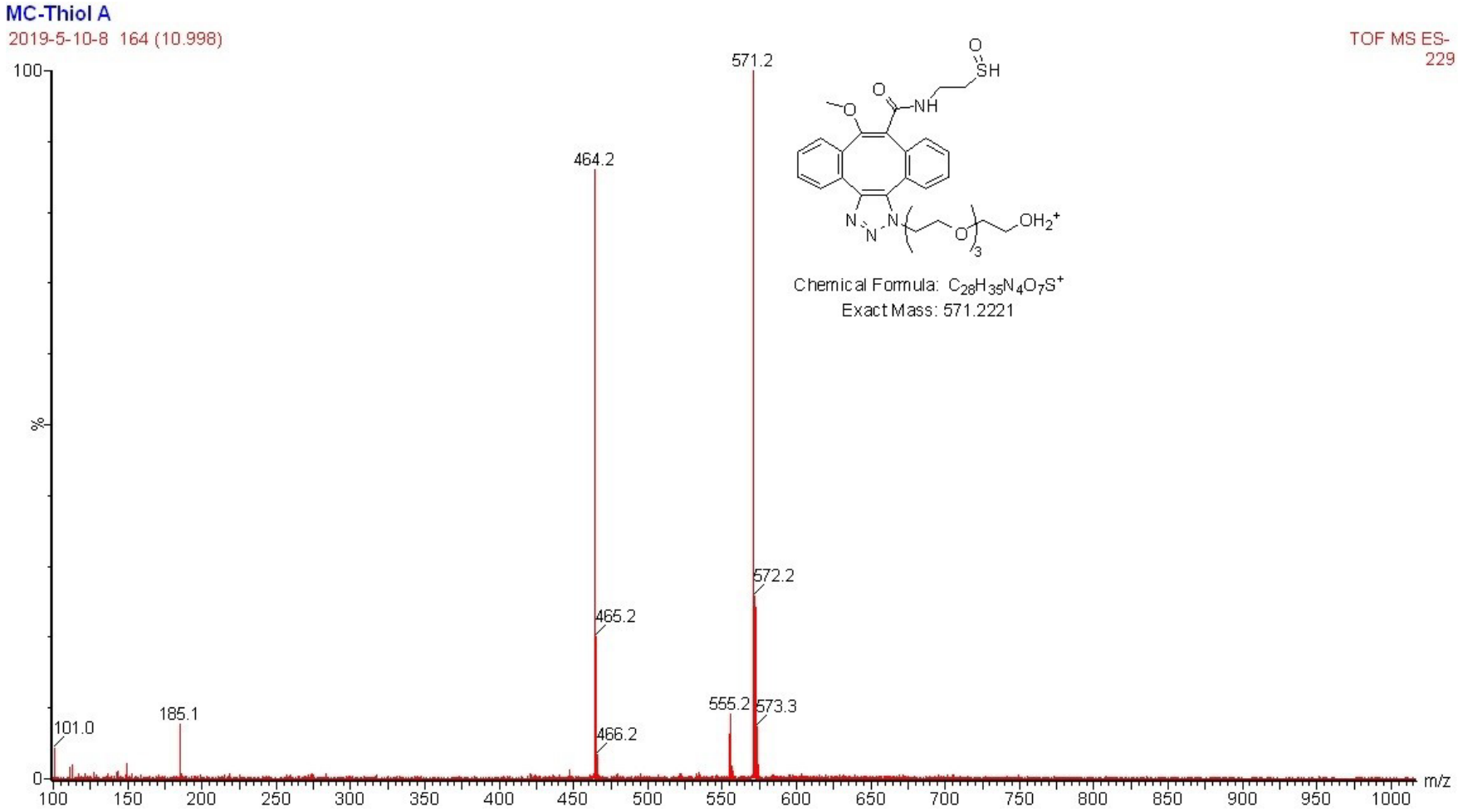
MC-Thiol A
2019-5-10-8 164 (10.998)
TOF MS ES-
229
100
%
0
571.2
464.2
572.2
465.2
555.2
573.3
185.1
101.0
466.2
m/z
100 150 200 250 300 350 400 450 500 550 600 650 700 750 800 850 900 950 1000
Chemical Formula: C28H35N4O7S+
Exact Mass: 571.2221

APPENDIX C

KINETICS DATA

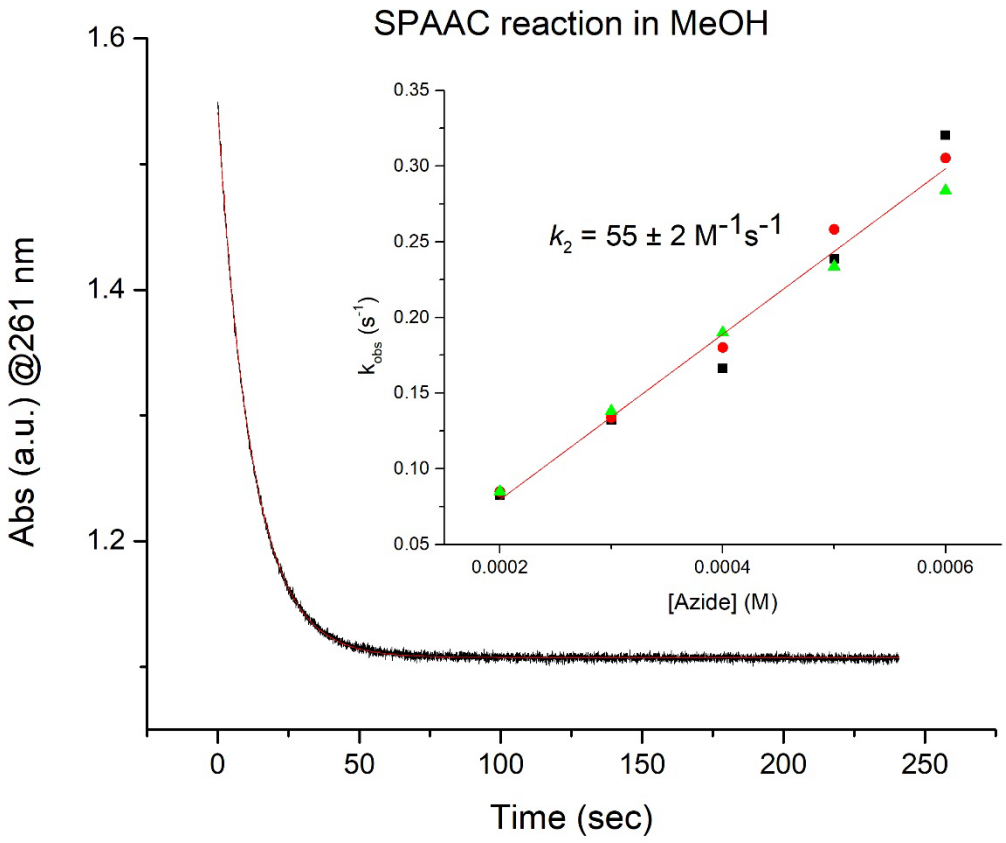

Figure C.1 Kinetics plot of the DIBOT + TEG-azide SPAAC reaction in methanol. Inset shows the linear fit of the observed rate constant vs various excess concentrations of TEG-azide.

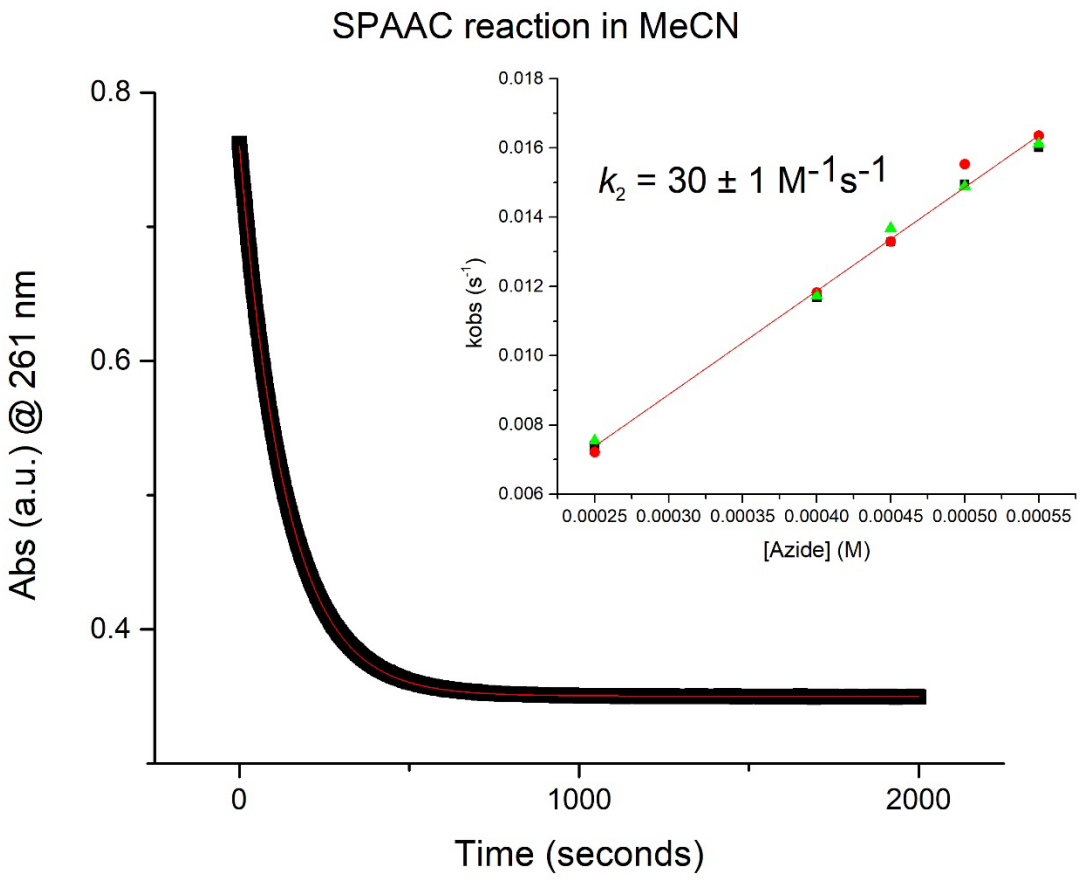

Figure C.2 Kinetics plot of the DIBOT + TEG-azide SPAAC reaction in acetonitrile. Inset shows the linear fit of the observed rate constant vs various excess concentrations of TEG-azide.

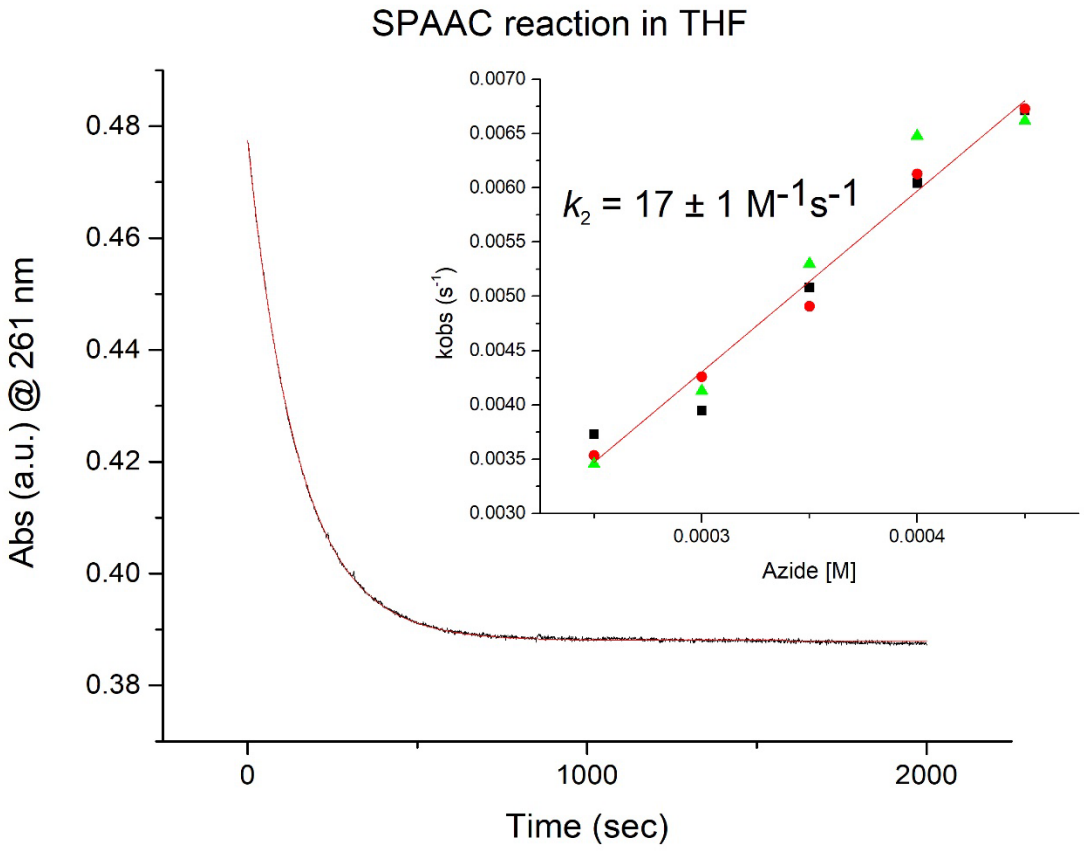

Figure C.3 Kinetics plot of the DIBOT + TEG-azide SPAAC reaction in THF. Inset shows the linear fit of the observed rate constant vs various excess concentrations of TEG-azide.

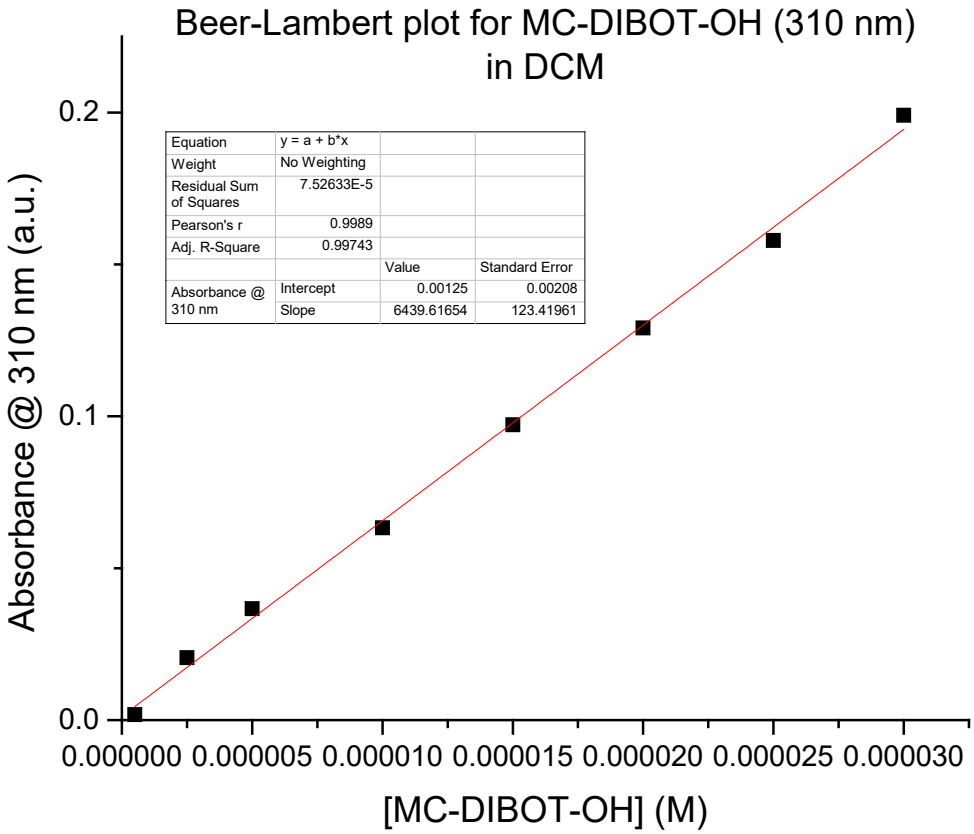

Figure C.4 Beer-Lambert plot for the 310 nm band of MC-DIBOT-OH in DCM. The slope of the line is the molar extinction coefficient.

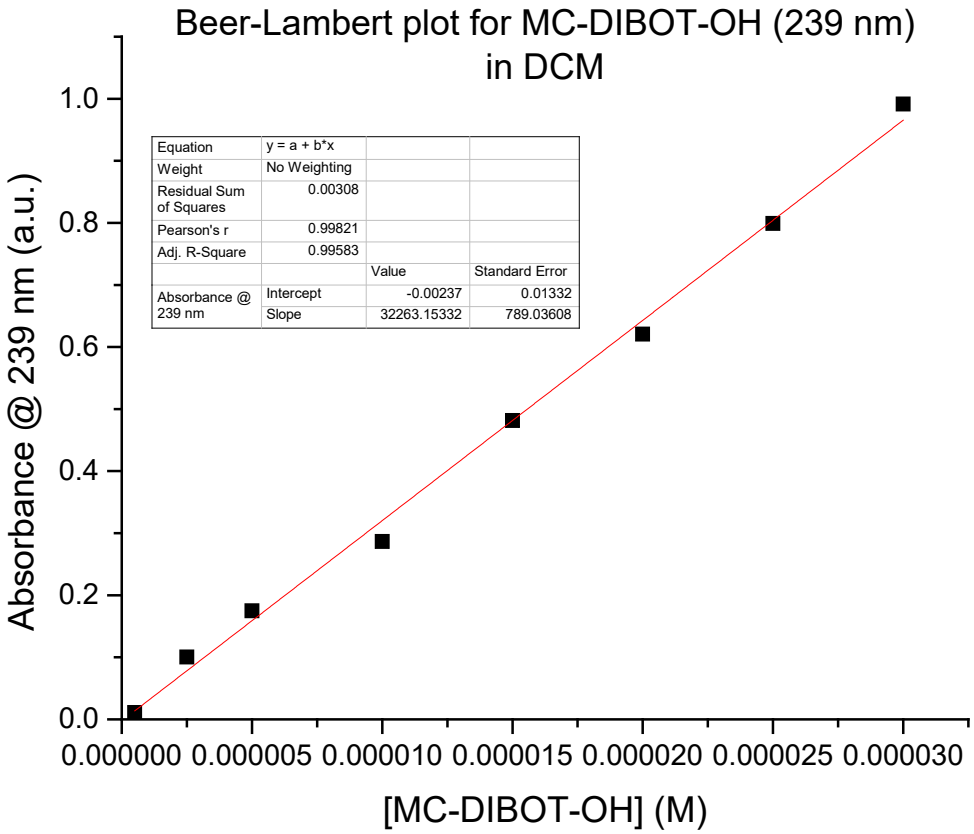

Figure C.5 Beer-Lamber plot for the 239 nm band of MC-DIBOT-OH in DCM. The slope of the line is the molar extinction coefficient.

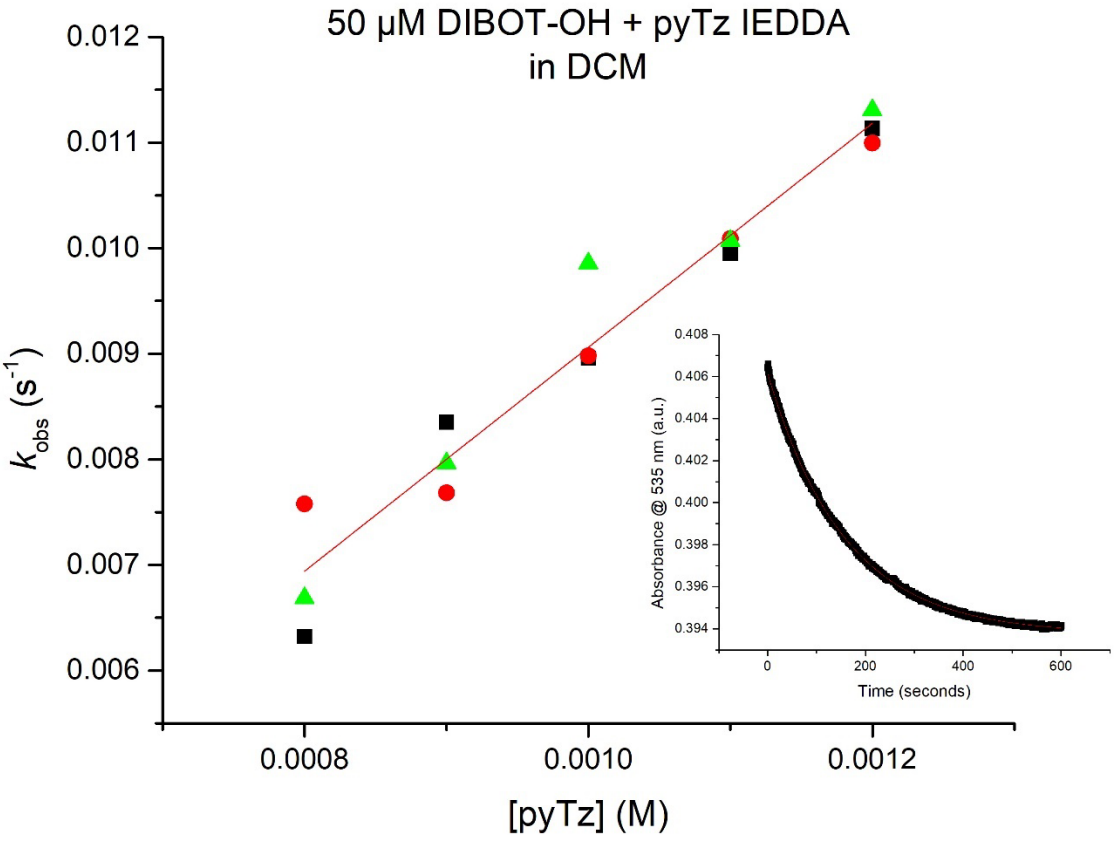

Figure C.6 Plot of k_{obs} vs [pyTz] for the DIBOT-OH + pyTz IEDDA reaction in DCM. Inset graph shows a sample kinetics plot obtained from UV-Vis analysis.

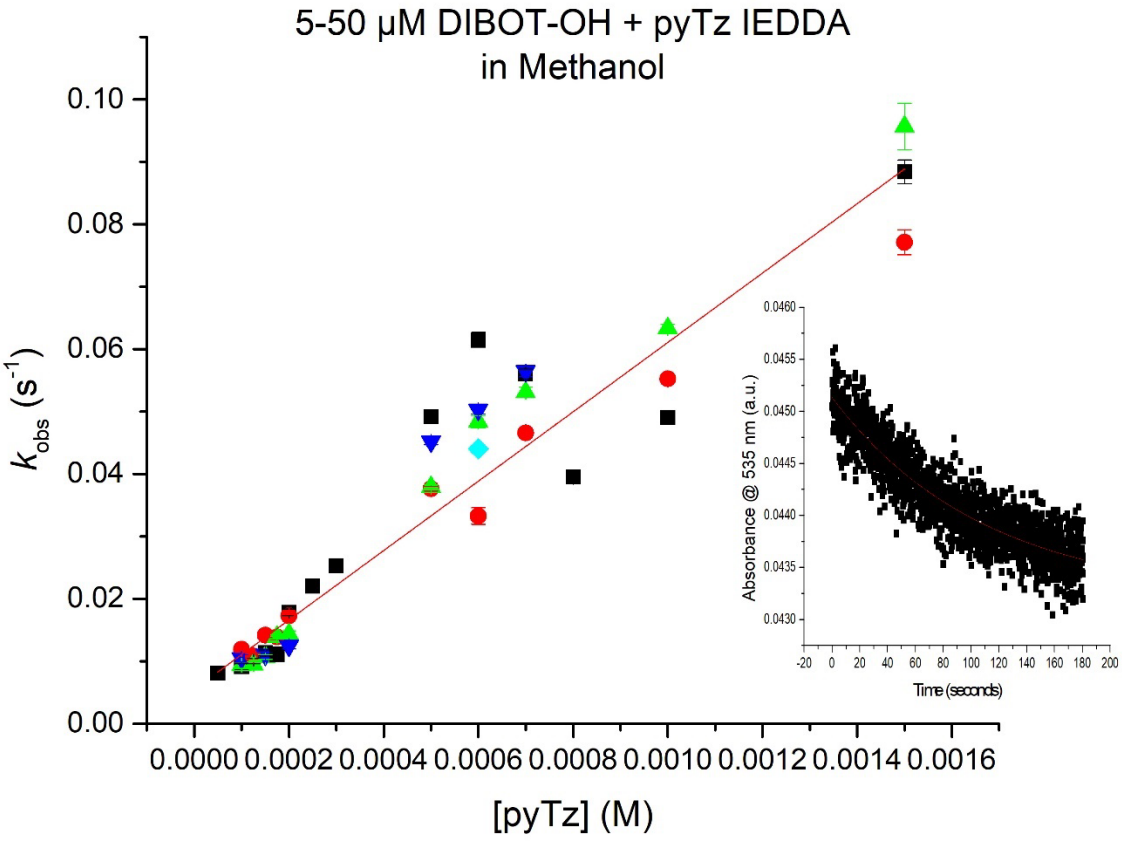

Figure C.7 Plot of k_{obs} vs [pyTz] for the DIBOT-OH + pyTz IEDDA reaction in MeOH. Inset graph shows a sample kinetics plot obtained from UV-Vis analysis.

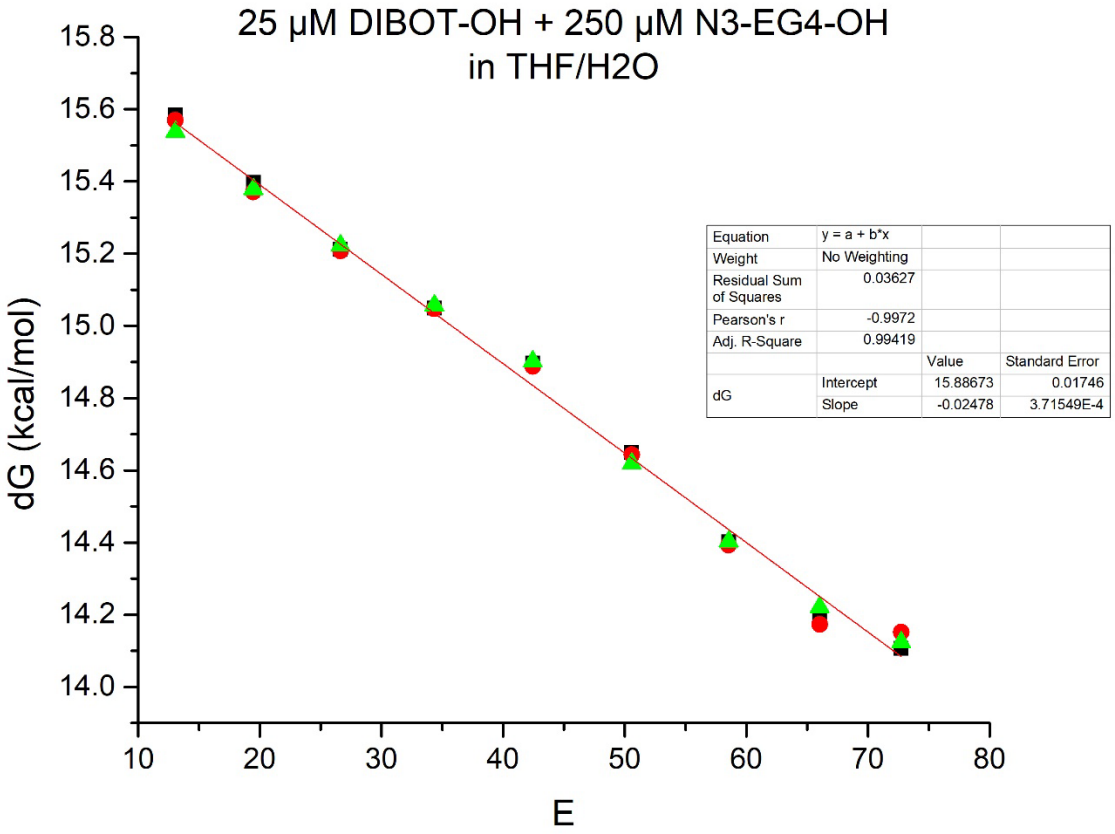

Figure C.8 Plot of the ΔG of activation vs dielectric constant of the solution for the DIBOT-OH + TEG-azide SPAAC reaction in THF/H_2O.

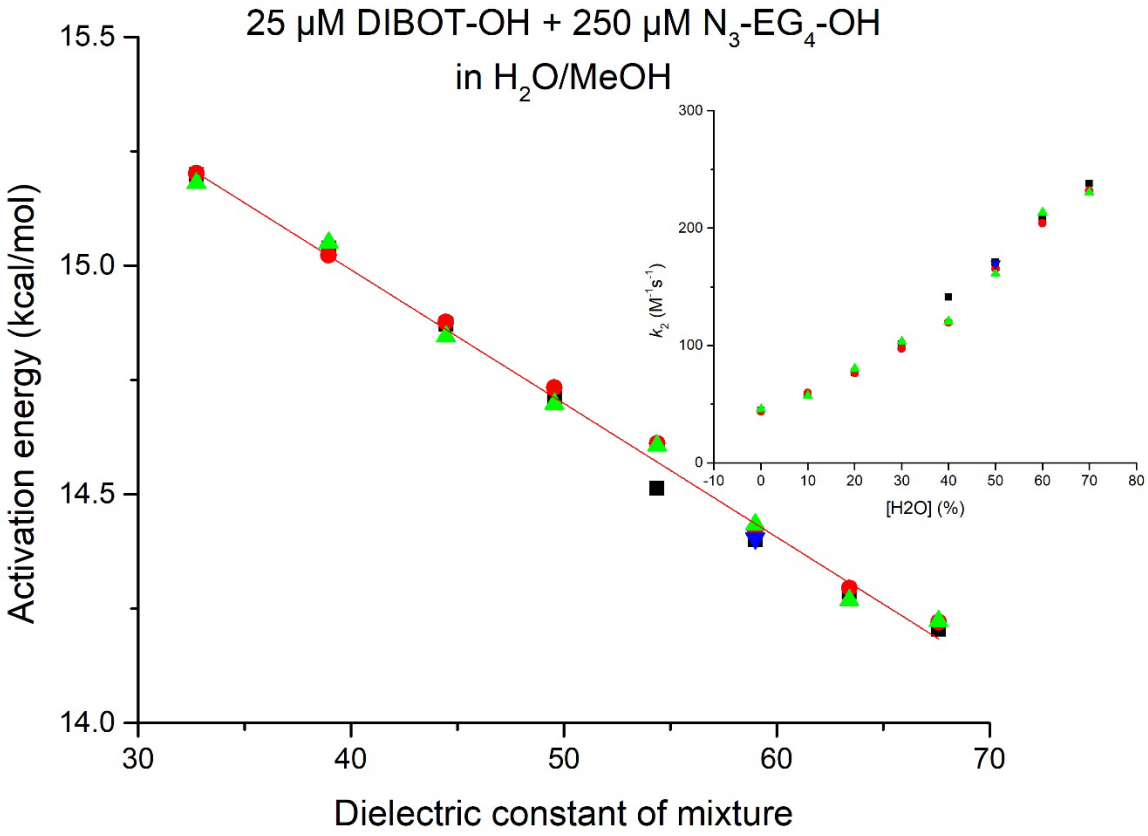

Figure C.9 Plot of the ΔG of activation vs dielectric constant of the solution for the DIBOT-OH + TEG-azide SPAAC reaction in methanol/H_2O. Inset graph shows second-order rate constant vs concentration of water as a percentage of the solvent.

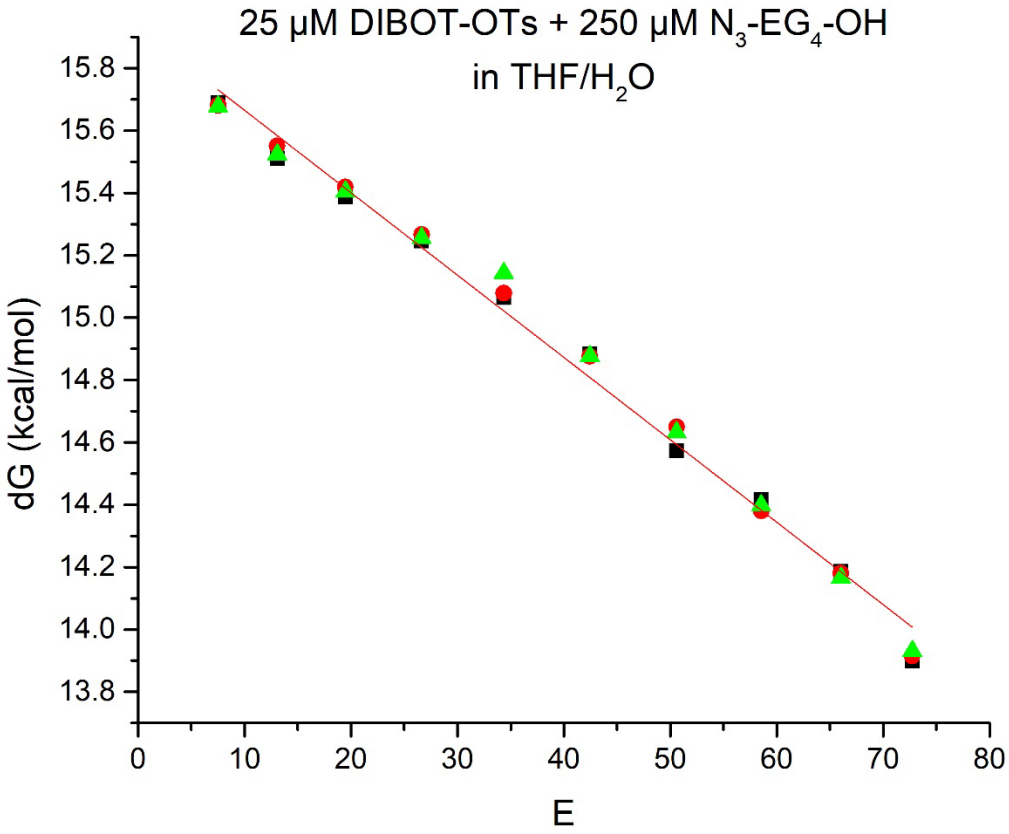

Figure C.10 Plot of the ΔG of activation vs dielectric constant of the solution for the DIBOT-OTs + TEG-azide SPAAC reaction in THF/H_2O.

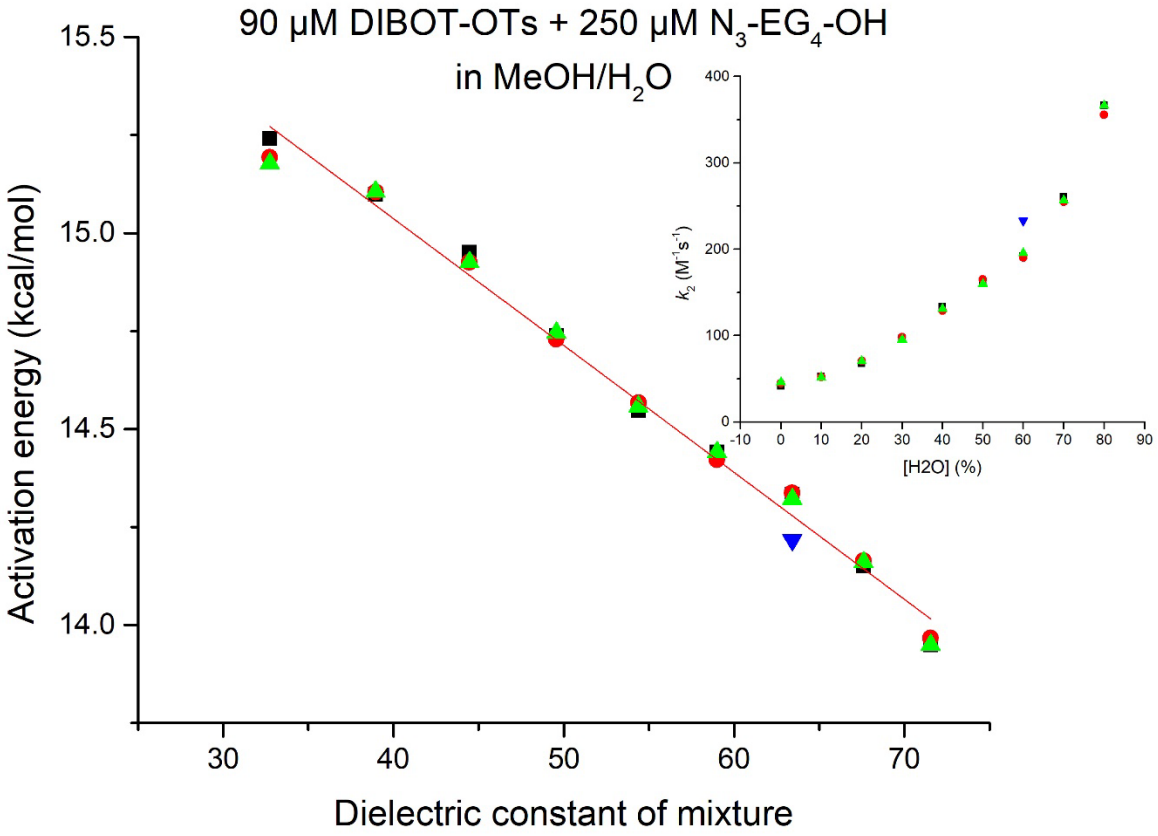

Figure C.11 Plot of the ΔG of activation vs dielectric constant of the solution for the DIBOT-OTs + TEG-azide SPAAC reaction in methanol/H_2O. Inset graph shows second-order rate constant vs concentration of water as a percentage of the solvent.

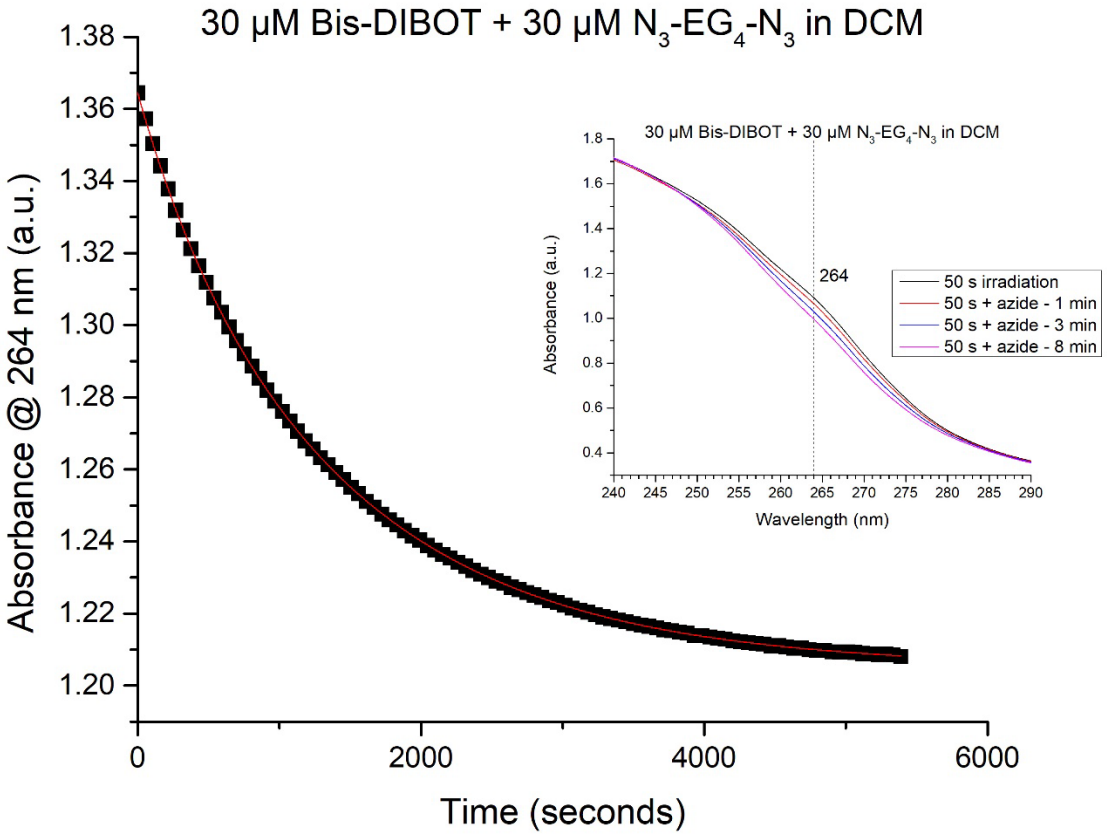

Figure C.12 Scanning kinetics plot for the bis-DIBOT + bis-azido-TEG tandem SPAAC reaction. The kinetics data fit a function with the formula $y = (A_1 \times e^{-k_1 t}) + (A_2 \times e^{-k_2 t})$.